UNIVERSITA'
CAMPUS BIO-MEDICO DI ROMA

FACOLTA' DI INGEGNERIA BIO-MEDICA

DOTTORATO DI RICERCA IN BIOINGEGNERIA E BIOSCIENZE

CURRICULUM IN INGEGNERI BIO-MEDICA

XXIX CICLO

MOTION CAPTURE SYSTEMS FOR RESPIRATORY, GAIT AND POSTURE ANALYSIS.

Supervisori:

Prof.ssa Loredana Zollo

Prof.ssa Silvia Sterzi

Dott. Michelangelo Morrone

INDEX

Introduction

Human motion analysis is the systematic study of human motion by careful observation, augmented by instrumentation for measuring body movements, body mechanics and the activity of the muscles. It aims to gather quantitative information about the mechanics of the musculoskeletal system during the execution of a motor task [1]. A special branch of human motion analysis is gait analysis which is specific to the study of human walking, and is used to assess, plan and treat individuals with conditions affecting their ability to walk.

In pursuing mental and physical excellence, the ancient Greeks found that harmony of mind and body required athletic activity to complement the pursuit of knowledge. Their interest in sport and human movement can be seen in the predominance of kinematic representations of Greek athletics in the artistic media. With the mechanical, mathematical and anatomical paradigms developed during Greek antiquity, the great philosopher Aristotle wrote the first book on human movement (About the Movements of Animals), which is the first scientific analysis of human and animal movement in terms of observing and describing muscular action and movement [2].

In the modern era (20th century e today), human motion analysis developed rapidly as the knowledge of anatomy and mechanics, and measurement technology was progressively established. In the 1940s, Harold Eugene Edgerton pioneered high-speed stroboscopic photography that was used to photograph objects in motion at a frequency of several million exposures per second. During the 1970s, video camera systems, such as infrared high-speed cameras, began their widespread application in the analysis of pathological gait, producing detailed motion analysis results within realistic cost and time constraints. With the collocation of high-speed computers and video camera systems, 3D analysis of human motion became feasible. However, it had to wait until after World War II to make its debut in clinical 3D applications.

After the war there were many retired soldiers who had sustained limb injuries and who needed orthopedic treatment, prostheses, orthoses and subsequent rehabilitation for recovery of functional activities, especially for level walking. In order to provide better medical services and achieve treatment goals, numerous investigators devoted themselves to the study of gait analysis for clinical applications. Among them was Verne Thompson Inman who began by applying the theory of mechanical engineering to clinical problems, such as designing prostheses for amputees. He studied the biomechanics of locomotion and proved the assumption that the most efficient gait pattern is achieved by minimizing vertical and lateral excursions of the body's center of gravity (COG). He also identified the so-called gait determinants for normal walking, i.e., features of the movement pattern that mini-mizes these COG excursions [1]. He suggested that these features be used to determine whether a movement pattern is normal or pathological. Following Inman's work, Jacquelin Perry divided the gait cycle into five stance phase periods and three swing phase periods [3]. David Sutherland refined the definition of the gait cycle to have three periods of stance, namely initial double support, single limb stance, and second double support [4]. Apart from kinematic measurements using video cameras, Dr J. Robert Close used a 16-mm movie camera with a sound track for studying the phasic action of muscles in subjects after muscle transfers for poliomyelitis. Doctor Close was the first to record synchronously the kinesiological electromyography (KEMG) of one muscle and kinematic data on cine film [5]. Jacquelin Perry pioneered using fine wire electrodes to record the gait electromyogram (EMG) and used it as a primary clinical tool in determining the appropriateness of surgical procedures to correct gait deformities [6]. Because muscles are the engines for producing active movements, EMG has been a useful assessment tool for detecting the electrical activity of specific muscles and assessing their contribution to movement or gait. Between 1944 and 1947, Vern Inman and colleagues added

KEMG to other measurements, i.e., 3D force and energy, in the study of walking in normal subjects and amputees, and thus significantly moved the science of gait analysis forward.

Starting from this historical background, actually instrumental motion analysis systems have widely spread their fields of application, moving from entertainment to military use. Namely, optoelectronic systems, which present poor invasivity and high reliability in objectively measuring body motion, have become the gold standard in movement analysis laboratories. Thus, the aim of this research is to present some recent applications of the optoelectronic systems to serve as clinical tools in respiratory, gait and posture analysis, highlighting possible technical advantages of this kind of motion analysis.

At this purpose, the paper is structured as follows: Chapter I reports technical considerations about marker-based motion analysis systems actually available in clinical settings. Chapter II provides an overview on the use of optoelectronic plethysmography in a wide range of respiratory patients. Chapter III and IV describe an interesting clinical application of marker-based motion analysis systems, respectively on the breathing kinematics of spinal cord injurd patients (and the influence of posture on this behavior), and the trunk alignment recovery in a group of parkinsonian patients undergone a specific rehabilitation protocol. Chapter V deals with technical aspects of ankle foot orthosis to be prescribed for foot drop syndrome. Finally, chapter VI presents preliminary data on the effect of wearing some different kinds of prosthesis in an upper limb amputee patient, as compared to age-matched healthy controls.

References

[1] Clinical Gait Analysis, University of Vienna, Austria. History of the study of locomotion. http://www.univie.ac.at/cga/ history/.

[2] Nigg BM, Herzog W. Biomechanics of the musculo-skeletal system. 3rd ed. Hoboken NJ: John Wiley & Sons; 2007.

[3] Watkins J. Structure and function of the musculoskeletal system. Champaign: Human Kinetics; 1999.

[4] Bergmann G, Deuretzbacher G, Heller M, Graichen F, Rohlmann A, Strauss J, et al. Hip contact forces and gait patterns from routine activities. J Biomech 2001;34:859e71.

[5] Heller MO, Bergmann G, Deuretzbacher G, Durselen L, Pohl M, Claes L, et al. Musculo-skeletal loading conditions at the hip during walking and stair climbing. J Biomech 2001;34:883e93.

[15] Perry J. Gait analysis: normal and pathological function. Thorofare, N.J.: Slack; 1992.

Chapter I - Motion Capture Systems for Human Motion Analysis

Introduction

Measurement of human posture and movement is an essential area of research in the bioengineering and rehabilitation fields. It is motivated by different goals in clinical application, such as in comparing normal with pathological movements, planning and evaluating treatment protocols, and assessing design of orthosis and prosthesis [1].

All movements and changes in movements arise from the action of forces, both internal and external. A change in the force acting on an object is necessary for moving an object from a stationary position or for changing its velocity. The amount of change in the velocity of an object depends on the magnitude and direction of the applied force. Newton's laws of motion give a clear relationship between the changing force and the resultant change in movement, and this is applicable to all forms of movement.

Human motion analysis can be defined as the systematic study of human motion; it can be realized by means of instrumentation for measuring body mechanics [2]. The essential aim of human motion analysis is to understand the mechanical function of the musculoskeletal system during the execution of a motor task. A special branch of human motion analysis is gait analysis which is specific to the study of human walking, and is used to assess, plan and treat individuals with conditions affecting their ability to walk.

Motion capture (MoCap) is the process of recording the movement of objects or human bodies. Among several scenarios (e.g., military, entertainment, sports), MoCap is extensively used in the medical field, both for clinical and research purposes [1].

Since 1970 when MoCap started as a photogrammetric analysis tool in biomechanics research, different technologies have been developed and tested to record the movement like acoustic [2], inertial [3], magnetic or reflective markers [4], wearables [5] or combinations of any of these. Since the beginning of the 21st century because of the rapidly growth of optical technologies, new

methods and methodologies have been developed based on optoelectronic systems. Because the enhancement of the performance of these systems, MoCap is used in a range of clinical and research application, ranging from gait analysis to small movements of different discrict like the chest, the head, the spine, the hand, the arm in healthy, athletes and in pathological subjects (e.g. amputees, extra-pyramidal disorders, neuro-vascular accidents), likewise in babies and adults.

Currently, within the large number of MoCap technologies, the most affordable and accurate analysis of the musculoskeletal system can be performed by using MoCap systems based on the tracking of markers positioned on specific body landmarks [6].

Photogrammetric systems have been used to record two- or three-dimensional image of posture. This type of system uses either light-reflective markers or light-emitting diodes affixed to the human body, and captures data with cameras and films for measuring the orientation of body segments through data reduction processing. Optoelectronic analysis applies the same principles as photogrammetric system to measure the position of joints and body segments. The optoelectronic sensing unit is used for collecting the data instead of films. Video systems also use the similar basic principles as both photogrammetric and optoelectronic systems but capture data with optoelectronic units or cameras of higher sampling rate. These systems can be used to capture and record three-dimensional body movements. The availability of these image-based methods has helped to achieve the goals of monitoring and analysing human posture and movement. However, inherent limitations of these methods, which are complicated to set up, time-consuming to operate, and limited to the laboratory environment (Hsiao and Keyserling 1990), so the chance of using these methods in the clinical applications are restricted. In recent years, low-powered and miniaturized electronic sensors, which are for use in robotic, industrial, aerospace and biomedical applications, have been developed by using advanced electronic circuit

technology. The use of these electronic sensors has been considered as alternative methods for human posture and movement analysis in clinical applications.

Marker-Based MoCap Systems: a brief overview

Based on the work carried out in collaboration with Massaroni et al. [19], the author of this paper briefly reports the last acquisitions on marker-based tracking motion analysis systems. Marker-based MoCap systems detect active or passive markers on the body, placed on the part of the body to analyse. These devices carry out indirect measurements of kinematic variables. Markers are less invasive than other sensors because they are lighter and smaller. For this reason, it is easier to apply them on the body and the subject can perform his/her natural movements. In addition, the weight and the size of markers allow to minimize skin motion artefact, one of the most serious problems to correctly quantify motion analysis, caused by muscle contraction, inertial effects and the weight of sensors. There are critical cases, like some joints, to regard with much more caution as this artefact produces even with optoelectronic systems.

Marker-based MoCap systems can be considered a measurement chain consisting of an interface (i.e.., IR cameras and/or video-cameras), sensors (markers), a signal processor (for the control of IR lights and light collection) and a computer (host pc with specific software) [7]. The processor can be embedded into the Host-PC (e.g., Oqus 7+ by QUALISYS®) or can be a remote device supplied by the vendor to be connected to a Host-PC (e.g., SMART-DX 100 by BTS Bioengineering®).

These MoCap systems utilize data captured from image sensors of cameras to triangulate the 3D position of a subject between two or more cameras calibrated to provide overlapping projections [8].

In order to obtain the tridimensional coordinates (x, y and z axis) of each marker apposed on the subject the following steps are mandatory: i) marker identification from each camera, ii) the post-processing of data collected from each camera sensor (i.e., camera sensor distortion correction), iii) stereophotogrammetric merge of data collected.

The identification and the tracking of markers are based on i) the recording of the light reflected back by markers illuminated by light sources (infrared light, IR), whose direction of emission is coaxial to cameras in the case of passive markers, and ii) the light emitted by the active markers. The camera's threshold can be adjusted in all the MoCap so only the bright reflective markers will be sampled, ignoring skin and fabric. Special cables allow the image sending by coded information from each camera to the the MoCap processor. The processor has: *i)* to process each camera image for all the camera synchronized during the time and *ii)* to recognize the shape by using a proper algorithm to identify markers. Algorithms are widely reviewed in [9].

Generally, the markers position collection is based on the estimation of the centroid. The grayscale value of each pixel can be used to provide sub-pixel accuracy by finding the centroid of the Gaussian [9].

After marker identification, the centroid of marker on the camera sensor is calculated. Therefore, trajectories of markers reconstructed. At this point, marker coordinates are sent to the processor host-pc that provide to transfer distorted camera coordinates into the undistorted world coordinates: this is possible by the primary calibration of the system that provides a calibration matrix per each camera [4]. An object with markers attached at known positions (differently from vendors to vendors) is used to calibrate the cameras and obtain their positions and the lens distortion of each camera is measured. If two calibrated cameras see a marker, a three-dimensional fix can be obtained.

Camera calibration

The triangulation is the process of determining a point in 3D space given into two or more projections and it is the basis process of the marker-based MoCap systems. Camera parameters include intrinsics, extrinsics, and distortion coefficients. To estimate the camera parameters, you need to have 3-D world points and their corresponding 2-D image points. You can get these correspondences using multiple images of a calibration pattern, such as a wand with fixed markers.

The most common calibration algorithms use the camera model which include i) the pinhole camera model and ii) lens distortion.

The pinhole camera model does not account for lens distortion because an ideal pinhole camera does not have a lens. To accurately represent a real camera, the full camera model used by the algorithm includes the radial and tangential lens distortion.

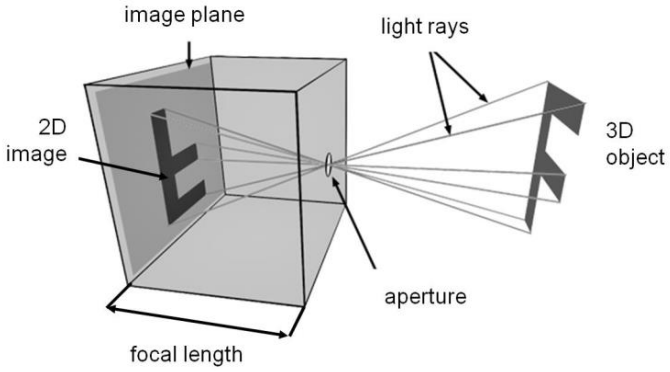

Figure 1.1. Pin hole camera model

A pinhole camera is a simple camera without a lens and with a single small aperture (Figure 1.1). Light rays pass through the aperture and project an inverted image on the opposite side of the

camera. Think of the virtual image plane as being in front of the camera and containing the upright image of the scene.

The pinhole camera parameters are represented in a 4-by-3 matrix called the *camera matrix* (see (1)). This matrix maps the 3-D world scene into the image plane. The calibration algorithm calculates the camera matrix using the extrinsic and intrinsic parameters. The extrinsic parameters represent the location of the camera in the 3-D scene. The intrinsic parameters represent the optical center and focal length of the camera.

$$W[x\ y\ 1] = [X\ Y\ Z\ 1]P \qquad (1)$$

where W is the scale factor, [x y 1] the image points, [X Y Z 1] the real tridimensional world point and P the camera matrix which can be expressed as in (2):

$$P = K\ (2)\ \begin{matrix} R \\ t \end{matrix}$$

where R and t are the rotational and translational contribution, respectively and K is the intrinsic matrix. The world points are transformed to camera coordinates using the extrinsics parameters. The camera coordinates are mapped into the image plane using the intrinsics parameters.

The calibration algorithm calculates the camera matrix using the extrinsic and intrinsic parameters. The extrinsic parameters represent a rigid transformation from 3-D world coordinate system to the 3-D camera's coordinate system. The intrinsic parameters represent a projective

transformation from the 3-D camera's coordinates into the 2-D image coordinates (scheme in Figure 1.2).

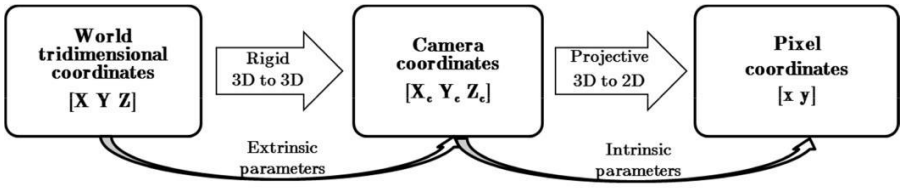

Figure 1.2. Camera calibration flowchart

The extrinsic parameters consist of a rotation, R, and a translation, t. The origin of the camera's coordinate system is at its optical center and its x- and y-axis define the image plane. The intrinsic parameters include the focal length (f_x, f_y), the optical center (c_x, c_y), also known as the principal point, and the skew coefficient (s) which is non-zero if the image axes are not perpendicular. The camera intrinsic matrix, K, is defined as in (3):

$$K = \begin{matrix} f_x & 0 & 0 \\ s & f_y & 0 \\ c_x & c_y & 1 \end{matrix} \qquad (3)$$

where skew coefficient and focal length are calculated as in (4):

$$s = f_y \tan\alpha$$
$$f_x = F\, p_x \qquad (4)$$
$$f_y = F\, p_y$$

and p_x and p_y the size of the pixel in world units. The camera matrix does not account for lens distortion because an ideal pinhole camera does not have a lens. To accurately represent a real camera, the camera model includes the radial and tangential lens distortion.

Radial distortion occurs when light rays bend more near the edges of a lens than they do at its optical center. The smaller the lens, the greater the distortion. The radial distortion coefficients model this type of distortion. The distorted points are denoted as ($x_{distorted}$, $y_{distorted}$):

$$\begin{aligned} x_{distorted} &= x \cdot (1 + k_1 \cdot r^2 + k_2 \cdot r^4 + k_3 \cdot r^6) \\ y_{distorted} &= y \cdot (1 + k_1 \cdot r^2 + k_2 \cdot r^4 + k_3 \cdot r^6) \end{aligned} \quad (5)$$

where x, y are the undistorted pixel locations. x and y are in normalized image coordinates. Normalized image coordinates are calculated from pixel coordinates by translating to the optical center and dividing by the focal length in pixels. Thus, x and y are dimensionless. Moreover, k_1, k_2, k_3 are the radial distortion coefficients of the lens and r^2 is x^2+y^2. Typically, two coefficients are sufficient for calibration. Exclusively in the case of severe distortion, such as in wide-angle lenses, 3 coefficients have to be used included the k_3.

Tangential distortion occurs when the lens and the image plane are not parallel. The tangential distortion coefficients model this type of distortion. The distorted points are denoted as ($x_{distorted}$, $y_{distorted}$) as in (6):

$$\begin{aligned} x_{distorted} &= x + [2 \cdot p_1 \cdot x \cdot y + p_2 \cdot (r^2 + 2 \cdot x^2)] \\ y_{distorted} &= y + [p_1 \cdot (r^2 + 2 \cdot y^2) + 2 \cdot p_2 \cdot x \cdot y] \end{aligned} \quad (6)$$

$$\cdot (r^2 \qquad 2 \cdot p$$

1

being *x*, *y* the undistorted pixel locations. *x* and *y* are in normalized image coordinates. Normalized image coordinates are calculated from pixel coordinates by translating to the optical center and dividing by the focal length in pixels. Thus, *x* and *y* are dimensionless. Moreover, p_1 and p_2 are the tangential distortion coefficients of the lens and r^2 is x^2+y^2. These principals are equal both in the case of active and passive markers used during the data collection.

Passive markers

Passive markers are markers coated with a thin-film of reflective material to reflect the light that is generated from the infrared (IR) LEDs coaxial with the camera. A ring or a square of IR emitting LEDs is placed around the lens of each camera composing the system, which gives a short (~2 ms) light flash at the end of each video frame.

These kinds of markers are usually spherical or hemispherical and their size depend on their body placement (Figure 1.3.A), system application [4] and movement amplitude [10]. Differently from active markers, the passive ones do not require any wiring, allow fast movements and are extremely cheap (the cost of 1 marker is around 1 dollar). Moreover, the use of passive markers allows the capture of high numbers of markers and the use of MoCap based on passive markers do not require the subject to wear wires or electronic equipment on the body. In conclusions, they are less impeding than active markers allowing fluent movements to the subject.

Active markers

Active optical MoCap triangulate positions by illuminating one LED at a time very quickly or multiple LEDs with software to identify them by their relative positions (Figure 1.3.B). Rather than reflecting light back that is generated externally by the cameras like in the passive marker based MoCap, the passive markers themselves are powered to emit their own light. The cost of 10 active marker is around 1000/1500 dollars.

Since Inverse Square law provides a quarter of the power at two times the distance, this can increase the distances and volume for capture. This also enables high signal-to-noise ratio, resulting in very low marker jitter and a resulting high measurement resolution (often < 0.1 mm within the calibrated volume). The power to each marker can be provided sequentially in phase with the capture system providing a unique identification of each marker for a given capture frame at a cost to the resultant frame rate. The ability to identify each marker in this manner is useful in realtime applications. The alternative method of identifying markers is to do it algorithmically requiring extra processing of the data. There are also possibilities to find the position by using coloured LED-Markers. In these MoCap systems, each colour is assigned to a specific point of the body.

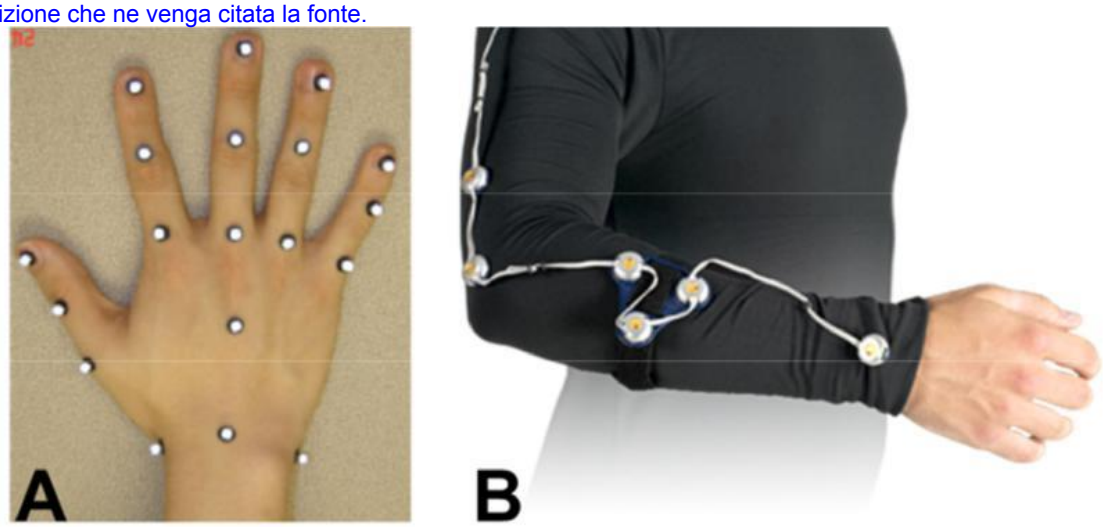

Figure 1.3. A) Passive markers (diameter of 5 mm) placed on the skin of the hand to collect the hand joint kinematics. B) Active markers fixed to a t-shirt to analyse the movement of the upper arm (elbow, shoulder joint kinematics) (Optotrak Smart Marker System, Northern Digital Inc.).

Marker-based MoCap in the investigation of small movements

In applications requiring small movement detection and analysis, the most viable solution implies the use of passive markers for reasons reported in the previous sections. Although the metrological performance of the motion capture system is strictly related to the specific system set-up, it is possible to achieve higher accuracy with a proper cameras choice, marker set and positioning of the cameras. Thus, MoCap can be used in clinical applications requiring the recording of small movement, < 0.2 m, in a workspace lower than the one used in gait analysis, equal to 4 m^3. Some benefits resulting in the use of marker-based MoCap in the study of small displacements can be found in the monitoring of upper arms, face and chest analysis. In particular the higher accuracy of these systems compared to the other non-invasive tools allows investigating fine movements tasks by monitoring the wrist joint and fingers movements (e.g., in musicians [11] and during handwriting [12]). MoCap systems are also employed in the study of fast and spatially complex upper limb movements during a task in several pathologies [13]. In the oral and maxillofacial sciences MoCap systems have been used to study the mandible movements [14] and the tooth displacements under load [15] by the use of a dozen of markers. By extending the focus on the face, MoCap systems allow detecting and quantitatively analyze the facial kinematics [16] in the follow-up of facial functional treatments. Moreover, the possibility of analyze the kinematics of the chest has been also explored by some researchers [17]. MoCap systems used in mechanics of breathing can improve the investigation of chest wall mechanics alterations and the relationships between lung and chest wall, especially in no-collaborative patients (i.e., intensive care patients, newborns) on which spirometry is infeasible. Section 4 will be completely focused on this application. The smaller it the movement to collect, the higher the

accuracy of the system employed in the data collection. Several parameters can affect the data quality.

Data quality

A number of variables strongly influence the accuracy and the precision of the MoCap computation of the 3D coordinates for each marker that we can consider the measurement. As far as it concerns the cameras composing the MoCap, accuracy is influenced by the resolution and the metrological performance of each camera sensor. The higher the resolution of the sensor (Figure 1.4), the smaller detail can be obtained from each marker. The right choice is crucial if the application requires precision in the tracking of small markers, or markers that are close together (e.g., applications in which a high number of markers are required).

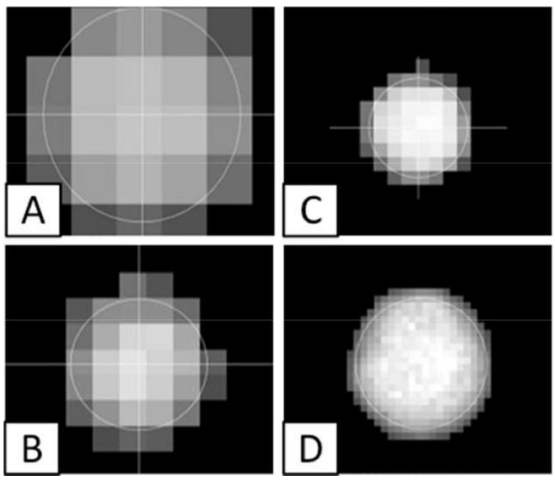

Figure 1.4. Comparison of a 1 MPixel (A) sensor marker view with a 16 MPixel sensor (D). The higher the resolution of the sensor (from A to D), the smaller detail can be obtained from the same marker.

The MoCap camera design represents a trade-off between high-resolution images and fast shutter speeds. A high camera shutter speed is important for those applications involving subjects moving quickly or in a very subtle, nuanced way (i.e., finger movements). Higher resolution cameras are able to better resolve smaller gestures and accommodate larger capture areas, at the expense of shutter speed. Alternatively, faster cameras are able to reduce the amount of blur caused by a fast moving subject, but at the expense of resolving power. Therefore, broader movements tend to require a faster camera, whereas more precise performances, such as face movements and mandibular displacements, require the accuracy of high-resolution cameras.

In Table 1.1, the main features of commercial MoCap systems including the maximum number of camera that can be connected, the system sensor resolution, the acquisition frequency, the declared accuracy as well as vendor's marker diameters are summarized. In the study of small displacements, MoCap systems are equipped with a number of cameras, which depends on the application (i.e., from 2 cameras are enough for tooth movement analysis and finger movements, at least, 6 cameras are required in the study of mechanics of breathing).

Circular, disc-shaped, spherical or semi-spherical, diamonds shaped reflective passive markers are customarily used, depending on the application. Likewise, the marker size depends on the skin localization, application, movement amplitude and distance from cameras. Marker placement, size, and shape are discussed in the next section of this review for each application.

The camera placement in the room is crucial for each application and influences the MoCap's data quality. In the study of small displacements, the area covered by cameras should be central as much as possible to maximize the volume that cameras are able to capture [18]. Tracking a large

number of markers or expanding the capture area is accomplished by the addition of more cameras.

Table 1.1. Features of the most common commercial motion capture systems

Manufacturer	Model	Cameras	Maximum Sensor resolution	Max acquisition frequency [fps]	Acquisition frequency at maximum resolution [fps]	Accuracy	Manufacturer's markers diameters (min-max)
BTS Bioengineering®	SMART-DX 100	up to 4 TvCs	640 x 480 (0.3 Mpixel)	280	140	<0.2mm*	3-20 mm
BTS Bioengineering®	SMART-DX 400	up to 16 TvCs	1366x768 (1 Mpixel)	300	100	<0.3mm**	3-20 mm
BTS Bioengineering®	SMART-DX 700	up to 16 TvCs	1500 x 1000 (1.5 Mpixel)	1000	250	<0.1mm**	3-20 mm
BTS Bioengineering®	SMART-DX 6000	up to 16 TvCs	2048 x 1088 (2.2 Mpixel)	2000	340	<0.1mm**	3-20 mm
BTS Bioengineering®	SMART-DX 7000	up to 16 TvCs	2048 x 2048 (4.0 Mpixel)	2000	500	<0.1mm***	3-20 mm
VICON®	T-Series T160	unlimited	4704 x 3456 16.0 Mpixel	-	120	-	1.5 – 25 mm
VICON®	T-Series T40S	unlimited	2336 x 1728 4.0 Mpixel	-	515	-	1.5 – 25 mm
VICON®	T-Series T20S	unlimited	1600 x 1280 2.0 Mpixel	-	690	-	1.5 – 25 mm
VICON®	T-Series T10S	unlimited	1120 x 887 1.0 Mpixel	-	1000	-	1.5 – 25 mm
VICON®	Bonita B10	unlimited	1366 x 768 1.0 Mpixel	-	250	-	1.5 – 25 mm
VICON®	Bonita B3	unlimited	640 x 480 0.3 Mpixel	-	250	-	1.5 – 25 mm
QUALISYS®	Oqus 1	unlimited	640 × 480 0.3 Mpixel	N/A§	250	-	2.5 – 50 mm
QUALISYS®	Oqus 3+	unlimited	1280 × 1024 1.3 Mpixel	1750§	500	-	2.5 – 50 mm
QUALISYS®	Oqus 5+	unlimited	2048 × 2048 4 Mpixel	360§	180	-	2.5 – 50 mm

Manufacturer	Model	Cameras	Maximum Sensor resolution	Max acquisition frequency [fps]	Acquisition frequency at maximum resolution [fps]	Accuracy	Manufacturer's markers diameters (min-max)
QUALISYS®	Oqus 7+	unlimited	4096 × 3072 12 Mpixel	1100§	300	-	2.5 – 50 mm
QUALISYS®	Pro Reflex	up to 7 TvCs, max 20 markers	640 x 480 0.3Mpixel	100 (4 cameras) 50 (2 cameras)	100	<0.02 mm****	n.d.
QUALYSIS®	MacReflex	up to 6 TvCs , max 50 markers	640 x 480 0.3Mpixel	50	50	1:30000 camera's field of view	n.d.
MOTION ANALYSIS®	Osprey Digital RealTime System	unlimited	640 x 480 0.3Mpixel	245	245	-	4 – 37.5 mm
MOTION ANALYSIS®	Kestrel Digital RealTime System	unlimited	2048 × 1088 2.2 Mpixel	600	300	-	4 – 37.5 mm
MOTION ANALYSIS®	Raptor-H	unlimited	640 × 480 0.3Mpixel	250	250	-	4 – 37.5 mm
MOTION ANALYSIS®	Raptor-E	unlimited	1280 × 1024 1.3 Mpixel	up to 10.000	500	-	4 –37.5 mm
MOTION ANALYSIS®	Raptor-4	unlimited	2352 × 1728 4.06 Mpixel	up to 10.000	200	-	4 - 37.5 mm
MOTION ANALYSIS®	Raptor-12HS	unlimited	4096 × 3072 12.5 Mpixel	300	300	-	4 - 37.5 mm
OPTITRACK®	Prime 41	96+	2048 × 2048 4.1 Mpixel	180	180	-	6.4 – 19 mm
OPTITRACK®	Prime 17W	96+	1664 × 1088 1.7 Mpixel	360	360	-	6.4 – 19 mm
OPTITRACK®	Prime 13	96+	1280 × 1024 1.3 Mpixel	240	240	-	6.4 – 19 mm

Manufacturer	Model	Cameras	Maximum Sensor resolution	Max acquisition frequency [fps]	Acquisition frequency at maximum resolution [fps]	Accuracy	Manufacturer's markers diameters (min-max)
OPTITRACK®	Prime 13W	96+	1280 × 1024 1.3 Mpixel	240	240	-	6.4 – 19 mm
OPTITRACK®	Slim 13E	96+	1280 × 1024 1.3 Mpixel	240	240	-	6.4 – 19 mm
OPTITRACK®	Flex 13	24	1280 × 1024 1.3 Mpixel	120	120	-	6.4 – 19 mm
OPTITRACK®	Flex 3	24	640 × 480 0.3 Mpixel	100	100	<0.6 mm [1]	6.4 – 19 mm

* on a volume 2×2×2m

** on a volume 4×3×3m

*** on a volume 6×6×3m

§ High-speed mode (full field of view)

**** on a volume 45×45×50 cm

[1] Kertis, Jeffrey D., "Biomechanical Evaluation of an Optical System for Quantitative Human Motion Analysis" (2012). Master's Theses (2009 -). Paper 166.

The simulation in Figure 1.5 shows how the tracking volume (i.e., the volume visible in at least 2 cameras), the volume rated as "good" (i.e., the volume visible in 3 or more cameras) and the volume rated as "excellent" (i.e., the volume visible in 4 or more cameras) grow up with the increase of number of cameras.

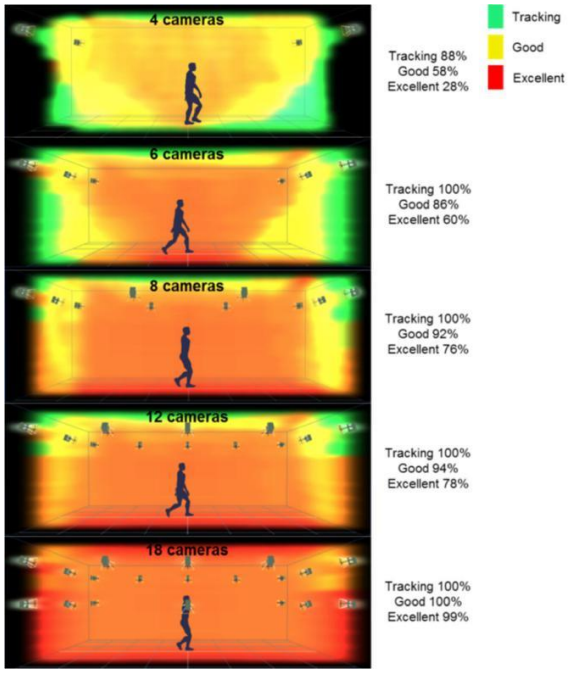

Figure 1.5. The higher the number of cameras in the room, the higher the coverage and the bigger the volume for data collection. These simulations were performed with the Vicon software chosing a 8 m x 5 m x 3 m room size and V8 Vantage cameras (8 Mpixels sensors, 12.5 mm lens, at 260 frame rate and a field of view of 62 x 47).

Unlike gait analysis in which good results are obtained by placing cameras above the maximum height of the entire marker set, for recording small movement different approaches should be take into account. If the MoCap is used to investigate the biomechanics of chest wall, the cameras

should be placed around the subject (circular perimeter) and at the same level of the chest wall to record it from all directions [19]. Differently, for mandibular movement and facial expression studies, the head of the patient need to stay in front of cameras placed at the same level of mouth and the number of cameras can be lower than other applications. The placement of cameras on adjustable tripods usually ensures good visibility, avoids possible problems caused by having strobes in the field of view and ensures good flexibility of the entire OS in recording small movements.

Metrological investigations of MoCap systems

Although MoCap systems born for the gait analysis and have been used in this field only for many years, today their range of application is moving more and more in the investigation of smaller displacements (eg, dental implants, facial motion analysis, trunk analysis, and so on.

In general, performance of optoelectronic motion systems heavily depends on the system's setup and the so-called boundary operational conditions, as markers size, use of property markers, use of focal lens on camera, digital conversion of the signal, the configuration of the rooms, the rigorous calibration procedure, and so on [20].

In this section our aim is to analyze the scientific literature about the precision and accuracy of marker-based MoCap for both small displacement and small calibrated volume. We will try to summarize the main potential sources of inaccuracy that affect measurements during the human movement analysis for respiratory chest wall mechanics.

Instrumental errors

The non-invasive measurement of markers in 3D space requires an analysis of non-stationary markers over time, even under static conditions, in order to determine the causes of the measurement system errors [21]. This implies a system estimate of the instantaneous position and orientation of each marker, and then the resulting estimate of musculoskeletal segment. In this field movements observed by the system can be attribute to two different type of movements [22]:

- due to systemic and random system error;
- due to human movement artifacts (i.e., related to the layer of fat).

In this discussion, we will focus on the analysis of the first kind of movements. This movements are the result of the measurement system error, depend on the inherent accuracy of the system, on its technology and its architecture. Such errors also may be defined as cumulative, referring to the error propagation from one to a plurality of markers.

It is well known that this kind of error is strongly dropped down by a correct and good calibration procedure of the system, as well as thanks to an appropriate setting of the discrimination threshold of the system and by a fitting use of tools for filtering and smoothing. The system performance of the system, metrological namely accuracy and precision, may still change due to a large number of factors as:

- system appropriateness, in terms of technical suitability and quality;
- movement analysis system setup:
  - number of cameras used
  - cameras placement in the laboratory
- size of the measurement volume (or workspace)
- size and shape of the calibration object used in the calibration procedure

- attention paid to calibration procedure.

Metrological tests and procedures on MoCap systems

Producers usually report that markers reconstructions precision, within a well-defined range of measurement, is about 1:3000 the calibrated volume diagonal. The accuracies reported by Shortis [23] in a series of morpho-metric studies ranged from 1:5000 with 4 cameras up to 1:15000 using 36 cameras. Schmid in [24] analyzed the achievable accuracy in displacement measurements within commercially available optoelectronic systems for movement analysis. The achievable accuracy of distance measurements in 2001's commercially available motion measurement systems usually ranged from about 0.09% to 1.77% and higher. Accuracy of 0.0373% was determined with the new calibration technique [24]. The 95% confidence interval ranged at +/- 0.023 mm, the RMS error at 0.188 mm.

The above mentioned values [23], [24] are widely acceptable in a system used for human movement analysis. However, the quality of the measurements could be further improved by performing precision and accuracy evaluations during laboratory routines.

Since producers provide general information, the system-in-use metrological characteristic evaluation can be directly performed by the investigator before starting the experimental session through the use of spot-checks, i.e. tests that the user may perform easily for verification of the preservation of the MoCap performance [21]. Several of such tests have been proposed in the literature, based on different target measurements.

In practice, the following metrological measurements can be carried out:

1. The measurements of inter-marker distance;

2. The measurement of a single-marker or of set-of-marker displacements compared to a defined initial position.

Inter-marker distance

Several studies have been conducted in order to evaluate the preservation of the relative distance between markers within the measurement volume of the system. These tests are considered a good indicator of the calibration maintenance.

A usual method for estimating the instrumental error consists in recording a rigid support on which are placed at least two markers at known distance, both in the static and in the dynamic conditions.

The inter-marker distance can be estimated for each recording frame in order to evaluate the MoCap system systematic and random errors relative to the reference measurement [21], [24].

An example of inter-marker test is the pendulum test [25] where a rigid pendular object is a base for two markers in known positions, and allows to evaluate the optoelectronic system performance, both at the end and at the center of the calibrated volume. Another example is the Full Volume Test, where a stiff rod mounts two spherical markers fixed at each end. The vertical axis of the rod is aligned approximately with the vertical axis of the laboratory frame and then moved parallel to each axis, throughout the entire measurement volume, while the speed of the rod movement is kept steady [25]. An evolution test dates back to 2000 and it is represented by the MAL test [21], where a rigid bar is a base for the two markers and ball point; a target is set to a known position with respect to these two markers, coinciding with the tip of the rod. This is placed in a fixed point on the floor. Acquisitions are made while the rod is kept stationary (static test), and while the rod is made rotating around the target point by moving the other end along a

pseudo-circular trajectory. The maneuver is performed manually at a speed approximating the physical exercise under analysis [21].

In the past, thanks to these spot-checks, several authors have conducted their studies in order to determine the performance of several commercially available systems for human movement analysis (Table 1.2).

Table 1.2. Metrological results on different motion analysis systems on the market. Abbreviation: MAE = % Mean Absolute Error, NA = not available data. * 2 cameras adopted, ** 4 cameras adopted, *** 6 cameras adopted, NA no information on cameras.

Model		Sample rate [Hz]	MAE [mm]	Std Dev [mm]	Absolute Max Error [%]
Peak 5 NA	[26]	60 - 2000	0.6	4.2	14.2
Ariel NA	[26]	60 - 400	0.7	6	26.3
Vicon NA	[26]	50 - 200	0.3	1.2	4.9
Elite System NA	[26]	50 - 100	0.4	0.9	5.6
Kinemetrix NA	[26]	50 - 200	0.4	3.8	12.1
Ariel Apas*	[27]	60	1.3	5.4	2.7
Dynas 3D*	[27]	60	2	0.2	5.7
Elite Plus**	[27]	50	0.1	0.3	0.1
Expert Vision**	[27]	60	0.1	0.53	1
Peak 5*	[27]	60	0.4	2	1.2
Primas*	[27]	100	0.3	0.14	0.7
Vicon 140**	[27]	60	0.1	1.82	0.7
Vicon 370***	[27]	60	0.8	0.4	1
Video Locus*	[27]	60	0.4	1.5	0.8
ND**	[28]	60	0.2	0.1	0.1
Motion Analysis*	[29]	60	NA	1.4 - 3.0	NA

Table 1.2 summarizes the results obtained in several studies, only including those conducted exclusively through passive reflective markers and dynamic test.

In Klein et al. [30], determined limits of accuracy and consistency of linear and angular measures were obtained by using the Ariel Performance Analysis System, and a meter and an universal 360° goniometer as reference. They used a rectangular volume of 2.0 m wide x 0.7 m deep x 1.3 m high, and two different camera placements (3.8 m apart, 3.8 m from the data acquisition region, and 1.75 m high; 3 m apart, 3 m from the data acquisition region, and 1.75 m high). The accuracy of the Ariel System was investigated by examining 12 marker coordinates located on the calibration frame. Average mean error for linear displacement was around 3.5 mm for a length of 500 mm and average mean angular error was 0.26° (measurement range was from 10° to 170°).

Vander Linden et al. [29] investigated the accuracy and reproducibility of angle measurements obtained by using the Motion Analysis video system, under static and dynamic conditions. Reflective markers placed on a goniometer were recorded by two video cameras at 17 angles, from 20 to 180 degrees, in 10-degree increments, in a calibrated volume of 1.6 m x 0.72 m x 1.27 m. Cameras were positioned at 180 cm from calibration cube. Average within-trial variability was less than 0.4°; the within-trial variability ranged from 1.39 to 3.04 mm for the inter-marker distance.

In another study [31] two markers are placed on rotating plate at both 90 mm and 500 mm each other and their distance has been measured by 7 motion analysis systems. Results indicated that 5 of 7 marker-based MoCaps produced less than 2.0 mm RMS errors in dynamic condition and 1.0 mm RMS error when measuring the stationary marker. Also the research group showed that all the MoCap confused marker identifications when markers moved within 2 mm of each other.

This result can be very important as design limitation in the development of various applications for the movement analysis systems. This result also represents a limit for the applications in which the number of markers is high (i.e., tracking of the chest wall kinematics).

In 2008 Windolf et al. proposed a robotic device with a two-fold purpose: evaluating the performance of Vicon-460 MoCap system and achieving a dynamic and repeatable calibration in order to obtain precision and accuracy of the system in a working volume of 180 x 180 x 150 mm^3. The researchers focused their attention on camera setup, calibration volume, marker size and application of lens filters. Equipped with four cameras, the MoCap system provided an overall accuracy of 63 μm and a overall precision of 15 μm for the most favorable parameter setting. Arbitrary changes in camera arrangement revealed variations in mean accuracy between 76 and 129 μm.

The research group also performed measurements including regions unaffected by the dynamic calibration where a considerably lower accuracy (221 ± 79 μm) was found.

Single-marker or set-of-marker displacements compared to a defined initial position

In the literature there are also protocols based on metrological analysis with a single marker and motorized systems to support that analysis, based on each instant knowledge of the marker's trajectory or the object on which the marker is placed. This kind of test allows the knowledge of the trajectories that are expected for the moving object and they are very useful to assess the accuracy of optoelectronic system in general. An example of using this kind of metrological assessment is the study of Thornton et al. [32] that assessed the accuracy of the Kinemetrix motion analysis system to measure horizontal movement by a single reflective marker, within

nine different camera arrangement. The marker was moved a known horizontal distance along a line bisecting the horizontal angular separation of the two cameras. At the smallest camera separation tested (15° and 0° horizontal and vertical separation, respectively), the opto-electronic system showed to be unable to calculate the 3D marker position.

Also Cappello et al. [33] used a rotating disk with an embedded marker as a mechanical tremor simulator to test the ability of the 3D analysis system to track marker trajectories also in a small calibrated volume. They observed deviations from the expected circular path mainly due to the flickering effect. Data analysis showed a standard error of 0.5 - 0.8 mm along the x and y axes and about 2 mm along the z axis, in agreement with the values declared by the manufacturer. This result [33] allowed a breakthrough for 3D movement analysis systems that proved robust assessments of movements for high frequencies and for very small movements.

In another Evaert study [28], video motion analysis system accuracy and precision has been measured by observing marker's motion in fixed position by 3D video motion analysis system specifically configured for measuring small and slow displacements within a small measurement volume (0.7 m x 0.5 m x 0.3 m), using 4 cameras. Displacements have been measured by manually sliding device with two markers applied; trials have been conducted in three different directions and in three different positions. Mean error found was 0.034 mm and mean absolute error was 0.094 mm ($p < 0.05$). Thanks to these results the motion analysis configured for registration within small volumes might be used for other clinical applications than gait analysis.

Tests and results reported until now are related to a generically motion analysis system, in terms of small calibration volumes and linear displacement less than 1 m. In literature there are also other kinds of work oriented to particular applications of the MoCap systems. Some clinical

applications have needed to measure surface and volume of human body. Therefore, optoelectronic systems performance must be evaluated also for these particular measurements.

Paul et al. [34] studied the reliability, stability, validity and precision of a stereophotogrammetry system (3dMDtorso) for quantifying the complex three-dimensional structure of the human torso, by using a human-form mannequin and different geometric solids, without markers. Surfaces and volumes of these ones were measured both by system and through mathematical equations, starting from linear measurements by caliper (accuracy of ±0.5 mm). Results show strong correlation ($R^2 > 0.993$) between caliper and optoelectronic system volume measurements. The percentage accuracy decreases exponentially by increasing geometric solid volumes (from 0.1 to 270 mL). Therefore, the system accuracy of volume measurement has been assessed for clinical applications, but only static trials have been carried out. By means of the mannequin, the group demonstrated that a 5% error in surface area calculations may occur in objects smaller than $23.5cm^2$ and also that, in volume measurement, a 5% error may occur in volumes less than 32mL. Our search in volume calculations into the literature revealed very few studies with marker-less approach as Paul et al. study [35], [36] and the sole [34] which have analyzed reliability or precision for surface area measurements.

Only two works [37], [38] aim to characterize the metrological system of optoelectronic plethysmography, motion analysis system specifically design and used for the analysis of ventilatory mechanics and compartmental analysis of breathing, both in supine and prone position. The purpose of these works was to assess the reliability, accuracy and precision of the MoCap used in the volume calculations, both in static and dynamic conditions.

In the first paper dated 2010, Bastianini et al. [37] have been realized a system using a DC-precision actuator and a single spherical marker fixed at the end of the motor shaft, in order to

evaluate the discrimination threshold of the system and optoelectronic plethysmography to measure the accuracy in small linear displacements. The study analyzed three different configurations of cameras (2, 4, 6) in a same workspace calibrated and two different types of markers (spherical 6 and 12 mm diameter). These tests have allowed to determine the discrimination threshold of the OEP in 30 microns.

Furthermore, it is seen how the increase in the number of cameras increases the accuracy of the system for marker of smaller diameter.

In another further study Bastianini et al. [38] investigate the MoCap accuracy on tidal volume and found that it does not depend on thorax displacement's magnitudes and it ranges from 9% to 20%. Accuracy was also well represented by a logarithmic regression (from 20% to 4%), whose trend decreases with the increase of geometric solid volumes (from 0.1 to 270 mL).

References

[1] G. Ferrigno, N. A. Borghese, and A. Pedotti, "Pattern recognition in 3D automatic human motion analysis," *ISPRS J. Photogramm. Remote Sens.*, vol. 45, no. 4, pp. 227–246, Aug. 1990.

[2] G. Ferrigno and A. Pedotti, "ELITE: a digital dedicated hardware system for movement analysis via real-time TV signal processing.," *IEEE Trans. Biomed. Eng.*, vol. 32, no. 11, pp. 943–50, Nov. 1985.

[3] P. Allard, J. P. Blanchi, and R. Aissaoui, "Bases of three-dimensional reconstruction," in *P. Allard, I. A. F. Stokes & J. P. Blanchi (Eds.), Three-dimensional analysis of human movement*, 1995, pp. 19–40.

[4] A. Leardini, L. Chiari, U. Della Croce, and A. Cappozzo, "Human movement analysis using stereophotogrammetry. Part 3. Soft tissue artifact assessment and compensation.," *Gait Posture*, vol. 21, no. 2, pp. 212–25, Feb. 2005.

[5] L. Turner-Stokes and K. Reid, "Three-dimensional motion analysis of upper limb movement in the bowing arm of string-playing musicians.," *Clin. Biomech. (Bristol, Avon)*, vol. 14, no. 6, pp. 426–33, Jul. 1999.

[6] Y. Gilboa, N. Josman, A. Fattal-Valevski, H. Toledano-Alhadef, and S. Rosenblum, "The handwriting performance of children with NF1.," *Res Dev. Disabil., vol. 31, no. 4, pp. 929–35, 2010.*

[7] T.W. Lu, C.F. Chang "Biomechanics of human movement and its clinical applications", *Kaohsiung J Med Sci.*, vol. 28, suppl. 2, S13–25, 2012.

[8] W. L. O. Kam and B. G. Ferguson, "Broadband passive acoustic technique for target motion parameter estimation," *IEEE Trans. Aerosp. Electron. Syst.*, vol. 36, no. 1, pp. 163–175, 2000.

[9] K. J. O'Donovan, R. Kamnik, D. T. O'Keeffe, and G. M. Lyons, "An inertial and magnetic sensor based technique for joint angle measurement," *J. Biomech.*, vol. 40, no. 12, pp. 2604–2611, 2007.

[10] W. Tao, T. Liu, R. Zheng, and H. Feng, "Gait analysis using wearable sensors," *Sensors*, vol. 12, no. 2. pp. 2255–2283, 2012.

[11] L. Turner-Stokes, K. Reid "Three-dimensional motion analysis of upper limb movement in the bowing arm of string-playing musicians", *Clin Biomech (Bristol)*, 1999 Jul;14(6):426-33.

[12] D.N. Fernandes, T. Chau "Fractal dimensions of pacing and grip force in drawing and handwriting production", *J Biomech*, 2008;41(1):40-6.

[13] E. E. Butler, A. L. Ladd, S. a Louie, L. E. Lamont, W. Wong, and J. Rose, "Three-dimensional kinematics of the upper limb during a Reach and Grasp Cycle for children.," *Gait Posture*, vol. 32, no. 1, pp. 72–7, May 2010.

[14] P. O. Eriksson, B. Häggman-Henrikson, E. Nordh, and H. Zafar, "Co-ordinated mandibular and head-neck movements during rhythmic jaw activities in man.," *J. Dent. Res.*, vol. 79, no. 6, pp. 1378–84, Jun. 2000.

[15] H. Liu, C. A. Holt, and S. L. Evans, "Measuring tooth movement in 3D: Resolution, accuracy and reliability of the optical motion capture system.," pp. 14–17, 2006.

[16] C. Sforza, A. Frigerio, A. Mapelli, F. Mandelli, F. V. Sidequersky, V. Colombo, V. F. Ferrario, and F. Biglioli, "Facial movement before and after masseteric-facial nerves

anastomosis: a three-dimensional optoelectronic pilot study.," *J. Craniomaxillofac. Surg.*, vol. 40, no. 5, pp. 473–479, Jul. 2012.

[17] P. A. Aliverti A, Dellaca R, "Optoelectronic plethysmography: a new tool in respiratory medicine," *Recenti Prog. Med.*, vol. 92, no. 11, pp. 644–647, 2001.

[18] S. Fleishman, D. Cohen-Or, and D. Lischinski, "Automatic camera placement for image-based modeling," *Comput. Graph. Forum*, vol. 19, no. 2, pp. 101–110, 2000.

[19] C. Massaroni, E. Schena, P. Saccomandi, M. Morrone, S. Sterzi, and S. Silvestri, "Evaluation of optoelectronic plethysmography accuracy and precision in recording displacements during quiet breathing simulation," in *37th Annual International Conference of the IEEE Engineering in Medicine and Biology Society.*, 2015, pp. 1291–1294.

[20] E. Furnée and Œ. Jobbágy, "Precision 3-D motion analysis system for real-time applications," *Microprocess. Microsyst.*, vol. 17, no. 4, pp. 223–231, 1993.

[21] U. Della Croce and A. Cappozzo, "A spot check for estimating stereophotogrammetric errors.," *Med. Biol. Eng. Comput.*, vol. 38, pp. 260– 266, 2000.

[22] A. Cappozzo, A. Cappello, U. D. Croce, and F. Pensalfini, "Surface-maker cluster design criteria for 3-D bone movement reconstruction," *IEEE Trans. Biomed. Eng.*, vol. 44, no. 12, pp. 1165–1174, 1997.

[23] M. Shortis, "Precision evaluations of digital imagery for close-range photogrammetric applications.," PHOTOGRAMM. ENG. Remote SENS., 1988.

[24] O. A. Schmid, "A New Calibration Method for 3-D Position Measurement in Biomedical Applications - Ein neues Kalibrierverfahren zur dreidimensionalen Positionsbestimmung für biomedizinische Anwendungen," *Biomed. Tech. Eng.*, vol. 46, no. 3, pp. 50–54, 2001.

[25] A. Cappozzo, U. Della Croce, F. Catani, A. Leardini, S. Fioretti, and M. Maurizi, "Stereometric system accuracy tests," in *Measurement and data processing methodology in clinical movement analysis-preliminary. CAMARC II Internal Report*, 1993.

[26] Y. Ehara, H. Fujimoto, S. Miyazaki, S. Tanaka, and S. Yamamoto, "Comparison of the performance of 3D camera systems," *Gait Posture*, vol. 3, no. 3, pp. 166–169, Sep. 1995.

[27] Y. Ehara, H. Fujimoto, S. Miyazaki, M. Mochimaru, S. Tanaka, and S. Yamamoto, "Comparison of the performance of 3D camera systems II," *Gait Posture*, vol. 5, no. 3, pp. 251–255, 1997.

[28] D. G. Everaert, A. J. Spaepen, M. J. Wouters, K. H. Stappaerts, and R. A. B. Oostendorp, "Measuring small linear displacements with a three-dimensional video motion analysis system: Determining its accuracy and precision," *Arch. Phys. Med. Rehabil.*, vol. 80, no. 9, pp. 1082–1089, 1999.

[29] D. W. Vander Linden, S. J. Carlson, and R. L. Hubbard, "Reproducibility and accuracy of angle measurements obtained under static conditions with the Motion Analysis video system.," *Phys. Ther.*, vol. 72, no. 4, pp. 300–5, 1992.

[30] P. J. Klein and J. J. DeHaven, "Accuracy of three-dimensional linear and angular estimates obtained with the ariel performance analysis system," *Arch. Phys. Med. Rehabil.*, vol. 76, no. 2, pp. 183–189, 1995.

[31] J. G. Richards, "The measurement of human motion: A comparison of commercially available systems," *Hum. Mov. Sci.*, vol. 18, no. 5, pp. 589– 602, 1999.

[32] M. J. Thornton, M. C. Morrissey, and F. J. Coutts, "Some effects of camera placement on the accuracy of the Kinemetrix three-dimensional motion analysis system," *Clin. Biomech.*, vol. 13, no. 6, pp. 452–454, 1998.

[33] A. Cappello, A. Leardini, M. G. Benedetti, R. Liguori, and A. Bertani, "Application of stereophotogrammetry to total body three-dimensional analysis of human tremor," *IEEE Trans. Rehabil. Eng.*, vol. 5, no. 4, pp. 388–393, 1997.

[34] S. M. Paul, A. P. Chamberlin, C. Hatt, A. V. Nayak, and J. V. Danoff, "Reliability, validity, and precision of an active stereophotogrammetry system for three-dimensional evaluation of the human torso," *Med. Eng. Phys.*, vol. 31, no. 10, pp. 1337–1342, 2009.

[35] A. Losken, H. Seify, D. D. Denson, A. A. Paredes, and G. W. Carlson, "Validating three-dimensional imaging of the breast.," *Ann. Plast. Surg.*, vol. 54, no. 5, pp. 471-6-8, May 2005.

[36] A. Losken, I. Fishman, D. D. Denson, H. R. Moyer, and G. W. Carlson, "An objective evaluation of breast symmetry and shape differences using 3-dimensional images.," *Ann. Plast. Surg.*, vol. 55, no. 6, pp. 571–5, Dec. 2005.

[37] F. Bastianini, E. Schena, and S. Silvestri, "Accuracy evaluation on linear measurement through opto-electronic plethysmograph," in *2012 Annual International Conference of the IEEE Engineering in Medicine and Biology Society*, 2012, pp. 1–4.

[38] F. Bastianini, E. Schena, P. Saccomandi, and S. Silvestri, "Accuracy evaluation of dynamic volume measurements performed by opto-electronic plethysmograph, by using a pulmonary simulator," *Proc. Annu. Int. Conf. IEEE Eng. Med. Biol. Soc. EMBS*, vol. 2013, pp. 930–933, Jan. 2013.

Chapter II - Chest wall motion analysis

Introduction

In clinical practice and scientific research, the evaluation of chest wall (CW) kinematics during breathing and the assessment of thoraco-abdominal volumes allow an additional perspective on the study of different pathologies and can tailor medical treatment during rehabilitation. From the middle of the 20th century, the scientific community started to study the respiratory system as a model [1–3] and founded its analysis on mechanical models of the different parts composing the system [3–6]. Mead et al. [7–9] published a series of scientific papers in which the possibility of measuring lung volume variations by the measure of thoracic and abdominal wall displacement was described. These studies led to hundreds of studies on respiratory mechanics in the 1980s with works of Mead et al. [10, 11], Hoppin et al. [4], Peslin et al. [6, 12], and others who contributed to the understanding of the respiratory drive and the mechanisms of pulmonary ventilation, and to the determination of how the ventilatory pump acts on respiratory structures.

The real technological breakthrough occurred in 1990 with Pedotti et al. [13, 14], who was the first to use a system based on motion analysis technology that provided the theoretical possibility of measuring and monitoring the movement of a number of points by photo-reflective markers. The ELITE system was the first motion analysis system used for the assessment of non-invasive optoelectronic breathing mechanics [14–16]. Since 2000, a growing number of studies have used optoelectronic plethysmography (OEP) to (a) assess breathing pattern, (b) measure asynchronies in breathing strategies in patients with various pathologies, and (c) investigate the healthy breathing biomechanics.

The following overview is extrapolated from a recent review about the clinical findings and research applications of OEP in the non-invasive assessment of breathing in a population of

healthy and diseased individuals and in a wide age range [17]. In March 2016, a search in 50 Digital Library and Bibliographic Search databases (e.g., SCOPUS®, PubMed® and Google Scholar®) with the terms "opto-electronic plethysmography," "optoelectronic plethysmography," and "optoelectronic plethysmograph" was performed. A total of 220 studies were found overall. After reading the titles and abstracts, those which referred to OEP were included, totalling 156 papers. After reading the full texts of these studies, 14 more studies were found by manual search. Thus, a total of 170 studies on OEP were selected.

OEP is a motion analysis system, which measures the changes of the CW during breathing by modelling the thoraco-abdominal surface. The OEP working principle is based on the general principles of 3D motion capture [18] (Fig. 1). OEP reconstructs the CW surface and then volume by placing a number of markers on the skin (Fig. 1). In a general clinical setting, 6- and 10-mm diameter hemispherical or spherical markers are used [35]. For standing evaluations, commonly an 89-marker protocol is used (as shown in Fig. 1, considered the "full marker" protocol) [19–25]. A 52-marker protocol can be used to assess subjects in the supine position, for example in the monitoring of breathing in intensive care [26–28]. A 24-marker protocol has been used to collect the upper and lower CW movements in the breathing analysis of newborn babies [29,30]. Furthermore, a recent study validated a new 52-marker-based 3-compartment model of the CW to record spontaneous sleeping in infants [31]. A number of infrared (IR) cameras (4 [14,32–34] to 8 [28,35,36]) capture the scene and track a number of IR-reflective markers within a previously

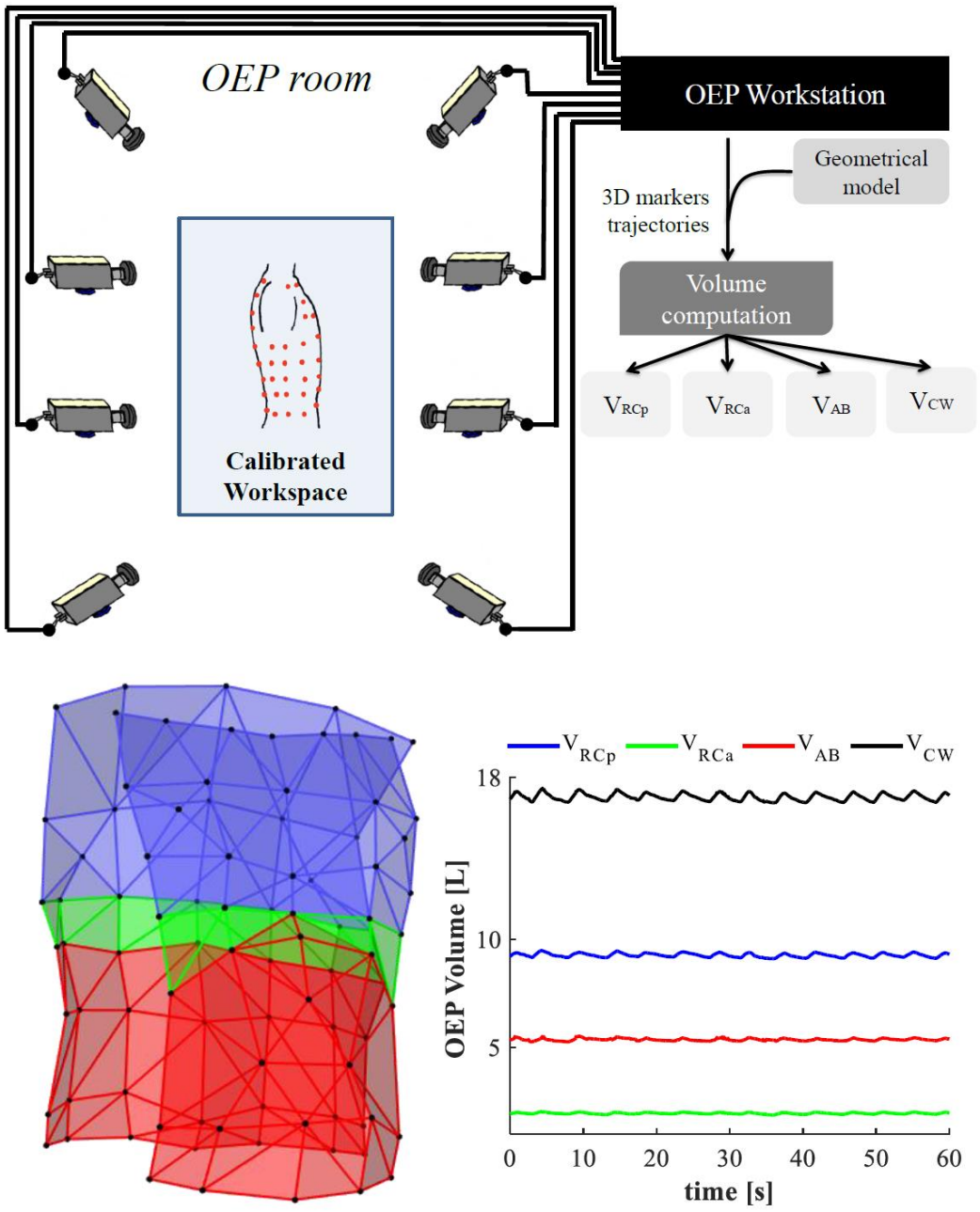

Fig. 1. Schematic of OEP working princi-ple; 3D human chest wall reconstructed starting from 89 markers: blue, green, and red surfaces represent the pulmonary rib cage (RCp), the abdominal rib cage (RCa), and the abdomen (AB), respectively. The rib cage (RC) volume is considered as the sum of RCp and RCa volumes. The plot shows the 3 compartmental volumes and the total chest wall volume during 60 s of OEP data collection in 1 healthy subject.

calibrated volume [37] defining the recording workspace [38]. A dedicated workstation (Fig. 1) synchronizes input and output information to and from cameras; an ad hoc-designed software in the workstation computes the marker 3D trajectories integrating the information collected from each camera.

Then, a geometrical model is applied: a closed surface is defined starting from connecting each triplet of markers to form a triangle. From each closed surface, the volume contained into this surface is calculated. For each triangle – identified by 3 markers – the area (S) and the direction of normal vector ($\vec{n}$) are calculated and from the volume contained in this surface can be calculated using the Gauss theorem [14, 38] as in equation (1):

$$\int_S \vec{F}\ x\ \vec{n} dS = \int_V dV = V,$$

where F is an arbitrary vector, S is a closed surface, V is the volume enclosed by S, and n is the normal unit vector on S.

The OEP CW model can be divided into 3 compartments, composed of the pulmonary rib cage (RCp), the abdominal rib cage (RCa), and the abdomen (AB) as highlighted in Figure 1. The 3-compartment model allows the following phenomena to be considered that (a) RCp and RCa are exposed at different pressures during the inspiration, (b) the diaphragm acts directly only on RCa, and (c) non-diaphragmatic inspiratory muscles act largely on RCp and not on RCa [7]. Regarding the AB, AB volume change is defined as the volume swept by the abdominal wall [7,25,35], and it is the result of the conjunct action of the diaphragm and expiratory abdominal muscles. RCa, and (c) non-diaphragmatic inspiratory muscles act largely on RCp and not on RCa [7]. Regarding the AB, AB volume change is defined as the volume swept by the abdominal wall [7,25,40], and it is the result of the conjunct action of the diaphragm and expiratory abdominal muscles.

Application in clinical settings: What Does OEP Measure?

CW Kinematics

OEP is a reliable tool for the analysis of CW kinematics partitioned into RCp, RCa, and AB, for both the left and right sides (also known as hemithoraxes). Results obtained from the breath-by-breath analysis of compartmental volumes can be further processed to assess if the thoraco-abdominal movement of the CW is synchronous, thus if RC (where RC = RCp + RCa) and AB are moving in phase. When the 2 compartments move in opposite directions, paradoxical movement occurs [41]. Konno and Mead [7] described one of the first models of movement of the CW: in healthy subjects, volume variations of the rib cage must be equal and opposite to volume variations of the AB, and the 2 compartments must move in phase. Several methods were designed in order to describe the synchrony of the thoraco-abdominal movement, also based upon ultrasound [42]. The most commonly used indexes are (a) the phase angle analysis and Lissajous loop evaluation [43–49], (b) the cross-correlation function [50], (c) the paradoxical inspiratory and expiratory time [51], (d) the inspiratory and expiratory phase ratio, and (e) the total phase ratio [51].

Breathing Volumes

The difference between the end-inspiratory volume and the end-expiratory volume is computed for each compartment, obtaining compartmental volumes. For each compartment, OEP gives information about the tidal volume (VT) [52] and end-expiratory and end-inspiratory volume [40,53,54]. OEP can also indirectly compute the following pulmonary volumes: expiratory reserve volume, inspiratory re-serve volume, forced expiratory volume in the first second (FEV1) [55,56], vital capacity (VC), and inspiratory capacity [57].

Breathing Time Assessment

By-breath analysis of compartmental volumes allows study of the respiratory cycle. The following variables are computed in order to analyze the respiratory cycle: inspiratory time (Ti), expiratory time (Te), and total time of the respiratory cycle (Ttot), inspiratory time in relation to the total time (Ti/Ttot), minute ventilation (MV), mean inspiratory flow (VCcw/Ti), and mean expiratory flow (VCCW/ Te) [51].

OEP Performance: Validity, Accuracy, and Reliability

The accuracy of OEP has been assessed in several ways. OEP is typically able to detect linear marker dis-placements higher than 30 μm, which was assessed to be its threshold for detecting linear movement [58]. This results in a volume threshold around 9 mL for typical adults. The effects of number of cameras (i.e., 4, 6, 8) and marker size (i.e., spherical, 6- and 12-mm diameters) on OEP accuracy in linear displacement have been evaluated: in-creasing the number of cameras generally increases OEP accuracy if spherical 6 mm markers are used [58]. On the other hand, OEP accuracy in dynamic volume estimation appears not to be influenced by the magnitude of the thorax's movement [59]. The OEP volume accuracy investigated by a volume calibration device in the range of 0–2.78 L is always better than 6.0% of measured volume. The OEP volume standard deviation for a known volume change delivered via a volume calibration device 10 times was ±2.7 mL, in the range of 0–2.78 L [60].

The validity of OEP in measuring respiratory volume variations was performed by the comparison between VCW changes estimated by OEP, and lung volume variations measured by spirometers and pneumotachometers as gold standard instruments [60]. OEP pemits to conduct a respiratroy breathing analysis with no need of noseclips and in a completely non-invasive manner.

OEP validity has been evaluated in healthy seated and standing subjects with the 89-marker protocol in different experimental situations (e.g., quiet breathing, incremental exercises). The maximum difference between spirometer and OEP measurements was reported to be <4% in all studies. VCW measurements of OEP, spirometry, and pneumotachography are highly correlated, with the mean discrepancy lower than 5%, in constrained postures like supine and prone position in healthy subjects during quiet and deep breathing [62].

Intra-rater and inter-rater reliability of OEP has been evaluated at rest and during submaximal exercise on a cycle ergometer. OEP showed an intra-class correlation coefficient higher than 0.75 and a coefficient of variation always lower than 10% [63].

Breathing Evaluation of Healthy Subjects

In the last decade, OEP has been extensively employed in studies looking at CW kinematics and volume changes in the 3 CW compartments in healthy subjects in relation to age, gender, weight, posture, and different physiological conditions, such as coughing and laughing. In pre-term and term infants, OEP has been demonstrated as a good tool to assess lung volume and compartmental changes and relative compartmental distribution [29]. The main advantage of this technology is that subject collaboration is not necessary. Typically, an easier marker protocol (24 markers on the anterior thoraco-abdominal surface) is used for such analysis. The non-invasive bedside evaluation of the respiratory status with OEP is especially useful in critically ill neonates to assess dis-ease severity and the response to pharmacological interventions [64] as well as to guide mechanical respiratory support (e.g., high-frequency oscillatory ventilation) [65].

In adulthood, OEP has been applied to study for the first time how the influence of posture and age can affect breathing variables (e.g., volumes, compartmental contribution to the VT, breathing frequency). Aliverti et al. [16] demonstrated that during quiet breathing, the RCa volume changes are higher in the prone position; and AB volume changes have the opposite behaviour; they are decreased when subjects lay down. Volume data collected during deep breathing in healthy adults demonstrated that the distribution of compartmental breathing volumes is posture independent. The volume changes in both hemithoraces are similar, as demonstrated by Nozoe et al. [66]. Moreover, Wang et al. [67] demonstrated that the motion of all 3 CW compartments is highly correlated with diaphragmatic movement distance in the inspiratory phase during both quiet and deep breathing. In particular, the AB movement is closely correlated with diaphragmatic movement in the supine position. The progressively increased inclination of the trunk (from seated to supine position) determines a progressive reduction of RC displacement, VT, and MV and a progressive increase in AB contribution to the VT [68]. In a recent study, Souza Mendes et al. [69] demonstrated that posture, gender, and age influence both the breathing pattern and the thoraco-abdominal motion.

The influence of age on ventilatory kinematics and the mechanisms adopted by the elderly population to overcome age-related physiological changes has been studied by Muniz de Souza et al. [70]. They showed that in the elderly, during moderate inspiratory resistance, the pattern is deep and slow. With respect to the influence of gender, different results have been found in the literature. On one hand, Romei et al. [68] showed that female subjects are characterized by smaller dimensions of the RC compartment and during quiet breathing by lower VT, minute ventilation and AB contribution to VT than males. On the other hand, Binazzi et al. [32] demonstrated no gender differences in breathing pattern or CW kinematics when normalized to

size-related VC. Moreover, Muniz de Souza et al. [70] investigated OEP differences in AB kinematics between young and elderly women during different inspiratory efforts. It was shown that in the elderly, the breathing pattern is deep and slow during moderate inspiratory resistance.

Barcelar et al. [71] investigated how both lung function and thoraco-abdominal volume variations during quiet breathing are altered in obese women. Obesity significantly reduced VRCp and increased VAB compared with normal weight. Additionally, the increased mass of AB modifies the position and the shape of the diaphragm, making this muscle more cranially displaced and its fibres lengthened.

New insights into OEP in the field of laughing and coughing have been gained. Filippelli et al. [72] highlighted that fits of laughter consistently lead to sudden and substantial decrease in lung volume in all the CW compartments and remarkable dynamic compression of the airways. Moreover, Cossette et al. [73] showed that flute support entails antagonistic contraction of non-diaphragmatic inspiratory muscles that tends to hold the RC at higher lung volume by collecting, for the first time, volume data with OEP in young professional flutists. OEP has been used to investigate the influence of cough on CW kinematics in healthy adults by Smith et al. [74] and Lanini et al. [20]. The operating volume was found to be the most important determinant of cough peak flow and volume expelled in healthy individuals [74]. A noticeable RC distortion ensues during coughing if the action of the muscle force acting on the RCa is not commensurate with the force acting on the RCp [20].

One study investigated the effect on the CW of the incentive spirometry in healthy adults [75], and Chihara et al. [81] analyzed the CW kinematics and respiratory muscle recruitment in 7 healthy men during rebreathing of a hypercapnic-hyperoxic gas mixture. The latter study showed that the end-inspiratory lung volume (EIV) increase in VCW was mainly achieved by increasing

end-inspiratory volumes of the RCp and RCa, reflecting the inspiratory RC muscle contribution to recruit the inspiratory reserve volume. Findings reported by Illi et al. [76] likely indicate that all inspiratory muscles fatigued simultaneously rather than in succession and that inspiratory RC muscles did not take over diaphragmatic work in the course of prolonged normocapnic hyperpnoea.

The comprehensive literature analysis reported in this section demonstrates that OEP can be considered both a reliable system for the basic physiological and patho-physiological studies thanks to its non-invasiveness measurements and no requirement of subject cooperation during the evaluations and an attractive tool for evaluating breathing under a wide variety of circumstances in health.

Evaluation of Chronic Obstructive Pulmonary Disease Patients

Although the origins of dyspnoea and exercise intolerance in chronic obstructive pulmonary disease (COPD) are complex and multifactorial, "dynamic hyperinflation" (DH), which is mainly due to expiratory flow limitation and gas accumulation/retention (usually termed "air trapping"), is presumably the most important factor in limiting exercise and contributing to dyspnoea by causing restrictive constraints onto volume expansion [77]. OEP has been used to confirm the hypothesis that COPD patients can dynamically hyperinflate or deflate lung/CW compartments during exercise. In one such study, Aliverti et al. [53] found that the patients with severe COPD showed DH during incremental exercise; patients with a greater expiratory flow reserve at rest, in-stead, adopted the more "normal" approach to reducing end-expiratory lung volume (EEV) of the CW (EEV CW) when they exercised. It remains nevertheless unclear if reduced lung volume

contributes to relieving dyspnoea and improving exercise tolerance in COPD patients [77]. When Aliverti et al. [53] used OEP to analyze the effect of nebulized salbutamol on endurance exercise time in subjects with severe airway obstruction, they described 2 different response patterns to bronchodilation therapy: while the less hyperinflated patients showed reduced EEV after active treatment, the more severely hyperinflated ones continued to allow EEVAB to rise during exercise [79]. Georgiadou et al. [54] described an increase in exercise dyspnoea both in individuals who progressively hyperinflated the CW as well as in those who did not. A lack of correlation between the degree of DH and exercise-induced dyspnoea has led to the hypothesis that abnormalities in CW motion, in particular, the paradoxical (inward) inspiratory movement of the lower rib cage, play a critical role in the onset of dyspnoea and exercise intolerance in COPD patients. OEP measurements have shown that although hyperinflated patients are especially likely to display abnormalities in RC motion, a paradoxical movement of the RCa is not entirely explained by static lung or dynamic RC hyperinflation [80–82].

Pursed-lip breathing (PLB), which involves nasal inspiration followed by exhalation through partially closed lips, has recently been used to assess volume changes in CW compartments and onset of dyspnoea in COPD patients. Bianchi et al. [83] utilized OEP measurement to analyze the displacement of the CW and its compartments and of the RC and AB during supervised PLB manoeuvre in a group of patients with mild to severe COPD. Compared to spontaneous breathing, the patients practicing PLB exhibited a significant reduction in EEV CW and a significant increment in EIV of the CW. The hypothesis that RC distortion plays a role in the onset of breathlessness during exercise in COPD patients raises the question if rehabilitation programs can reduce abnormalities in CW motion in these patients, thereby restoring exercise capacity and relieving breathlessness.

Gagliardi et al. [84] recently used OEP to evaluate the VCW, VRC, and VAB in COPD patients before and after a 24-session exercise program that included education, breathing retraining, unsupported arm exercise, and cycling. Study results showed that exercise training (a) had no effect on operational thoraco-abdominal volumes, (b) contributed to dyspnoea relief by improving patients' ventilatory profile, (c) increased tolerance to the dynamic restriction of CW volumes, and (d) improved RC distortion, albeit only to a small extent.

By using the OEP, Bruni et al. [85] evaluated the effect of oxygen therapy on dyspnoea, CW DH, and RC distortion in a group of COPD individuals. At isotime during exercise, while breathing supplemental oxygen, dyspnoea relief was associated with a decrease in ventilation regard-less of whether patients distorted the RC or dynamically hyperinflated or deflated the CW. In the light of these results, the authors concluded that dyspnoea, CW DH, and RC distortion were not interrelated phenomena and that benefit from oxygen therapy was unrelated to its possible effect on RC distortion or dynamic CW hyperinflation.

When Coutinho Myrrha et al. [86] analyzed CW volumes and breathing patterns in COPD patients at rest and during inspiratory loaded breathing (ILB), they found that the AB was the main compartment responsible for VT during both situations. The authors noted that the COPD patients overcame the load imposed by ILB and improved VT by changing the inspiratory VCW without modifying the predominant mobility of the AB at rest and without affecting the EEVCW.

Authors – year	**Pathology stage, Sample characteristics**	**Topic**	**Findings**
Aliverti et al. [50] – 2004	Clinically stable, n=20	Pathogenesis of DH during incremental exercise	Response pattern may vary according to disease severity
Aliverti et al. [72] – 2005	Severely obstructed, n=18	Effect of salbutamol on endurance exercise	Less hyperinflated patients show reduced EELV
Vogiatzis et al. [73] - 2005	Clinically stable, n=20	Change in V_T pattern during recovery from exercise	Presence of two patterns during exercise: early and late hyperinflation.
Georgiadou et al. [51] – 2007	Severely obstructed, n=20	Influence of chest wall volumes on dyspnoea	EEV_{CW} attenuation in "hyperinflators" doesn't

		during exercise	reduce dyspnoea
Bianchi et al. [80] – 2007	Mild to severe obstruction, n=30	Volume changes in chest wall compartments during PLB	Symptom relief associated to decreased end-expiratory volumes of the chest wall and abdomen in more severely obstructed
Bruni et al. [77] – 2012	Clinically stable, n=15	Effect of oxygen therapy on dyspnoea, chest wall DH, and rib cage distortion	Benefit unrelated to a possible effect on rib cage distortion or dynamic chest wall hyperinflation
Coutinho Myrrha et al. [78] – 2013	Clinically stable, n=13	Chest wall volumes and breathing patterns during ILB	Increment in V_T of the chest wall as a result of higher EEV_{CW} during ILB

Gagliardi et al. [79] – 2014	Severely obstructed, n=14	Effect of exercise program on chest wall volume, and exercise-induced dyspnoea	No effect on thoraco-abdominal volumes; improved rib cage distortion
Rocha et al. [81] – 2015	Clinically stable with age > 60 y.o., n=20	Effect of MDRT on improvement of diaphragmatic mobility	MFRT significantly improved diaphragmatic mobility over the course of treatments and significantly improved the 6-minute walk distance over the treatment course
Borges-Santos et al. [82] – 2015	Clinically stable, n=54: n=17 no symptoms, n=12 anxiety	Relationship between the presence of symptoms of anxiety or	Symptoms of depression report more dyspnoea. No impact of

	symptoms, n=13 depressive symptoms, n=12 both symptoms	depression with breathing pattern and thoracoabdominal mechanics at rest and during exercise in COPD	anxiety and depression on breathing pattern and thoracoabdominal mechanics.
Lima et al. [76] - 2016	Meta-analysis considering 6 studies	The effects of a constant load or incremental cycle ergometer tests on dyspnoea and CW volumes	Euvolumic COPD patients respond more favourable with less dyspnoea to constant load and incremental protocol.

Table 1: Studies utilizing OEP in the evaluation of patients with COPD (DH= Dynamic Hyperinflation; EELV=End-Expiratory Lung Volume; ILB= Inspiratory Loaded Breathing; PLB= Pursed-Lip Breathing, MDRT=Manual Diaphragm Release Technique, EEV_{CW}=end-expiratory lung volume (EEV) of the CW).

OEP in Intensive Care Units

The OEP system has been used to evaluate the effect of invasive and non-invasive ventilatory strategies on VT and thoraco-abdominal synchrony and to monitor CW mechanics and the distribution of VCW variations in patients undergoing mechanical ventilation. Aliverti et al. [30] found that volumes measured using OEP in patients with acute lung injury and acute respiratory distress syndrome receiving continuous positive pressure ventilation or pressure support ventilation (PSV) were highly correlated with measurements taken using spirometry and pneumotachography. They also assessed accuracy of the compartmentalization procedure (RCp, RCa, and AB) by calculating compartmental volume changes during isovolume manoeuvres, and concluded that OEP is able to provide relevant data on the distribution of CW volume variations in ventilated patients.

Dellacà et al. [87] set out to investigate the efficacy of OEP in assessing PEEP-induced variations of lung gas volume in mechanically ventilated, paralyzed patients with acute respiratory failure. The authors measured the EEVCW breath-by-breath by OEP before, during, and after the PEEP increase/decrease and compared its variations with the corresponding EEV ones measured using the helium dilution technique. The regression line between EEV changes measured by helium and EEV CW changes measured by OEP was found to be quite close to the identity line, and the difference was not related to their absolute magnitude.

Finally, OEP was used to study lung volume distribution during the administration of neurally adjusted ventilator assist (NAVA) ventilation, which assists spontaneous breathing proportionally to diaphragmatic electrical activity, compared to administration of PSV at different levels of support [88]. Although NAVA and PSV similarly reduced the abdominal contribution to VT, subject-ventilator synchronization was better during NAVA with respect to PSV, and the difference between the 2 modes in regional ventilation distribution was not significant.

OEP in the Neuromuscular Disease Evaluation

Muscular diseases are characterized by progressive loss of muscle strength, resulting in cough ineffectiveness with its deleterious effects on the respiratory system. Assessment of cough effectiveness is, therefore, a prominent component of the clinical evaluation and respiratory care in these patients. OEP has been used to investigate pulmonary volumes, respiratory muscle strength, peak cough flow, and CW kinematics in neuromuscular patients. A recent review suggests the use of OEP as a non-invasive method to study the thoraco-abdominal kinematics in children with neuromuscular diseases [89]. Subjects with these conditions are unable to reduce EECW volume and exhibit greater RC distortion during cough. Peak cough flow is negatively correlated with RC distortion (the greater the former, the smaller the latter), but is not correlated with respiratory muscle strength [90]. So, this suggests that in-sufficient deflation of CW compartments and marked RC distortion resulted in cough ineffectiveness in these neuromuscular patients.

In patients with Duchenne muscular dystrophy (DMD), OEP highlighted that the CW motion during spontaneous breathing in awake conditions and in the supine position is an important indicator of the degree of respiratory muscle impairment in DMD [26]. Moreover, the contribution of abdominal volume change is a strong indicator of diaphragm impairment [91] such that it could discriminate between efficient end inefficient coughs [92,93]. However, AB contribution is not only an important marker of the progression of the disease but is also an early indicator of nocturnal hypoxaemia [27]. Al-though, even in other dystrophic diseases as Becker muscular dystrophy, facio-scapulo-humeral dystrophy, and Limb-girdle dystrophy, OEP is able to reveal mild initial modifications in the respiration, which could be helpful for functional and new therapeutic strategy evaluation. Moreover, OEP has been used in spinal muscular atrophy (SMA) patients with the aim to investigate

if the RC motion was similar in mild SMA (with onset of lower limbs muscular weakness after 3 years) and healthy subjects [28, 94].

Authors – year	**Pathology, Sample characteristics**	**Aim**	**Findings**
Lo Mauro et al. [26] – 2010	DMD patients at different stages of the disease, n=66	To investigate if V_{AB} contribution to V_T should be considered an early indicator of respiratory impairment in DMD	• In the supine position, the average contribution of ^{V}AB to ^{V}T progressively decreased with age. • NH patients showed significantly lower contribution of VAB changes.
Romei et al. [91] – 2012	DMD, n=40	To determine if V_{RC} and V_{AB} can be helpful to distinguish between those patients who are	• In supine position during the slow VC manoeuvre, ventilator parameters are significantly lower in DMD patients.

		in the early stages of NH development and those who do not yet.	• In seated position, DMD patients showed lower MV than healthy subjects during quiet breathing.
D'Angelo et al. [92] – 2011	DMD patients (4 groups according to age), n=114	To identify early markers of respiratory insufficiency and rule out the role of pharmacological and surgical therapies in DMD	• A subgroup of adolescent DMD patients showed differences in AB contribution to V_{CW} related to the time spent with low oxygen saturation during night, despite similar spirometric parameters. • The inadequate pre-inspiration and insufficient expiratory flow, particularly of the RC muscles seemed to be the cause underlying the progressive inefficient cough typical of the natural course of the disease.

Bonato et al. [93]-2011	DMD patients, n=40	To investigate the relation between the reduction of VC and inspiratory muscles weakness and the ability to breath autonomously	Relationship between the CW variations and the saturations showed differences in AB contribution to V_{CW} variations related to the time spent with low oxygen saturation during night, despite similar spirometric parameters.

• Lo Mauro et al. [88] - 2014 • Lo Mauro et al. [89] - 2012	DMD patients, n=36 (3 groups according to the peak cough flow)	To investigate if thoraco-abdominal operating volumes during coughing determine the effectiveness of cough in DMD patients	• During the inspiration preceding cough, patients with efficient cough showed normal volume variations whereas patients with intermediate cough efficiency showed low AB volume variation. • Patients with inefficient cough were characterized by reduced total and compartmental CW volumes during the inspiration preceding cough and reduced AB contribution to V_T during quiet breathing.
D'Angelo et al. [87]- 2012	DMD, n=45: • with Spinal Fusion,	To compare the rate of decline in respiratory	The decline of V_{AB} contribution to the CW in the DMD patients who

	n=15, • with severe scoliosis (Cobb angle >20°), n=22 • with mild scoliosis Cobb angle <20°), n=8	function in 3 groups of non-ambulant DMD patients, divided on the basis of Cobb angle and Spinal fusion	underwent spinal fusion is far less evident and steep that the one indicated by the FVC and it occurs in a longer period of time.
Lanini et al. [86] - 2008	• BMD,n=3 • FSHD, n=1 • LGMD, n=2 • Myotonic dystrophy, n=2 • Healthy subjects,	To test the hypothesis that operating forces on the CW may impact on distribution of inspired gas volume to RC compartments, resulting in RC distortion and	The cough peak flow was negatively correlated with the distortion of the CW, but not with respiratory muscle strength.

	n=12	decrease in cough effectiveness.	
D'Angelo et al. [94] - 2011	• LGMD,n=38 • BMD, n=20 • FSHD, n=30 • Healthy subjects, n=20	To study the CW behaviour in a large population of patients affected with LGMD, BMD and FSHD.	• Both IC and VC were significantly lower in LGMD and FSHD patients than in healthy subjects. • BMD patients showed slightly lower values of IC and normal values of VC. • AB contribution was reduced in wheelchair bound patients with LGMD and FSHD in the seated position.
Bourdarham et al. [25] – 2013	• Myotonic Dystrophy, n=6	To determine whether OEP	In subjects with various degrees of restrictive respiratory

	• Acid Maltase deficiency, n=5 • Mitochondrial Myopathy, n=1 • DMD, n=1 • Spinal muscular atrophy, n=1 • Neuralgic amyotrophy, n=6	accurately evaluated VC in patients with respiratory muscle dysfunction of variable severity, including those with paradoxical AB movements.	disease VC evaluated with spirometry and OEP showed a strong positive correlation and relatively good agreement.

LoMauro et al. [27] - 2014	• SMA, n=18 • Healthy subjects, n=18	To study how CW kinematics and respiratory muscles change in relation to SMA severity.	In mild SMA and intermediate SMA, RC motion was significantly reduced and sometime paradoxical during quiet breathing in supine position.
Lissoni et al [90] - 1998	• SMA type II, n=9 • Healthy subjects, n=13	To analyse CW kinematics during spontaneous breathing (healthy subjects) and during spontaneous breathing and while using mechanically assisted ventilation (SMA patients).	CW kinematic analysis may be helpful for choosing the ventilation parameters to optimize therapeutic benefits.
Lissoni et al. [95]	• SMA, n=12	To analyse thoraco-	kinematic analysis can be helpful in

- 1996	• Healthy subjects, n=13	abdominal volume changes when breathing spontaneously and when breathing deeply.	determining differences in regional lung mobility and risk for nocturnal ventilatory dysfunction in children with SMA.

Table 2: Studies utilizing OEP in the evaluation of patients with neuromuscular diseases (DMD= Duchenne Muscular Distrophy, NH=nocturnal hypoxemia, MV=minute volume, BMD=Becker's muscular dystrophy, FSHD=Facioscapulohumeral dystrophy, LGMD=Limb-girdle dystrophy Myotonic, SMA= Spinal muscular atrophy).

Outcome Assessment after Thoracic Surgery

Thoracic surgery deeply affects CW kinematics, mainly in the early post-operative period. Patients who underwent surgical procedures involving the CW may benefit from pulmonary rehabilitation (PR) in order to restore correct function of respiratory muscles [95]. OEP represents a suitable tool to identify muscular dysfunctions related to chest surgery.

Lung transplantation (LT) represents the most burdensome CW dynamics' alteration surgical procedures. Wilkens et al. [96] utilized OEP to measure CW volumes of 39 patients affected by COPD, idiopathic pulmonary fibrosis and cystic fibrosis (CF), waiting for LT, and 16 transplanted subjects. Three distinctive breathing pat-terns were observed to cope with the disease, which includes higher VT due to increased EIV for COPD and increased respiratory rate

without VT changes in CF and pulmonary fibrosis patients. Chronic adaptations of the ventilatory pump to advanced lung diseases seem to be reversible, as the authors demonstrate that LT restores a normal breathing pattern regardless of the underlying disease. Nosotti et al. [97] focused the attention on the rearrangement of the VCW and its compartments in CF patients receiving a double LT. Results showed that 2 months after surgery, total lung capacity, functional residual capacity, and residual volume significantly de-crease, mainly due to the reduction in AB amplitude and to a lesser extent in RCp displacement. Based on these findings, the authors argued that with a healthy lung the diaphragm restores its normal curvature, thus decreasing the abdominal distension.

OEP has been used to reveal post-operative ventilatory asymmetries. De Groote et al. [98] analyzed how 2 lungs with different mechanical properties may influence CW dynamics. Imbalances in the extent and rate of inflation or deflation between native and transplanted lung could be explained by different changes in the volume of the 2 hemithoraxes (due to hyperinflation of the native lung), by displacement of the mediastinum, or by a combination of both. Changes in the volume of each hemithorax were measured by OEP during CO2-induced hyperpnoea and forced expiration in male patients who had undergone single LT for emphysema [98]. The authors reported similar volumes of the 2 hemithoraxes at both functional residual capacity and total lung capacity, thus showing that the unequal volumes of the native lung and the graft are accommodated by displacement of the mediastinum rather than by volume distortion. A widespread application of OEP is in tailoring post-operative PR. Several studies have pointed out the efficacy of PR for COPD patients, but less evidence exists for surgical conditions. In Bastianini et al. [55], patients receiving superior lobectomy for non-small cell lung cancer underwent CW kinematic assessment before and immediately after surgery, as well as after 2

weeks of PR. FEV 1 and FVC were found to be decreased between the pre-surgery (PreS) phase and the post-surgery phase (PostS) and partially recovered after rehabilitation (PostR). Notably, the authors reported a significant negative correlation between FEV1 measured during PreS and the FEV1 decreasing from PreS to PostR. The above-mentioned findings agree with the results of Cesario et al. [98], al-though a lower improvement in the latter study was observed after 4-week PR. In another study aimed at testing an OEP system as a diagnostic tool to assess the efficacy of asymmetric PR, Bastianini et al. [100] assessed VT variations of the 6 compartments (the left and right sides of RCp, RCa, and AB) in patients who had undergone left or right superior lobectomy, in PreS, PostS, and PostR phases. Even though PR did not improve the overall volumes, the VT of the non-operated side increased between PreS and PostR. This indicates that PR was more effective on the non-operated side, which then compensates the contralateral one. The negative effect of CW tumours on global CW mechanics during quiet breathing and exercise has been confirmed by Elshafie et al. [101] in a recent study on a patient with unilateral extra-thoracic CW sarcoma. They demonstrated that surgery reverses this abnormality, but only at rest.

Evaluation of Other Health Conditions

OEP has been used in several clinical applications to study different pathological conditions. OEP has been used to study thorax and CW deformity, in children with pectus excavatum [102, 103] with osteogenesis imperfecta type III and type IV (connective tissue disorder characterized by bone fragility, multiple fractures, and significant CW deformities) [108], and in adults with ankylosing spondylitis [104, 105], and to evaluate the effect of posture on breathing kinematics in sub-jects with spinal cord injury [56]. OEP has also been used to investigate VT differences between paretic and healthy sides during quiet breathing, voluntary hyperventilation, and

hypercapnic stimulation in post-stroke patients with hemiparesis [22]. One study analyzed the ventilator breathing pattern in patients with late-onset glycogen storage disease type II. This is an autosomal recessive lysosomal storage disease due to glucosidase alpha acid deficiency, a slowly progressive disease predominantly affecting skeletal and respiratory muscles [106]. Frazão et al. [106] used the OEP to assess the outcome of a respiratory rehabilitative treatment using PEP-Mask in Parkin-son disease patients. In patients with chronic heart failure plus cardiomegaly, significant differences in the regional distribution of RC volumes were found among patients with heart failure associated with cardiomegaly and healthy controls [108].

Barcelar et al. [71] demonstrated, with the use of the OEP, in obese women (BMI >40), that not only lung but also CW function is altered.

Authors – year	**Pathology, Sample characteristics**	**Findings**
• Binazzi et al. [104] – 2012 • Redlinger et al . [105] – 2011	Pectus Excavatum, • n=24 • n=119	• The V_{CW}, V_{RCp}, V_{RCa} and V_{AB} at rest are similar in patients with PE and in healthy subjects. During maximal respiration, PE patients had a significant increase in the

		volume within the RCa compared with healthy ones. • Patients with PE demonstrated significantly decreased midline marker excursion at the level of the pectus defect.
LoMauro et al. [40] – 2012	Osteogenesis Imperfecta type III and type IV, n=22	• Pectus carinatum characterizes Osteogenesis Imperfecta type III patients and alters respiratory muscles coordination, leading to CW and RC distortions and an inefficient ventilator pattern.
• Ferrigno et al. [106] – 1998 • Romagnoli et al. [107] – 2004	Ankylosing spondylitis • n=17 • n=6	• During rebreathing, CW expansion increased (AB component increased more) to a similar extent in patients with ankylosing spondylitis to that unhealthy

		subjects. • RC inspiratory peak and muscle pressure was significantly lower in patients than in controls subjects, but not the AB.
Boudarham et al. [112] – 2013	Unilateral diaphragm weakness, n=13	• OEP detected asymmetric ventilation in all patients diagnosed with unilateral diaphragm weakness and in no patients without this diagnosis. • OEP is an effective non-invasive alternative that is preferred by the patients over diaphragm compound muscle action potentials response and lateral twitch transdiaphragmatic pressure
Meric et al. [113] – 2016	Late-onset Pompe disease, n=11	• AB contribution and V_{AB} during the VC manoeuvre are reliable and non-invasive

		indices of diaphragmatic function in Pompe disease

Remiche et al. [109] – 2013	Late onset Glycogen storage disease type II, n=10	• Higher MV in supine position were found in patients with diaphragmatic weakness (supine FVC fall higher than 25%) respect patients without diaphragmatic weakness (supine FVC change lower or equal to 25%). • In seat and in supine position, patients were characterized by reduced CW IC and by a poor ability to mobilize the AB, being both AB IC and AB ERV significantly lower than in control subjects.
Lanini et al. [21] – 2003	Hemiplegia due to a cerebrovascular accident, n=8	• V_T of paretic and healthy sides were similar during quiet breathing • Hemiparetic stroke produces asymmetric ventilation with an increase in carbon dioxide sensitivity and a decrease in voluntary ventilation

		on the paretic side
Frazão et al. [110] – 2014	Parkinson Patients, n=15	• The study did not find significant difference for AB compartment contribution between Parkinson's patients and healthy subjects during quiet breathing even with Parkinson's showed higher V_T values.
Brandão et al. [111] – 2012	Chronic heart failure plus cardiomegaly patients, n=19	• Left side of the RCa is characterized by lower displacement during inspiratory loaded breathing. • Regional distribution differences in V_{CW} are correlated with other functional parameters, namely left ventricular ejection fraction and dyspnoea.

Table 3: Studies utilizing OEP in the evaluation of other pathological conditions (VC=Vital Capacity, MV=minute volume, FVC=functional ventilatory capacity, IC=inspiratory capacity, ERV= expiratory reserve volume).

OEP in Exercise Science

The function of the respiratory system during exercise is usually assessed by the analysis of expired air to calculate breathing frequency, VT, minute ventilation, oxygen consumption, and carbon dioxide production. These methods are commonly used and are valuable in the quantification of fitness status and diagnosis of a range of cardiovascular and respiratory diseases [109].

Until recently, the movement of the chest and AB during exercise has not been considered in either the understanding of optimal breathing pattern nor in relation to exercise respiratory diseases. The assessment of chest and AB wall movement during exercise may also assist in the understanding of breathing pattern disorders and exercise-triggered dysfunctional breathing [110].

Dickinson et al. [111] have previously reported that using breathing technique and inspiratory muscle training has been successful in eliminating exercise respiratory symptoms during high-intensity exercise in an elite athlete; however, the absence of a method to track chest and AB wall movements meant it was impossible to quantify any changes in breathing mechanics.

Investigations into the use of OEP to assess the movement of the chest and AB during exercise are emerging. Initial reports suggest EIV increases during exercise are mainly achieved by increasing end-inspiratory volumes of the RCp and RCa reflecting the inspiratory RC muscle contribution [112]. Initial work from Layton et al. [113, 114] using OEP suggests that during exercise females have less contribution from VAB and greater contribution of VRCp when compared to males. Table 4 provides an overview of the studies that have used OEP to evaluate the breathing pattern and CW movement during exercise.

Further investigations using OEP during exercise will assist our understanding of the relationship between respiratory and locomotor muscle fatigue, posture, and CW movement. These types of investigations can then aid the delivery of specific therapy and breathing training programmes

targeted towards reducing exercise respiratory symptoms and optimizing chest and AB wall movement during exercise.

Authors – year	**Sample characteristics**	**Aims**	**Findings**
Vogiatzis et al. [120] – 2005	n=15 (10 males, 5 females)	• To investigate the pattern of response in operational lung volumes and relative contribution of respiratory muscle groups between men and women of similar fitness.	• Men exhibited significantly greater operational lung volumes than women during symptom-limited exercise. • During the incremental exercise VCW, EI is progressively increased and VCW, EE is decreased and that both genders utilised primarily the muscles of the rib cage compartment rather than those

			of the abdomen.
Layton et al. [118] –2011	n=18 ET (11 males, 7 females) n=14 UT (9 males, 5 females)	• To determine how increased ventilatory demand impacts kinematic ventilatory s and if there is any difference in the total chest wall volume variations (V_{CW}) of male and endurance-female trained athlete s (ET) compared to untraine d individuals (UT) during exercise.	• With peak exercise, female ET did not change EEV_{CW} or EEV_{RCp} while female UT significantly decreased both parameters . • ET have significant increases in EIV_{RCp}, while UT do not. • Women demonstrated less contribution of the V_{AB} and greater contribution of V_{RCp} when compared to men. • Men demonstrated similar

			contribution of the V_{RCp} and the V_{AB}.
Layton et al. [119] – 2013	n=16 ET n=14 UT	To compare measurements of V_T by OEP and spirometry during a maximal cycling exercise test	Discrepancy of -2.4±3.9% between the two methods during maximal exercise and -2.0±7.2% during submaximal exercise

Table 4: Studies that have used OEP to evaluate chest wall movement and breathing pattern during exercise. (FVC=Functional Vital Capacity, $V_{CW, EI}$ = End-inspiration chest wall volume, EEV_{CW} = End-expiration chest wall volume, V_{CW}= total chest wall volume variations, EEV_{RCp} = End-expiration pulmonary rib cage volume, EIV_{RCp} = End-inspiration pulmonary rib cage volume, V_{AB}= abdominal volume, ET=endurance-trained athletes, UT=untrained athletes).

Conclusions

OEP is an innovative non-invasive tool for measuring different compartments of the CW and thus lung volume variations. OEP has been shown to be a valuable and ac-curate assessment tool that

can provide crucial information about CW mechanics across the respiratory field. The high accuracy and validity of the OEP to measure volume variations assessed in different populations and experimental protocols allow to successfully use this tool in newborns, children, and healthy and pathological sub-jects; OEP allows the study of both breathing volumes and biomechanical indexes for a better comprehension of the work of breathing without interferences using invasive instrumentation.

Although OEP has been used in research, the large number of markers strongly discourage its employment in the daily clinical practice as an alternative tool for traditional flow-based instrument to assess respiratory parameters. In fact, the marker placement can be tedious and complicated, especially in subjects in which the landmarks are difficult to identify. Marker placement is also time-consuming and therefore requires dedicated staff. In order to make OEP more practical for an applied patient setting, future investigations should focus on reducing the marker set or integrate OEP into wearable technology.

OEP may be used in the future to assist in the understanding of breathing patterns in respiratory conditions that are difficult to diagnose objectively, e.g. dysfunctional breathing, and therefore it may have the potential to contribute to an improvement in therapeutic strategies.

References

[1] H. T. Milhorn, R. Benton, R. Ross, and A. C. Guyton, "A mathematical model of the human respiratory control system.," Biophys. J., vol. 5, pp. 27–46, 1965.

[2] A. B. Otis, W. O. Fenn, and H. Rahn, "Mechanics of breathing in man.," J. Appl. Physiol., vol. 2, pp. 592–607, 1950.

[3] M. D. Goldman, G. Grimby, and J. Mead, "Mechanical work of breathing derived from rib cage and abdominal V-P partitioning.," J. Appl. Physiol., vol. 41, pp. 752–763, 1976.

[4] F. J. Hoppin, J. J. Stothert, I. Greaves, Y.-L. Lai, and J. Hildebrandt, "Lung recoil: elastic and rheological properties.," in Macklem PT, Mead J (eds) Handbook of physiology. The respiratory system. Mechanics of breathing, Section 3, vol III, part 1, 1986, pp. 195–215.

[5] L. E. Bayliss and G. W. Robertson, "The visco-elastic properties of the lungs," Q. J. Exp. Physiol. Cogn. Med. Sci., vol. 29, no. 1, pp. 27–47, Mar. 1939.

[6] R. Peslin, J. Papon, C. Duviver, and J. Richalet, "Frequency response of the chest: modeling and parameter estimation.," J. Appl. Physiol., vol. 39, no. 4, pp. 523–34, Oct. 1975.

[7] K. Konno and J. Mead, "Measurement of the separate volume changes of rib cage and abdomen during breathing.," J. Appl. Physiol., vol. 22, no. 3, pp. 407–422, 1967.

[8] J. Mead, "The control of respiratory frequency.," Ann. N. Y. Acad. Sci., vol. 109, pp. 724–729, 1963.

[9] J. Mead, N. Peterson, G. Grimby, and J. Mead, "Pulmonary ventilation measured from body surface movements.," 1967.

[10] G. M. Barnas, K. Yoshino, D. Stamenovic, Y. Kikuchi, S. H. Loring, and J. Mead, "Chest wall impedance partitioned into rib cage and diaphragm-abdominal pathways.," J. Appl. Physiol., vol. 66, pp. 350–359, 1989.

[11] G. M. Barnas, K. Yoshino, S. H. Loring, and J. Mead, "Impedance and relative displacements of relaxed chest wall up to 4 Hz.," J. Appl. Physiol., vol. 62, pp. 71–81, 1987.

[12] R. Peslin, C. Duvivier, and C. Gallina, "Total respiratory input and transfer impedances in humans.," J. Appl. Physiol., vol. 59, no. 2, pp. 492–501, Aug. 1985.

[13] G. Ferrigno and A. Pedotti, "ELITE: a digital dedicated hardware system for movement analysis via real-time TV signal processing.," IEEE Trans. Biomed. Eng., vol. 32, no. 11, pp. 943–50, Nov. 1985.

[14] S. J. Cala, C. M. Kenyon, G. Ferrigno, P. Carnevali, A. Aliverti, A. Pedotti, P. T. Macklem, and D. F. Rochester, "Chest wall and lung volume estimation by optical reflectance motion analysis.," J. Appl. Physiol., vol. 81, pp. 2680–2689, 1996.

[15] G. Ferrigno, P. Carnevali, A. Aliverti, F. Molteni, G. Beulcke, and A. Pedotti, "Three dimensional optical analysis of chest wall motion.," J. Appl. Physiol., vol. 77, pp. 1224–1231, 1994.

[16] A. Aliverti, R. Dellacà, P. Pelosi, D. Chiumello, L. Gattinoni, and A. Pedotti, "Compartmental analysis of breathing in the supine and prone positions by optoelectronic plethysmography," Ann. Biomed. Eng., vol. 29, no. 1, pp. 60–70, Jan. 2001.

[17] Massaroni M, Carraro E, Vianello A, Miccinilli S, Morrone M, Levai K, Schena E, Saccomandi P, Sterzi S, Dickinson JW, Silvestri S. Optoelectronic Plethysmography in Clinical Practice and Research: A Review. Respiration 2017;93(5):339-354.

[18] I. Iandelli, E. Rosi, and G. Scano, "The ELITE system.," in Monaldi archives for chest disease = Archivio Monaldi per le malattie del torace / Fondazione clinica del lavoro, IRCCS [and] Istituto di clinica tisiologica e malattie apparato respiratorio, Università di Napoli, Secondo ateneo, 1999, vol. 54, no. 6, pp. 498–501.

[19] C. Massaroni, E. Schena, F. Bastianini, A. Scorza, P. Saccomandi, G. Lupi, F. Botta, S. A. A. Sciuto, and S. Silvestri, "Development of a bio-inspired mechatronic chest wall simulator for evaluating the performances of opto-electronic plethysmography.," Open Biomed. Eng. J., vol. 8, pp. 120–30, Jan. 2014.

[20] B. Lanini, R. Bianchi, B. Binazzi, I. Romagnoli, F. Pala, F. Gigliotti, and G. Scano, "Chest wall kinematics during cough in healthy subjects," Acta Physiol., vol. 190, no. 4, pp. 351–358, Aug. 2007.

[21] I. Vogiatzis, D. Athanasopoulos, R. Boushel, J. A. Guenette, M. Koskolou, M. Vasilopoulou, H. Wagner, C. Roussos, P. D. Wagner, and S. Zakynthinos, "Contribution of respiratory muscle blood flow to exercise-induced diaphragmatic fatigue in trained cyclists.," J. Physiol., vol. 586, no. Pt 22, pp. 5575–5587, Nov. 2008.

[22] B. Lanini, R. Bianchi, I. Romagnoli, C. Coli, B. Binazzi, F. Gigliotti, A. Pizzi, A. Grippo, and G. Scano, "Chest wall kinematics in patients with hemiplegia.," Am. J. Respir. Crit. Care Med., vol. 168, no. 1, pp. 109–13, Jul. 2003.

[23] S. Hostettler, S. K. Illi, E. Mohler, A. Aliverti, and C. M. Spengler, "Chest wall volume changes during inspiratory loaded breathing," Respir. Physiol. Neurobiol., vol. 175, no. 1, pp. 130–139, Jan. 2011.

[24] M. Gorini, I. Iandelli, G. Misuri, F. Bertoli, M. Filippelli, M. Mancini, R. Duranti, F. Gigliotti, and G. Scano, "Chest wall hyperinflation during acute bronchoconstriction in asthma," Am. J. Respir. Crit. Care Med., vol. 160, pp. 808–816, 1999.

[25] BTS Bioengineering, Optoelectronic Plethysmography Compedium Marker Setup; A handbook about marker positioning on subjects in standing and supine positions. 2011.

[26] J. Boudarham, D. Pradon, H. Prigent, I. Vaugier, F. Barbot, N. Letilly, L. Falaize, D. Orlikowski, M. Petitjean, and F. Lofaso, "Optoelectronic vital capacity measurement for restrictive diseases.," Respir. Care, vol. 58, no. 4, pp. 633–8, Apr. 2013.

[27] A. Lo Mauro, M. G. D'Angelo, M. Romei, F. Motta, D. Colombo, G. P. Comi, A. Pedotti, E. Marchi, A. C. Turconi, N. Bresolin, and A. Aliverti, "Abdominal volume contribution to tidal volume as an early indicator of respiratory impairment in Duchenne muscular dystrophy.," Eur. Respir. J., vol. 35, no. 5, pp. 1118–25, May 2010.

[28] A. LoMauro, M. Romei, R. Priori, M. Laviola, M. G. D'Angelo, and A. Aliverti, "Alterations of thoraco-abdominal volumes and asynchronies in patients with spinal muscle atrophy type III," Respir. Physiol. Neurobiol., vol. 197, no. 1, pp. 1–8, Jun. 2014.

[29] R. Dellacà, M. M. L. Ventura, E. A. Zannin, M. Natile, A. Pedotti, and P. Tagliabue, "Measurement of total and compartmental lung volume changes in newborns by optoelectronic plethysmography," Pediatr. Res., vol. 67, no. 1, pp. 11–16, Jan. 2010.

[30] A. Aliverti, R. Dellacà, P. Pelosi, D. Chiumello, A. Pedotti, and L. Gattinoni, "Optoelectronic plethysmography in intensive care patients," Am. J. Respir. Crit. Care Med., vol. 161, no. 5, pp. 1546–1552, May 2000.

[31] C. M. A. Reinaux, A. Aliverti, L. G. M. da Silva, R. J. da Silva, J. N. Gonçalves, J. B. Noronha, J. E. C. Filho, A. D. de Andrade, and M. C. de Amorim Britto, "Tidal volume measurements in infants: Opto-electronic plethysmography versus pneumotachograph," Pediatr. Pulmonol., p. in press, Mar. 2016.

[32] B. Binazzi, B. Lanini, R. Bianchi, I. Romagnoli, M. Nerini, F. Gigliotti, R. Duranti, J. Milic Emili, and G. Scano, "Breathing pattern and kinematics in normal subjects during speech, singing and loud whispering.," Acta Physiol. (Oxf)., vol. 186, no. 3, pp. 233–46, Mar. 2006.

[33] R. L. Dellacà, L. D. Black, H. Atileh, A. Pedotti, and K. R. Lutchen, "Effects of posture and bronchoconstriction on low-frequency input and transfer impedances in humans.," J. Appl. Physiol., vol. 97, no. 1, pp. 109–118, Jul. 2004.

[34] M. Filippelli, R. Duranti, F. Gigliotti, R. Bianchi, M. Grazzini, L. Stendardi, and G. Scano, "Overall Contribution of Chest Wall Hyperinflation to Breathlessness in Asthma," Chest, vol. 124, no. 6, pp. 2164–2170, Dec. 2003.

[35] M. Laviola, A. Zanini, R. Priori, F. Macchini, E. Leva, M. Torricelli, C. Ceruti, and A. Aliverti, "Thoraco-abdominal asymmetry and asynchrony in congenital diaphragmatic hernia.," Pediatr. Pulmonol., Jul. 2014.

[36] A. Aliverti, R. L. Dellacà, P. Lotti, S. Bertini, R. Duranti, G. Scano, J. Heyman, A. Lo Mauro, A. Pedotti, and P. T. Macklem, "Influence of expiratory flow-limitation during exercise on systemic oxygen delivery in humans," Eur. J. Appl. Physiol., vol. 95, no. 2–3, pp. 229–242, Oct. 2005.

[37] P. Allard, J. P. Blanchi, and R. Aissaoui, "Bases of three-dimensional reconstruction," in P. Allard, I. A. F. Stokes & J. P. Blanchi (Eds.), Three-dimensional analysis of human movement, 1995, pp. 19–40.

[38] J. G. Andrews, "Euler's and Lagrange's equations for linked rigid-body models of three-dimensional human motion.," in P. Allard, I. A. F. Stokes & J. P. Blanchi (Eds.), Three dimensional analysis of human movement, 1995, pp. 145–175.

[39] A. Aliverti and A. Pedotti, "Opto-electronic plethysmography," Monaldi Arch. Chest Dis. - Pulm. Ser., vol. 59, no. 1, pp. 12–16, 2003.

[40] I. Romagnoli, B. Lanini, B. Binazzi, R. Bianchi, C. Coli, L. Stendardi, F. Gigliotti, and G. Scano, "Optoelectronic plethysmography has improved our knowledge of respiratory physiology and pathophysiology," Sensors, vol. 8, no. 12, pp. 7951–7972, Dec. 2008.

[41] A. Lo Mauro, S. Pochintesta, M. Romei, M. G. D'angelo, A. Pedotti, A. C. Turconi, A. Aliverti, and M. G. D'Angelo, "Rib cage deformities alter respiratory muscle action and chest wall function in patients with severe osteogenesis imperfecta.," PLoS One, vol. 7, no. 4, p. e35965, Jan. 2012.

[42] M. A. Sackner, H. Gonzalez, M. Rodriguez, A. Belsito, D. R. Sackner, and S. Grenvik, "Assessment of asynchronous and paradoxic motion between rib cage and abdomen in normal subjects and in patients with chronic obstructive pulmonary disease.," Am. Rev. Respir. Dis., vol. 130, no. 4, pp. 588–93, 1984.

[43] M. J. Tobin, T. S. Chadha, G. Jenouri, S. J. Birch, H. B. Gazeroglu, and M. A. Sackner, "Breathing patterns. 1. Normal subjects," Chest, vol. 84, no. 2, pp. 202–205, 1983.

[44] J. L. Allen, M. R. Wolfson, K. McDowell, and T. H. Shaffer, "Thoracoabdominal asynchrony in infants with airflow obstruction.," Am. Rev. Respir. Dis., vol. 141, no. 2, pp. 337–42, Feb. 1990.

[45] N. M. Kiciman, B. Andréasson, G. Bernstein, F. L. Mannino, W. Rich, C. Henderson, and G. P. Heldt, "Thoracoabdominal motion in newborns during ventilation delivered by endotracheal tube or nasal prongs," Pediatr. Pulmonol., vol. 25, no. 3, pp. 175–181, 1998.

[46] O. H. Mayer, R. G. Clayton, A. F. Jawad, J. M. McDonough, and J. L. Allen, "Respiratory inductance plethysmography in healthy 3- to 5-year-old children.," Chest, vol. 124, no. 5, pp. 1812–9, Nov. 2003.

[47] E. Agostoni and P. Mognoni, "Deformation of the chest wall during breathing efforts.," J. Appl. Physiol., vol. 21, no. 6, pp. 1827–32, Nov. 1966.

[48] N. Beydon, S. D. Davis, E. Lombardi, J. L. Allen, H. G. M. Arets, P. Aurora, et al. "An Official American Thoracic Society/European Respiratory Society Statement: Pulmonary

function testing in preschool children," Am. J. Respir. Crit. Care Med., vol. 175, no. 12, pp. 1304–1345, Jun. 2007.

[49] R. K. Millard, "Inductive plethysmography components analysis and improved non-invasive postoperative apnoea monitoring." Physiol. Meas., vol. 20, pp. 175–186, 1999.

[50] V. F. Parreira, D. S. R. Vieira, M. a C. Myrrha, I. M. B. S. Pessoa, S. M. Lage, and R. R. Britto, "Optoelectronic plethysmography: a review of the literature," Rev. Bras. Fisioter., vol. 16, no. 6, pp. 439–53, Jan. 2012.

[51] A. Aliverti, N. Stevenson, R. L. Dellacà, A. Lo Mauro, A. Pedotti, and P. M. a Calverley, "Regional chest wall volumes during exercise in chronic obstructive pulmonary disease," Thorax, vol. 59, no. 3, pp. 210–6, Mar. 2004.

[52] O. Georgiadou, I. Vogiatzis, G. Stratakos, A. Koutsoukou, S. Golemati, A. Aliverti, C. Roussos, and S. Zakynthinos, "Effects of rehabilitation on chest wall volume regulation during exercise in COPD patients.," Eur. Respir. J., vol. 29, no. 2, pp. 284–91, Feb. 2007.

[53] F. Bastianini, E. Schena, and S. Silvestri, "Accuracy evaluation on linear measurement through opto-electronic plethysmograph," in 2012 Annual International Conference of the IEEE Engineering in Medicine and Biology Society, 2012, pp. 1–4.

[54] F. Bastianini, E. Schena, P. Saccomandi, and S. Silvestri, "Accuracy evaluation of dynamic volume measurements performed by opto-electronic plethysmograph, by using a pulmonary simulator," Proc. Annu. Int. Conf. IEEE Eng. Med. Biol. Soc. EMBS, vol. 2013, pp. 930–933, Jan. 2013.

[55] C. Massaroni, E. Schena, P. Saccomandi, and S. Silvestri, "Motion capture systems for breathing analysis: calibration procedure and experimental trials by the use of a novel in-situ tool for volumetric calibration," in 38th Annual International Conference of the IEEE Engineering in Medicine and Biology Society.

[56] E. Schena, C. Massaroni, P. Saccomandi, and S. Cecchini, "Flow measurement in mechanical ventilation: A review.," Med. Eng. Phys., vol. 37, no. 3, pp. 257–264, Feb. 2015.

[57] A. Aliverti, R. Dellacà, P. Pelosi, D. Chiumello, L. Gattinoni, and A. Pedotti, "Compartmental analysis of breathing in the supine and prone positions by optoelectronic plethysmography.," Ann. Biomed. Eng., vol. 29, no. 1, pp. 60–70, Jan. 2001.

[58] D. S. R. Vieira, M. Hoffman, D. A. G. Pereira, R. R. Britto, and V. F. Parreira, "Optoelectronic plethysmography: intra-rater and inter-rater reliability in healthy subjects.," Respir. Physiol. Neurobiol., vol. 189, no. 3, pp. 473–6, Dec. 2013.

[59] F. Reiterer, E. Sivieri, and S. Abbasi, "Evaluation of bedside pulmonary function in the neonate: From the past to the future." Pediatr. Pulmonol., vol. 50, no. 10, pp. 1039–50, Oct. 2015.

[60] M. Perego, E. Zannin, L. Marconi, G. Dognini, M. L. Ventura, T. Fedeli, P. Tagliabue, and R. Dellaca', "Regional distribution of chest wall displacements in infants during high frequency oscillatory ventilation (HFOV)," Eur. Respir. J., vol. 46, no. suppl 59, p. PA1856, Oct. 2015.

[61] M. Nozoe, K. Mase, S. Takashima, K. Matsushita, Y. Kouyama, H. Hashizume, Y. Kawasaki, Y. Uchiyama, N. Yamamoto, Y. Fukuda, and K. Domen, "Measurements of chest wall volume variation during tidal breathing in the supine and lateral positions in healthy subjects," Respir. Physiol. Neurobiol., vol. 193, no. 1, pp. 38–42, Mar. 2014.

[62] H. K. Wang, T. W. Lu, R. J. Liing, T. T. F. Shih, S. C. Chen, and K. H. Lin, "Relationship Between Chest Wall Motion and Diaphragmatic Excursion in Healthy Adults in Supine Position," J. Formos. Med. Assoc., vol. 108, no. 7, pp. 577–586, 2009.

[63] M. Romei, A. Lo Mauro, M. G. D'Angelo, A. C. Turconi, N. Bresolin, A. Pedotti, and A. Aliverti, "Effects of gender and posture on thoraco-abdominal kinematics during quiet breathing in healthy adults.," Respir. Physiol. Neurobiol., vol. 172, no. 3, pp. 184–91, Jul. 2010.

[64] L. Souza Mendes, M. Hoffman Barbosa, L. Silva Gabriel, G. Ribeiro-Samora, G. Freitas Fregonezi, A. Dornelas Andrade, R. Rodrigues Britto, and V. Franco Parreira, "Influence of posture, gender and sex on breathing pattern and thoracoabdominal motion during quiet breathing in healthy subjects," Eur. Respir. J., vol. 46, no. suppl 59, p. PA4218, Oct. 2015.

[65] H. Muniz de Souza, T. Rocha, S. L. Campos, D. C. Brandão, J. B. Fink, A. Aliverti, and A. D. de Andrade, "Acute effects of different inspiratory efforts on ventilatory pattern and chest wall compartmental distribution in elderly women.," Respir. Physiol. Neurobiol., vol. 227, pp. 27–33, Feb. 2016.

[66] J. de M. Barcelar, A. Aliverti, T. L. L. D. B. Melo, C. S. Dornelas, C. S. F. R. Lima, C. M. a Reinaux, and A. D. de Andrade, "Chest wall regional volumes in obese women.," Respir. Physiol. Neurobiol., vol. 189, no. 1, pp. 167–173, Oct. 2013.

[67] M. Filippelli, R. Pellegrino, I. Iandelli, G. Misuri, J. R. Rodarte, R. Duranti, V. Brusasco, and G. Scano, "Respiratory dynamics during laughter." J. Appl. Physiol., vol. 90, no. 4, pp. 1441–1446, Apr. 2001.

[68] I. Cossette, P. Monaco, A. Aliverti, P. T. Macklem, and G. J. Agarwal R1, Yadav R, Anand S, Suri JC, "Chest wall dynamics and muscle recruitment during professional flute playing," Respir. Physiol. Neurobiol., vol. 160, no. 2, pp. 187–195, Feb. 2008.

[69] J. A. Smith, A. Aliverti, M. Quaranta, K. McGuinness, A. Kelsall, J. Earis, and P. M. Calverley, "Chest wall dynamics during voluntary and induced cough in healthy volunteers.," J. Physiol., vol. 590, no. Pt 3, pp. 563–74, Feb. 2012.

[70] D. de M. Paisani, A. C. Lunardi, C. C. B. M. da Silva, D. C. Porras, C. Tanaka, and C. R. F. Carvalho, "Volume rather than flow incentive spirometry is effective in improving chest wall expansion and abdominal displacement using optoelectronic plethysmography.," Respir. Care, vol. 58, no. 8, pp. 1360–6, Aug. 2013.

[71] S. K. Illi, S. Hostettler, A. Aliverti, and C. M. Spengler, "Compartmental chest wall volume changes during volitional hyperpnoea with constant tidal volume in healthy individuals.," Respir. Physiol. Neurobiol., vol. 185, no. 2, pp. 410–5, Jan. 2013.

[72] D. E. O'Donnell, "Hyperinflation, dyspnea, and exercise intolerance in chronic obstructive pulmonary disease." Proc. Am. Thorac. Soc., vol. 3, no. 2, pp. 180–4, 2006.

[73] A. Aliverti, K. Rodger, R. L. Dellacà, N. Stevenson, A. Lo Mauro, A. Pedotti, and P. M. and Calverley, "Effect of salbutamol on lung function and chest wall volumes at rest and during exercise in COPD.," Thorax, vol. 60, no. 11, pp. 916–924, Nov. 2005.

[74] A. Jubran and M. J. Tobin, "The effect of hyperinflation on rib cage-abdominal motion.," Am. Rev. Respir. Dis., vol. 146, no. 6, pp. 1378–82, Dec. 1992.

[75] K. Chihara, C. M. Kenyon, and P. T. Macklem, "Human rib cage distortability.," J. Appl. Physiol., vol. 81, no. 1, pp. 437–47, 1996.

[76] I. Romagnoli, F. Gigliotti, B. Lanini, G. I. Bruni, C. Coli, B. Binazzi, L. Stendardi, and G. Scano, "Chest wall kinematics and breathlessness during unsupported arm exercise in COPD patients." Respir. Physiol. Neurobiol., vol. 178, no. 2, pp. 242–9, Sep. 2011.

[77] R. Bianchi, F. Gigliotti, I. Romagnoli, B. Lanini, C. Castellani, M. Grazzini, and G. Scano, "Chest Wall Kinematics and Breathlessness during Pursed-Lip Breathing in Patients with COPD," Chest, vol. 125, no. 2, pp. 459–65, Feb. 2004.

[78] G. I. Bruni, F. Gigliotti, B. Binazzi, I. Romagnoli, R. Duranti, and G. Scano, "Dyspnea, chest wall hyperinflation, and rib cage distortion in exercising patients with chronic obstructive pulmonary disease.," Med. Sci. Sports Exerc., vol. 44, no. 6, pp. 1049–56, Jun. 2012.

[79] M. A. Coutinho Myrrha, D. S. R. Vieira, K. S. Moraes, S. M. Lage, V. F. Parreira, and R. R. Britto, "Chest wall volumes during inspiratory loaded breathing in COPD patients.," Respir. Physiol. Neurobiol., vol. 188, no. 1, pp. 15–20, Aug. 2013.

[80] E. Gagliardi, G. Bruni, and I. Presi, "Thoraco-abdominal motion/displacement does not affect dyspnea following exercise training in COPD patients," Respir. Physiol. 2014.

[81] R. Bianchi, F. Gigliotti, I. Romagnoli, B. Lanini, C. Castellani, B. Binazzi, L. Stendardi, M. Grazzini, and G. Scano, "Patterns of chest wall kinematics during volitional pursed-lip breathing in COPD at rest." Respir. Med., vol. 101, no. 7, pp. 1412–1418, Jul. 2007.

[82] T. Rocha, H. Souza, D. C. Brandão, C. Rattes, L. Ribeiro, S. L. Campos, A. Aliverti, and A.D. de Andrade, "The Manual Diaphragm Release Technique improves diaphragmatic mobility, inspiratory capacity and exercise capacity in people with chronic obstructive pulmonary disease: a randomised trial.," J. Physiother., vol. 61, no. 4, pp. 182–9, Oct. 2015.

[83] E. Borges-Santos, J. T. Wada, C. M. da Silva, R. A. Silva, R. Stelmach, C. R. Carvalho, and A. C. Lunardi, "Anxiety and depression are related to dyspnea and clinical control but not with thoracoabdominal mechanics in patients with COPD.," Respir. Physiol. Neurobiol, vol. 210, pp. 1–6, May 2015.

[84] R. L. Dellacà, A. Aliverti, P. Pelosi, E. Carlesso, D. Chiumello, A. Pedotti, and L. Gattinoni, "Estimation of end-expiratory lung volume variations by optoelectronic plethysmography.," Crit. Care Med., vol. 29, no. 9, pp. 1807–11, Sep. 2001.

[85] B. Henri Meric, Pascale Calabresec, 1, Didier Pradona, b, Michèle Lejaillea and N. T. Frédéric Lofasoa, b, d, "Physiological comparison of breathing patterns with neurally adjusted ventilatory assist (NAVA) and pressure-support ventilation to improve NAVA settings.," Respir. Physiol. Neurobiol. 2014.

[86] B. Fauroux and S. Khirani, "Neuromuscular disease and respiratory physiology in children: putting lung function into perspective.," Respirology, vol. 19, no. 6, pp. 782–91, Aug. 2014.

[87] B. Lanini, M. Masolini, R. Bianchi, B. Binazzi, I. Romagnoli, F. Gigliotti, and G. Scano, "Chest wall kinematics during voluntary cough in neuromuscular patients," Respir. Physiol. Neurobiol., vol. 161, no. 1, pp. 62–68, Mar. 2008.

[88] M. G. D'Angelo, M. Romei, S. Gandossini, S. Bonato, E. Brighina, A. LoMauro, E. Marchi, A. Pedotti, A. C. Turconi, N. Bresolin, and A. Aliverti, "Advantages of the optoelectronic plethysmography in the evaluation of respiratory muscle function in DMD boys with scoliosis and spinal fusion," Gait Posture, vol. 35, pp. S7–S8, Apr. 2012.

[89] A. LoMauro, M. Romei, M. G. D'Angelo, and A. Aliverti, "Determinants of cough efficiency in Duchenne muscular dystrophy.," Pediatr. Pulmonol., vol. 49, no. 4, pp. 357–65, Apr. 2014.

[90] A. Lo Mauro, M. G. D'Angelo, M. Romei, S. Gandossini, A. C. Turconi, A. Pedotti, and A. Aliverti, "Chest wall kinematics during cough in Duchenne Muscular Dystrophy," Gait Posture, vol. 35, p. S8, Apr. 2012.

[91] A. Lissoni, A. Aliverti, A.C. Tzeng, and J. R. Bach, "Kinematic analysis of patients with spinal muscular atrophy during spontaneous breathing and mechanical ventilation.," Am. J. Phys. Med. Rehabil., vol. 77, no. 3, pp. 188–92, 1998.

[92] M. Romei, M. G. D'Angelo, A. LoMauro, S. Gandossini, S. Bonato, E. Brighina, E. Marchi, G. P. Comi, A. C. Turconi, A. Pedotti, N. Bresolin, and A. Aliverti, "Low abdominal contribution to breathing as daytime predictor of nocturnal desaturation in adolescents and young adults with Duchenne Muscular Dystrophy.," Respir. Med., vol. 106, no. 2, pp. 276–83, Feb. 2012.

[93] M. G. D'Angelo, M. Romei, A. Lo Mauro, E. Marchi, S. Gandossini, S. Bonato, D. Colombo, A. C. Turconi, A. Pedotti, N. Bresolin, and A. Aliverti, "P1.12 Duchenne muscular dystrophy

and optoelectronic plethysmography: A longitudinal study of respiratory function," Neuromuscul. Disord. vol. 21, no. 9–10, p. 645, Oct. 2011.

[94] S. Bonato, M. G. D'Angelo, S. Gandossini, M. Romei, D. Colombo, A. C. Turconi, A. Aliverti, and N. Bresolin, "P03.5 Optoelectronic Plethysmography for respiratory assessment in Muscular Duchenne Dystrophy," Eur. J. Paediatr. Neurol., vol. 15, p. S43, May 2011.

[95] M. G. D'Angelo, M. Romei, A. Lo Mauro, E. Marchi, S. Gandossini, S. Bonato, G. P. Comi, F. Magri, A. C. Turconi, A. Pedotti, N. Bresolin, A. Aliverti, M. G. D'Angelo, M. Romei, A. Lo Mauro, E. Marchi, S. Gandossini, S. Bonato, G. P. Comi, F. Magri, A. C. Turconi, A. Pedotti, N. Bresolin, and a. Aliverti, "Respiratory pattern in an adult population of dystrophic patients.," J. Neurol. Sci., vol. 306, no. 1–2, pp. 54–61, Jul. 2011.

[96] A. Lissoni, A. Aliverti, F. Molteni, and J. R. Bach, "Spinal muscular atrophy: kinematic breathing analysis.," Am. J. Phys. Med. Rehabil., vol. 75, no. 5, pp. 332–339, 1996.

[97] A. Cesario, V. Dall'Armi, G. Cusumano, L. Ferri, S. Margaritora, V. Cardaci, S. Cafarotti, P. Russo, L. Paleari, S. Sterzi, F. Pasqua, S. Bonassi, and P. Granone, "Post-operative pulmonary rehabilitation after lung resection for NSCLC: a follow up study.," Lung Cancer, vol. 66, no. 2, pp. 268–9, Nov. 2009.

[98] H. Wilkens, B. Weingard, A. Lo Mauro, E. Schena, A. Pedotti, G. W. Sybrecht, and A. Aliverti, "Breathing pattern and chest wall volumes during exercise in patients with cystic fibrosis, pulmonary fibrosis and COPD before and after lung transplantation.," Thorax, vol. 65, no. 9, pp. 808–14, Sep. 2010.

[99] M. Nosotti, M. Laviola, S. Mariani, E. Privitera, P. Mendogni, I. F. Nataloni, A. Aliverti, and L. Santambrogio, "Variations of thoracoabdominal volumes after lung transplantation measured by opto-electronic plethysmography.," Transplant. Proc., vol. 45, no. 3, pp. 1279–81, Apr. 2013.

[100] A. De Groote, A. Van Muylem, P. Scillia, G. Cheron, G. Verleden, M. Paiva, et al., "Ventilation asymmetry after transplantation for emphysema: role of chest wall and mediastinum.," Am. J. Respir. Crit. Care Med., vol. 170, no. 11, pp. 1233–1238, Dec. 2004.

[101] F. Bastianini, S. Silvestri, E. Schena, S. Cecchini, and S. Sterzi, "Evaluation of pulmonary rehabilitation after lung resection through opto-electronic plethysmography.," Conf. Proc. Annu. Int. Conf. IEEE Eng. Med. Biol. Soc. IEEE Eng. Med. Biol. Soc. Annu. Conf., vol. 2010, pp. 2481–4, Jan. 2010.

[102] A. Cesario, L. Ferri, D. Galetta, F. Pasqua, S. Bonassi, E. Clini, G. Biscione, V. Cardaci, S. di Toro, A. Zarzana, S. Margaritora, A. Piraino, P. Russo, S. Sterzi, and P. Granone, "Postoperative respiratory rehabilitation after lung resection for non-small cell lung cancer.," Lung Cancer, vol. 57, no. 2, pp. 175–80, Aug. 2007.

[103] F. Bastianini, S. Silvestri, G. Magrone, E. Gallotta, and S. Sterzi, "A preliminary efficacy evaluation performed by opto-electronic plethysmography of asymmetric respiratory rehabilitation.," Conf. Proc. Annu. Int. Conf. IEEE Eng. Med. Biol. Soc. IEEE Eng. Med. Biol. Soc. Annu. Conf., vol. 2009, pp. 849–852, Jan. 2009.

[104] G. Elshafie, A. Aliverti, L. Pippa, P. Kumar, M. Kalkat, and B. Naidu, "Surgery corrects asynchrony of ribcage secondary to extra-thoracic tumor but leads to expiratory dysfunction during exercise.," J. Cardiothorac. Surg., vol. 10, no. 1, p. 187, Jan. 2015.

[105] B. Binazzi, G. Innocenti Bruni, C. Coli, I. Romagnoli, A. Messineo, R. Lo Piccolo, G. Scano, and F. Gigliotti, "Chest wall kinematics in young subjects with Pectus excavatum.," Respir. Physiol. Neurobiol., vol. 180, no. 2–3, pp. 211–7, Mar. 2012.

[106] R. E. Redlinger, R. E. Kelly, D. Nuss, M. Goretsky, M. A. Kuhn, K. Sullivan, A. E. Wootton, A. Ebel, and R. J. Obermeyer, "Regional chest wall motion dysfunction in patients

with pectus excavatum demonstrated via optoelectronic plethysmography.," J. Pediatr. Surg., vol. 46, no. 6, pp. 1172–6, Jun. 2011.

[107] G. Ferrigno and P. Carnevali, "Principal component analysis of chest wall movement in selected pathologies", Med. Biol. Eng. Comput., vol. 36, no. 4, pp. 445–451, Jul. 1998.

[108] I. Romagnoli, F. Gigliotti, A. Galarducci, B. Lanini, R. Bianchi, D. Cammelli, and G. Scano, "Chest wall kinematics and respiratory muscle action in ankylosing spondylitis patients.," Eur. Respir. J., vol. 24, no. 3, pp. 453–60, Sep. 2004.

[109] S. Miccinilli, M. Morrone, F. Bastianini, M. Molinari, G. Scivoletto, S. Silvestri, F. Ranieri, and S. Sterzi, "Optoelectronic plethysmography to evaluate the effect of posture on breathing kinematics in spinal cord injury: a cross sectional study.," Eur. J., Apr. 2015.

[110] G. Remiche, A. Lo Mauro, P. Tarsia, D. Ronchi, A. Bordoni, F. Magri, G. P. Comi, A. Aliverti, and M. G. D'Angelo, "Postural effects on lung and chest wall volumes in late onset type II glycogenosis patients.," Respir. Physiol. Neurobiol., vol. 186, no. 3, pp. 308–14, May 2013.

[111] M. Frazão, E. Cabral, I. Lima, V. Resqueti, R. Florêncio, A. Aliverti, and G. Fregonezi, "Assessment of the acute effects of different PEP levels on respiratory pattern and operational volumes in patients with Parkinson's disease.," Respir. Physiol. Neurobiol., vol. 198, no. 1, pp. 42–7, Jul. 2014.

[112] D. C. Brandão, S. M. Lage, R. R. Britto, V. F. Parreira, W. A. de Oliveira, S. M. Martins, A. Aliverti, L. de Andrade Carvalho, J. F. do Nascimento Junior, L. Alcoforado, I. Remígio, and A. D. de Andrade, "Chest wall regional volume in heart failure patients during inspiratory loaded breathing.," Respir. Physiol. Neurobiol., vol. 180, no. 2–3, pp. 269–274, Mar. 2012.

[113] J. Boudarham, D. Pradon, H. Prigent, L. Falaize, M.-C. C. Durand, H. Meric, M. Petitjean, and F. Lofaso, "Optoelectronic plethysmography as an alternative method for the diagnosis of unilateral diaphragmatic weakness.," Chest, vol. 144, no. 3, pp. 887–95, Sep. 2013.

[114] H. Meric, L. Falaize, D. Pradon, D. Orlikowski, H. Prigent, and F. Lofaso, "3D analysis of the chest wall motion for monitoring late-onset Pompe disease patients.," Neuromuscul. Disord., vol. 26, no. 2, pp. 146–52, Feb. 2016.

[115] A. Mezzani, P. Agostoni, A. Cohen-Solal, U. Corrà, A. Jegier, E. Kouidi, S. Mazic, P. Meurin, M. Piepoli, A. Simon, C. Van Laethem, and L. Vanhees, "Standards for the use of cardiopulmonary exercise testing for the functional evaluation of cardiac patients: a report from the Exercise Physiology Section of the European Association for Cardiovascular Prevention and Rehabilitation.," Eur. J. Cardiovasc. Prev. Rehabil., vol. 16, no. 3, pp. 249–67, Jun. 2009.

[116] J. Dickinson, A. McConnell, E. Ross, P. Brown, and J. Hull, "The BASES Expert Statement on Assessment and Management of Non-asthma Related Breathing Problems in Athletes," 2015.

[117] J. Dickinson, G. Whyte, and A. McConnell, "Inspiratory muscle training: a simple cost-effective treatment for inspiratory stridor.," Br. J. Sports Med., vol. 41, no. 10, pp. 694–5; discussion 695, Oct. 2007.

[118] A. M. Layton, C. E. Garber, R. C. Basner, and M. N. Bartels, "An assessment of pulmonary function testing and ventilatory kinematics by optoelectronic plethysmography," Clin. Physiol. Funct. Imaging, vol. 31, no. 5, pp. 333–336, Sep. 2011.

[119] A. M. Layton, C. E. Garber, B. M. Thomashow, R. E. Gerardo, B. O. Emmert-Aronson, H. F. Armstrong, R. C. Basner, P. Jellen, and M. N. Bartels, "Exercise ventilatory kinematics in endurance trained and untrained men and women," Respir. Physiol. Neurobiol., vol. 178, no. 2, pp. 223–229, Sep. 2011.

[120] A. M. Layton, S. L. Moran, C. E. Garber, H. F. Armstrong, R. C. Basner, B. M. Thomashow, and M. N. Bartels, "Optoelectronic plethysmography compared to spirometry during maximal exercise.," Respir. Physiol. Neurobiol., vol. 185, no. 2, pp. 362–8, Jan. 2013.

[121] I. Vogiatzis, A. Aliverti, S. Golemati, O. Georgiadou, A. LoMauro, E. Kosmas, E. Kastanakis, and C. Roussos, "Respiratory kinematics by optoelectronic plethysmography during exercise in men and women.," Eur. J. Appl. Physiol., vol. 93, no. 5–6, pp. 581–7, Mar. 2005.

Chapter III - OEP application to spinal cord injured patients.

Introduction

A clear correlation utility of motion capture analysis os in the evaluation of breathing kinematics of patients suffering from chest wall mechanical or neurological impairment. Lung function is usually studied with spirometry or with pneumotachograph, which are unable to detect neither if a mechanical distortion in the chest wall ventilatory pattern exists or if a segmental abnormality drives to breathing impairment. In spinal cord injured (SCI) subjects chest wall compartments are differently affected depending on the level of the lesion, therefore a tool able to analyse separately the movement of each part of the chest wall would be useful [1-9]. Plethysmography has been extensively used for the study of respiratory motion in healthy subjects under different conditions (cough, speech, singing and walk) [10-12]. In a clinical setting the OEP was at first used for the evaluation of patients with chronic obstructive pulmonary disease, in order to study chest wall volume regulation according to illness severity [13], the efficacy of respiratory rehabilitation and the response to exercise [14-16]. More recently this technique was used to evaluate the kinematics of the chest wall and its components in patients affected by ankylosing spondylitis and hemiplegia [17,18] and the efficacy of cough in patients with neuromuscular diseases [19]. In all of these studies, the OEP was compared with spirometry, providing the same reliability and validity. In the following section it is reported the findings of a study carried out by the author in collaboration with Miccinilli et al [20], the effect of posture (sitting and supine) on respiratory kinematics in chronic SCI subjects and the differences between paraplegia and tetraplegia has been investigated by means of OEP. Breathing pattern was assessed studying the contribution of each thoracic-abdominal compartment to respiratory kinematics and the degree of synchronization among the different compartments, as well as OEP-derived lung functional parameters.

To this purpose, a cross-sectional study involving patients diagnosed with radiologically confirmed post-traumatic spinal cord injury was set up. Twenty chronic SCI patients (distance from onset > 1

year), referring to a Spinal Cord Hospital Unit were enrolled and compared to twenty healthy subjects matched for gender, age and lifestyle (in particular for smoking habits).

The level of the lesion was cervical (ranging from C3 to C7) in 9 patients (tetraplegics) and thoracic (ranging from T1 to T8) in 11 patients (paraplegics). Each patient underwent neurological evaluation according to the American Spinal Injury Association (ASIA) standards. Demographic and clinical characteristics of healthy and SCI subjects are reported in Table 1.

Table 1. Demographic and clinical characteristics of healthy and SCI subjects.

Study group	Age	Sex	Time from injury (months)	AIS (A-E)
Paraplegics (n=11)	36.6 ± 10.3	9M / 2F	81.1 ± 95.0	9A / 1B / 1C
Tetraplegics (n=9)	29.4 ± 10.5	7M / 2F	71.4 ± 70.8	6A / 0B / 3C
Controls (n=20)	33.6 ± 10.5	16M/4F	-	-

AIS: American Spinal Injury Association (ASIA) Impairment Score

To avoid possible confounding biases, the following exclusion criteria were defined: presence of airways/lung diseases (asthma, chronic bronchitis, etc.), presence of cardiac pathologies, use of drugs influencing breathing or cardiac activity or any condition which could have influenced patients' compliance.

Experimental protocol

Volume variations of the chest wall (CW) and of its compartments were measured by means of OEP. Three different compartments contributing to CW were analyzed: Pulmonary Rib Cage (RCp), corresponding to lungs, Abdominal Rib Cage (RCa), corresponding to diaphragm costal insertion, and Abdomen (AB); thus RCp + RCa = RC and RC + AB = CW (Figure1).

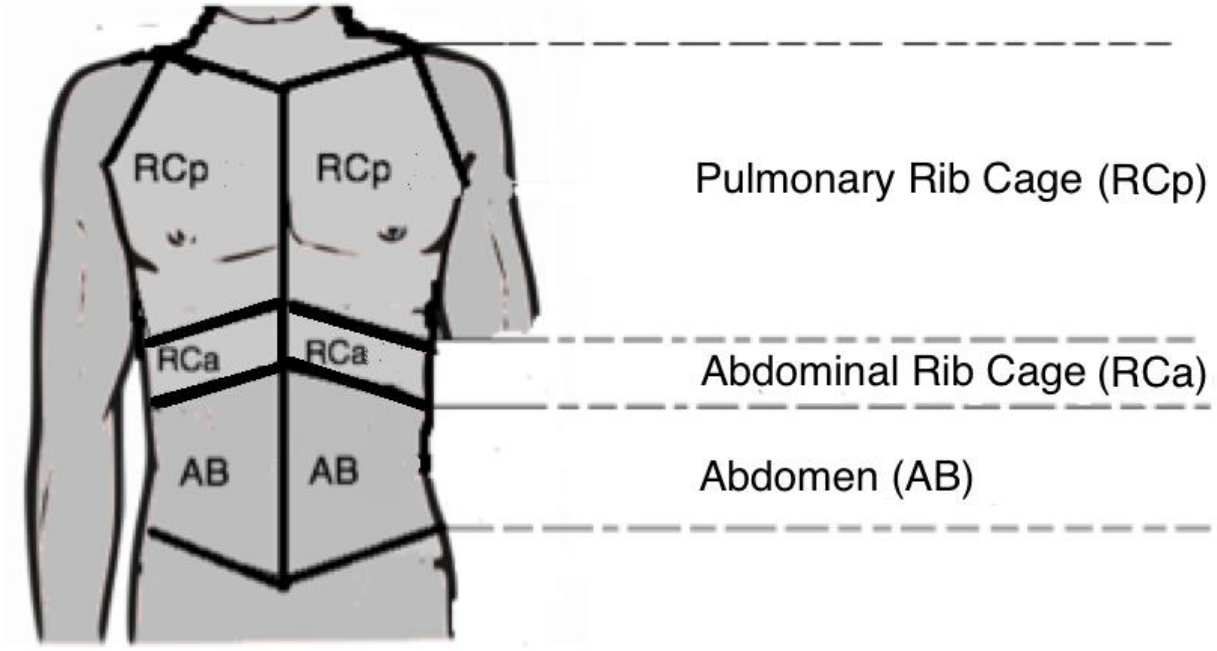

Figure 1. OEP compartmental volumes. Thoracic-abdominal wall divided into three compartments (RCp: Pulmonary Rib Cage, RCa: Abdominal Rib Cage, AB: Abdomen).

OEP compartmental volumes were measured in healthy and SCI subjects, in two different postures (sitting in the wheelchair and in supine position) during both quiet breathing (QB) and hyperventilation (HP). Thus, four experimental conditions were obtained: 1) sitting-QB; 2) sitting-HP; 3) supine-QB 4) supine-HP. One trial was performed for each condition. During each QB trial patients were asked to breath normally for 2 min; during HP trials patients were asked to breath in and out deeply for 1 min.

Additional trials were performed to derive respiratory functional parameters (VC, FEV1) in sitting and in supine position, in both healthy and SCI subjects. Two main parameters were considered: a) expiratory Vital Capacity (VC) (patients were asked to breath in until inspiratory capacity was reached and then to slowly breathe out until residual volume was reached) and b) Forced Expiratory Volume in the first second (FEV1) (patients were asked to make a maximal inspiration immediately followed by a quick and forced expiration); FEV1 was equal to the air volume exhaled during the

first second of the expiratory maneuver started from the level of Total Lung Capacity. The arithmetic mean of three FEV1 measures was computed.

Opto-Electronic Plethysmography

The OEP system is composed by a series of retro-reflective passive markers, fixed on thoracic-abdominal surface by means of a bi-adhesive tape, and a number of special cameras equipped with CCDs (solid-state charge-coupled devices) which operate at a rate of up to 100 fps, synchronized with coaxial infrared flashing light-emitting diodes. This system is therefore able to detect the movement of the CW during breathing measuring spatial displacements of markers placed on specific anatomical landmarks. The OEP system is also mouthpiece and noseclips-free: in this way a non-invasive recording can be provided.

A registration setup based on 52 markers, placed on the anterior and lateral surface of the thoracic-abdominal wall, and six infrared cameras was used (Figure 2A and 2B).

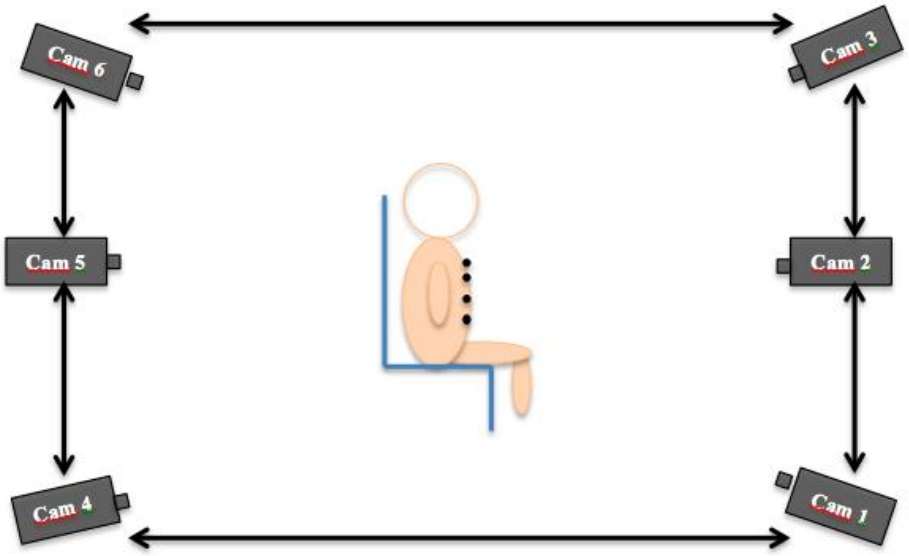

Figure 2A. Experimental setup. OEP: schematic representation of patient in sitting position.

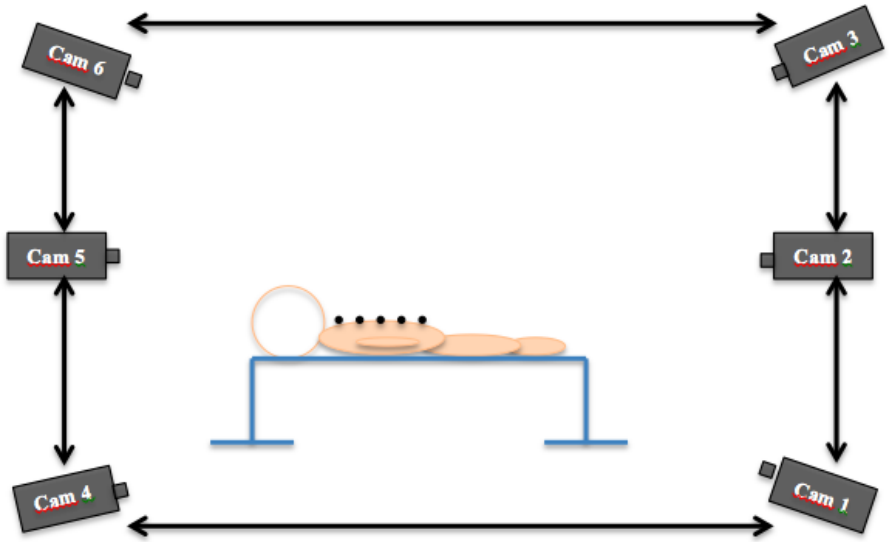

Figure 2B. Experimental setup. OEP: schematic representation of patient in supine position.

The three-dimensional (3D) coordinates of the different markers are computed using stereo-photogrammetric methods. The next step is to compute the volume obtained connecting the marker points to form triangles (using Gauss's theorem) that overall describe a closed surface. Volume accuracy, according to manufacturer's specifications, is between 0.02 and 0.2 L depending on patient's placement and on the calibration process. Starting from the measured points a special Ward's geometrical modelling of the chest wall is developed to describe its surface [7,8,20].

Phase angle analysis

The thoracic-abdominal asynchrony was quantified measuring the phase shift between the RCp and AB volume using the phase angle analysis, as already done in previous studies [22,23]. Phase angle analysis shows the relationship between RCp and AB movements and changes in shape of RCp and AB by continuous monitoring. Phase angle (θ) is calculated as: $\theta=\sin^{-1}(m/s)$, where m is the

distance between the two midpoints of the RCp excursion and *s* represents the AB excursion (Figure 3).

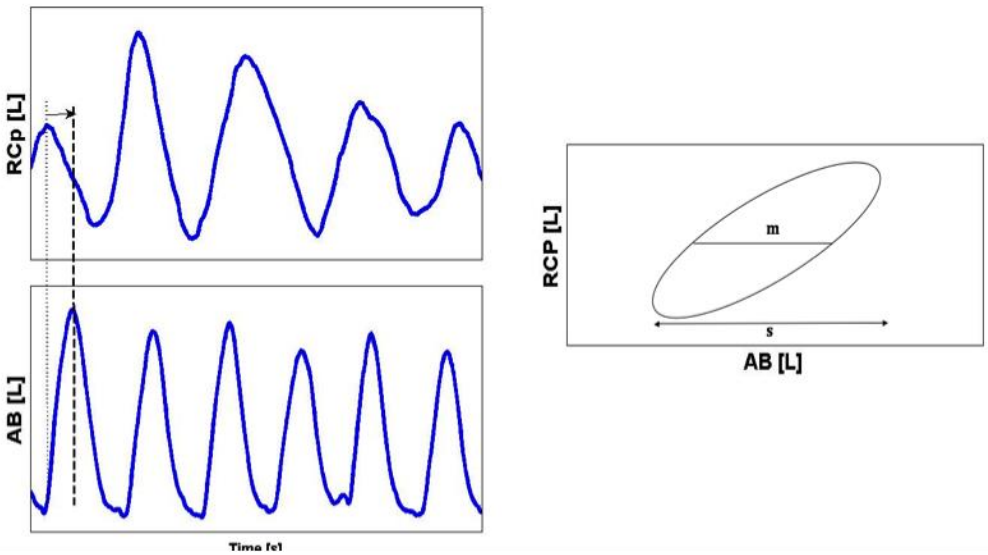

Figure 3. Phase angle analysis. m is the distance between the two midpoints of the RCp excursion and s represents the AB excursion.

RC and AB movements can be continuously displayed as an X-Y plot giving optical information about changes in loop shape and loop direction. A closed or very narrow loop with a positive slope on the X-Y plot is produced if RC and AB expand and decrease in synchrony. As RC and AB asynchrony worsens the loop opens and becomes progressively wider and the phase lag between the RC and AB movements increases until the phase angle reaches 90°. Above a phase angle of 90°, the loop starts to narrow again with increasing asynchrony, but its slope turns progressively negative. Complete paradoxical motion of the RC and AB also creates a closed or very narrow loop, but with a negative slope [22]. In order to assess the timing-relationship of the movement of the thoracic and the abdominal wall Konno and Mead plots were done [24]. Direction of loop rotation depends on which compartment (RC or AB) precedes the other. Anticlockwise loops indicate that the AB compartment (diaphragm) leads the RC, as usually observed in normal QB; on the contrary, clockwise loop means that RC movement precedes AB movement. Konno and Mead diagrams were

obtained plotting on the horizontal axis data relating to the movement of the RCp and on the ordinate axis, data relating to the movement of the AB during the whole breathing cycle in QB.

Statistical analysis

OEP compartmental volumes and OEP-derived lung volumes were analyzed by means of analysis of variance (ANOVA). For compartmental volumes, a three-way factorial model was used, with 'Disease' (2 levels: control/SCI), 'Posture' (2 levels: sitting/supine) and 'Type of breathing' (2 levels: QB/HP) as main factors. For lung volumes, we used a two-way factorial model, with 'Disease' (2 levels: control/SCI) and 'Posture' (2 levels: sitting/supine) as main factors. Post-hoc comparisons by means of t-tests were performed to analyze differences of interest within and between study groups. Phase angle values in sitting and supine position were compared by means of paired t-tests.

Results

Respiratory compartmental volumes

Three-way factorial ANOVA was performed in order to analyze the influence of disease, posture and type of breathing on respiratory compartmental volumes. Post-hoc comparisons were then performed in order to analyze differences within and between study groups in different experimental conditions. Figure 4 shows values of compartmental volumes in SCI patients and control subjects, in the different postural (sitting/supine) and breathing (QB/HP) conditions.

Effect of disease

ANOVA showed a significant effect of 'Disease' factor (controls/SCI patients) on CW ($F_{1,154}$=16.43; P=0.0001), RC ($F_{1,154}$=26.22; P<0.0001), RCp ($F_{1,154}$=22.52; P<0.0001) and RCa ($F_{1,154}$=22.43; P<0.0001) volumes. This reflects the global reduction of total and thoracic volumes in SCI patients in all experimental conditions. Compartmental volumes differences between patients and healthy subjects are summarized in Table 2.

Table 2. Effects of disease.

	RCp	**RCa**	**RC**	**AB**	**CW**
Sitting QB					
SCI	**↓↓**	↓↓	**↓↓**	=	↓
Para	**↓↓**	↓	**↓↓**	=	↓
Tetra	**↓↓**	↓↓↓	**↓↓**	↑	=
Sitting HP					
SCI	**↓↓↓**	**↓↓↓**	**↓↓↓**	↓	**↓↓↓**
Para	**↓↓↓**	**↓↓↓**	**↓↓↓**	↓↓	**↓↓↓**
Tetra	**↓↓↓**	**↓↓↓**	**↓↓↓**	**=**	**↓↓↓**

Volume differences between spinal cord injured (SCI), paraplegic (Para), tetraplegic (Tetra) and control subjects are coded as follows: = 80-120% of volume of control condition; ↑ 121-150% of volume of control condition; ↑↑ 151-200% of volume of control condition; ↑↑↑ 201-400% of volume of control condition; ↑↑↑↑ >400% of volume of control condition; ↓ 79-67% of volume of control condition; ↓↓ 66-50% of volume of control condition; ↓↓↓ 49-25% of volume of control condition; ↓↓↓↓ <25% of volume of control condition. Bold symbols represent significant variations (two-tail unpaired t-test, $p<0.05$). QB: quite breathing; HP: hyperventilation.

Post-hoc comparisons show that, in sitting position and QB, SCI patients have lower RC volume compared to controls (0.18±0.08 vs 0.31±0.2 l, $p<0.01$), while abdominal volume is comparable between patients and controls (0.16±0.11 vs 0.14±0.12 l, $p=0.53$). This accounts for a greater contribution of abdominal expansion, and a lesser contribution of RC expansion, to the total CW volume in SCI patients (AB/CW ratio: 46±16% vs 29±9%, $p<0.001$) (Figure 4, Table 2). In the standard sitting position, the differences between patients and healthy subjects become more evident during HP, that requires the activation of voluntary muscles, with lower RC and AB volumes in SCI subjects (RC: 0.67±0.55 vs 1.55±0.83 l, $p<0.001$; AB: 0.28±0.16 vs 0.41±0.31 l, $p=0.11$) (Figure 4, Table 2). The comparison of paraplegics and tetraplegics in sitting position reveals that in tetraplegics, during both QB and HP, the total CW volume is composed by a significantly greater contribution of AB and, parallely, by a lesser contribution of RC compartment (AB/CW ratio during QB: 55±16% vs 39±13%, $p<0.05$; AB/CW ratio during HP: 39±8% vs 27±10%, $p<0.05$; Figure R1).

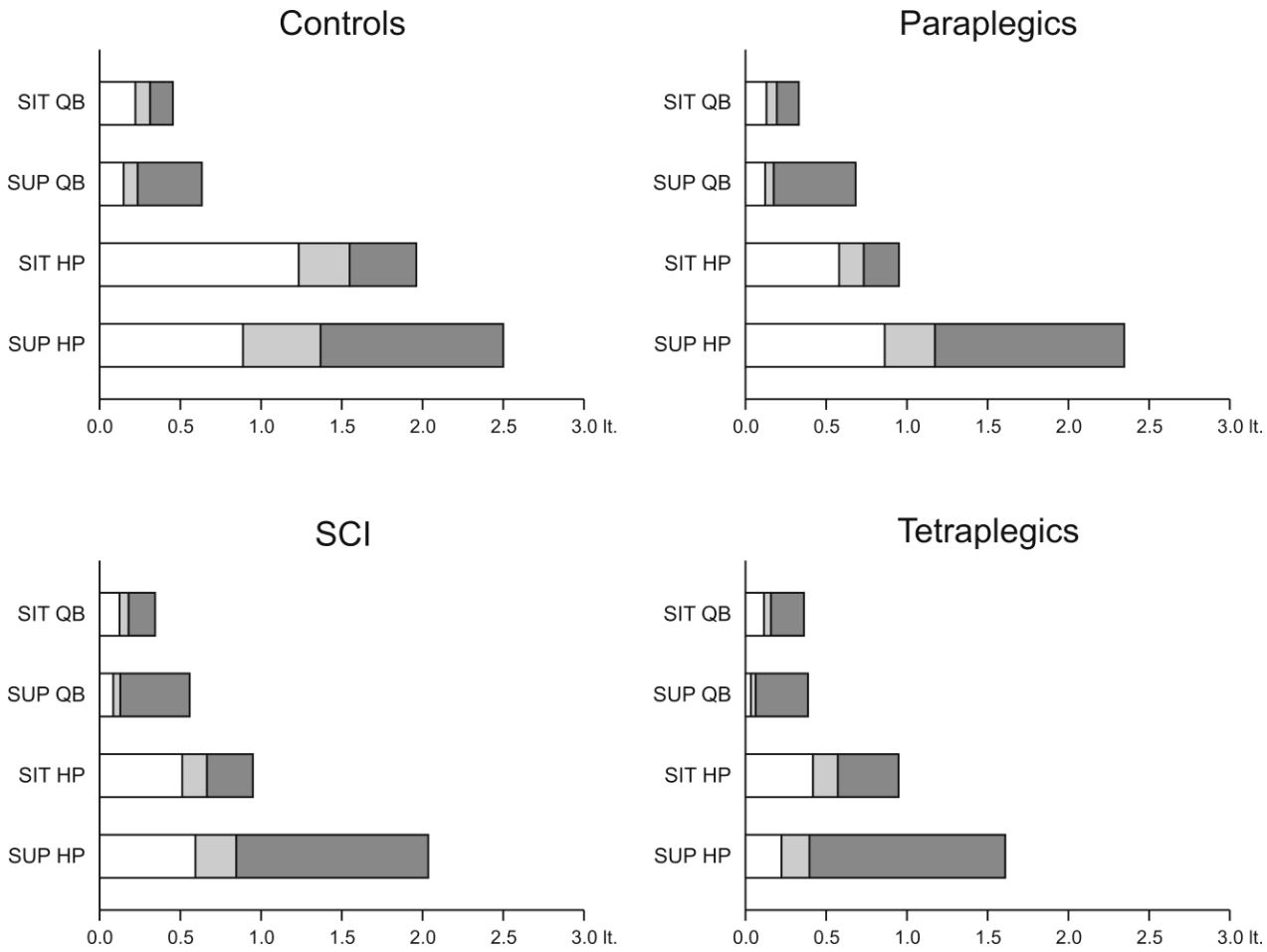

Figure 4. Results for compartmental volumes analysis. Compartmental volume variations in control, SCI patients, paraplegic and tetraplegic subjects, measured in the different positions (SIT: sitting; SUP: supine) and breathing conditions (QB: quite breathing; HP: hyperventilation).

Effect of posture

ANOVA showed a significant effect of 'Posture' (sitting/supine) on CW ($F_{1,154}$=24.23; P<0.0001), AB ($F_{1,154}$=134.5; P<0.0001), and RCa ($F_{1,154}$=6.29; P=0.013) volumes. Table 3 summarizes the direction and size of compartmental volume variations passing from sitting to supine position. Post-hoc comparisons show that during QB, both in SCI and in control subjects total CW volume is increased: this is determined by a markedly increased abdominal expansion despite a less pronounced reduction of RC expansion. Nanely, in supine compared to sitting position, CW volume

was increased by 62% in SCI patients (0.56±0.37 vs 0.34±0.15 l, $p<0.05$) and of 40% in controls (0.63±0.27 vs 0.45±0.30 l, $p<0.05$); AB volume was increased of 161% in SCI patients (0.43±0.34 vs 0.16±0.11 l, $p<0.01$) and of 180% in controls (0.40±0.13 vs 0.14±0.12 l, $p<0.0001$); RC volume was non significantly decreased of 29% in SCI patients (0.13±0.11 vs 0.18±0.08 l, $p=0.14$) and of 24% in controls (0.24±0.17 vs 0.31±0.20 l, $p=0.12$).

Table 3. Effects of posture.

	RCp	**RCa**	**RC**	**AB**	**CW**
Controls					
QB	**↓**	=	**↓**	**↑↑↑**	**↑**
HP	**↓**	**↑↑**	=	**↑↑↑**	**↑**
SCI					
QB	↓	↓	↓	**↑↑↑**	**↑↑**
HP	=	**↑↑**	↑	**↑↑↑↑**	**↑↑↑**
Paraplegics					
QB	=	=	=	**↑↑↑**	**↑↑↑**
HP	↑	**↑↑**	↑↑	**↑↑↑↑**	**↑↑↑**
Tetraplegics					
QB	**↓↓↓**	↓	**↓↓↓**	↑↑	=
HP	**↓↓**	=	↓	**↑↑↑**	**↑↑**

Volume variations from sitting to supine position are coded as follows: = 80-120% of volume in sitting condition; ↑ 121-150% of volume in sitting condition; ↑↑ 151-200% of volume in sitting condition; ↑↑↑ 201-400% of volume in sitting condition; ↑↑↑↑ >400% of volume in sitting condition; ↓ 79-67% of volume in sitting condition; ↓↓ 66-50% of volume in sitting condition; ↓↓↓ 49-25% of volume in sitting condition; ↓↓↓↓ <25% of volume in sitting condition. Bold symbols represent significant variations (two-tail paired t-test, $p<0.05$). QB: quite breathing; HP: hyperventilation.

Thus, in supine position and QB abdominal volume contributes to the greatest part of CW expansion, both in SCI (75±17% vs 46±16% of sitting position, $p<0.0001$) and control subjects (65±12% vs 29±9% of sitting position, $p<0.0001$). Moreover, in supine position we found a significant difference between AB/CW ratio in SCI patients compared to healthy subjects (75±17% vs 65±12%, $p<0.05$) (Figure 4). The sub-analysis on paraplegic and tetraplegic patients reveals that

tetraplegics have a significantly lower RC expansion in supine position (0.06±0.03 vs 0.17±0.12 l, $p<0.05$; Table 2), with AB compartment becoming the largely prevalent contributor to the total CW expansion in this respiratory condition (AB/CW ratio: 81±8%; Figure 4). Moreover, when considering the compartmental volume variations in the passage from sitting to supine position, paraplegics show a significantly increased AB and total CW expansion (AB: 0.51±0.41 vs 0.14±0.11 l, $p<0.01$; CW: 0.68±0.42 vs 0.33±0.19 l, $p<0.01$), while tetraplegics have a significantly reduced RCp and RC expansion (RCp: 0.03±0.02 vs 0.11±0.04 l, $p<0.01$; RC: 0.06±0.03 vs 0.16±0.05 l, $p<0.01$), that is partially balanced by a non-significantly increased AB expansion (0.32±0.18 vs 0.20±0.09 l, $p=0.16$), with a net effect of an unvaried total CW volume (0.39±0.19 vs 0.36±0.06 l, $p=0.75$) (Table 3).

Effect of type of breathing

ANOVA showed a significant effect of 'Type of breathing' (QB/HP) on all compartmental volumes: CW ($F_{1,154}=111.11$; $P<0.0001$), RC ($F_{1,154}=123.37$; $P<0.0001$), RCp ($F_{1,154}=113.88$; $P<0.0001$), RCa ($F_{1,154}=87.08$; $P<0.0001$) and AB ($F_{1,154}=103.82$; $P<0.0001$) volumes. This reflects the global increase of thoracic and abdominal volumes during HP in all study groups and postural conditions (Table 4). We also found a significant 'Disease' × 'Type of breathing' interaction for all compartmental volumes, except for AB: CW ($F_{1,152}=9.91$; $P<0.01$), RC ($F_{1,152}=13.11$; $P<0.001$), RCp ($F_{1,152}=11.85$; $P<0.001$), RCa ($F_{1,152}=9.82$; $P<0.01$). The comparison between SCI and control subjects shows that in the SCI group there is a significantly lower increase of CW and AB volumes induced by HP (expressed as HP/QB ratio) in sitting position (CW: 3.0±2.4 vs 4.8±1.9, $p<0.05$; AB: 2.0±1.0 vs 3.3±1.5, $p<0.01$) (Figure 4). Moreover, we found a significant 'Posture' × 'Type of breathing' interaction for CW ($F_{1,152}=9.01$; $P<0.01$), AB ($F_{1,152}=35.56$; $P<0.0001$) and RCa volumes ($F_{1,152}=8.02$; $P<0.01$). This is related to the overall more pronounced increase of respiratory volumes due to HP in supine than in sitting position: the comparisons of these variations in supine

versus sitting position, expressed as HP/QB ratio, revealed a significant variation of RCa in SCI and healthy subjects and of AB only in the SCI group (RCa in SCI: 7.4±7.1 vs 3.6±3.2, $p<0.05$; RCa in controls: 7.1±4.7 vs 4.6±3.2, $p<0.05$; AB in SCI: 3.7±2.1 vs 2.0±1.0, $p<0.01$; AB in controls: 2.9±0.9 vs 3.3±1.5, $p=0.2$) (Figure 4). No significant differences were found from the comparison of volume variations induced by HP between paraplegics and tetraplegics, both in sitting and in supine position.

Table 4. Effects of breathing.

	RCp	**RCa**	**RC**	**AB**	**CW**
Controls					
Sitting	**↑↑↑**	**↑↑**	**↑↑**	**↑**	**↑↑**
Supine	**↑↑↑**	**↑↑↑**	**↑↑↑**	**↑**	**↑↑**
SCI					
Sitting	**↑↑**	**↑**	**↑**	**↑**	**↑**
Supine	**↑↑↑↑**	**↑↑↑**	**↑↑↑↑**	**↑**	**↑↑**
Paraplegics					
Sitting	**↑↑**	**↑**	**↑**	**↑**	**↑**
Supine	**↑↑↑↑**	**↑↑↑**	**↑↑↑↑**	**↑**	**↑↑**
Tetraplegics					
Sitting	**↑↑**	**↑↑**	**↑↑**	**↑**	**↑**
Supine	**↑↑↑↑**	**↑↑↑**	**↑↑↑**	**↑↑**	**↑↑**

Volume variations from QB (quiet breathing) to HP (hyperventilation) are coded as follows: = 80-120% of volume in QB; ↑ 121-400% of volume in QB; ↑↑ 401-600% of volume in QB; ↑↑↑ 601-800% of volume in QB; ↑↑↑↑ >800% of volume in QB. Bold symbols represent significant variations (two-tail paired t-test, $p<0.05$).

Pulmonary function testing

Figure 5 shows OEP-derived lung volumes (VC and FEV1) measured in sitting and supine position in SCI and control individuals. A global analysis of VC and FEV1 data was initially performed by means of two-way ANOVA on each parameter. ANOVA on VC showed a significant effect of 'Disease' ($F_{1,76}=18.41$; $P<0.0001$), of 'Posture' ($F_{1,76}=11.70$; $P<0.01$) and of 'Disease' × 'Posture' interaction ($F_{1,74}=4.31$; $P<0.05$). ANOVA on FEV1 revealed a tendency to a significant effect of

'Disease' ($F_{1,76}$=3.23; P=0.08), a significant effect of 'Posture' ($F_{1,76}$=10.58; P<0.01) and a tendency to a significant effect of 'Disease' × 'Posture' interaction ($F_{1,74}$=3.35; P=0.07).

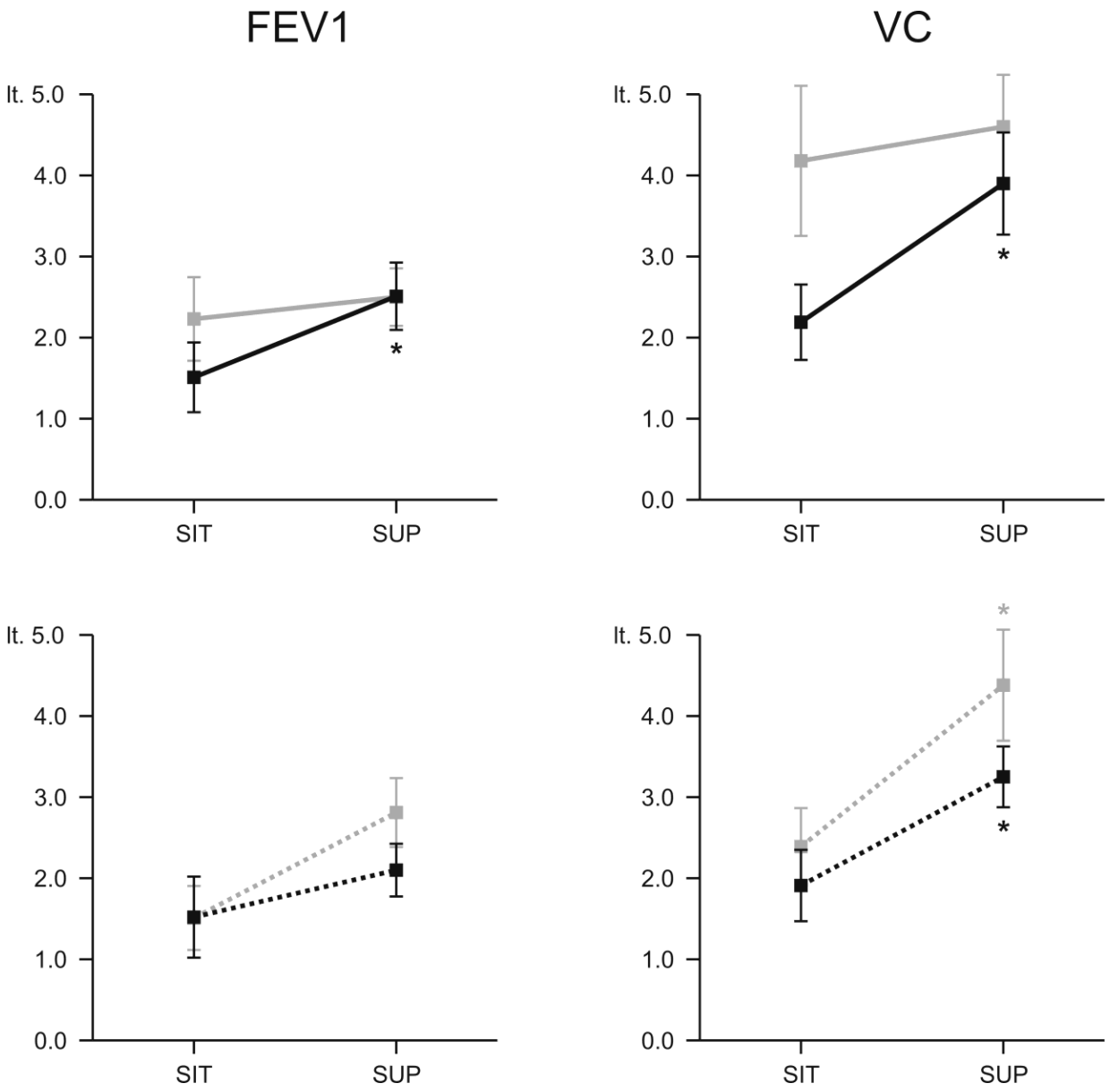

Figure 5. Results for pulmonary function analysis. OEP-derived lung volumes in control (gray line), SCI (black line), paraplegic (gray dotted line) and tetraplegic (black dotted line) subjects, measured in sitting (SIT) and supine (SUP) positions. VC: vital capacity; FEV1: forced expiratory volume in the 1st second. * p<0.05 (supine vs sitting condition).

Individual comparisons show that, in sitting position, volumes are significantly lower in SCI compared to control subjects, both for VC (2.19±0.93 vs 4.18±1.86 l, $p<0.001$) and FEV1 (1.51±0.86 vs 2.23±1.03 l, $p<0.05$). Supine position restores a near to normal ventilation in SCI patients, mainly due to a marked increase of volumes in supine position in this group: indeed, the increase of VC was 79% in SCI ($p<0.0001$) compared to 10% ($p>0.05$) of control subjects and the increase of FEV1 was 66% in SCI ($p<0.001$) compared to 12% ($p>0.05$) of controls. This determines a tendency towards a normalization of the SCI/control volume ratio in the passage from sitting to supine position, both for VC (0.85 vs 0.52) and FEV1 (1.00 vs 0.68). A separate analysis for paraplegic and tetraplegic patients revealed a similar trend in the two groups towards a normalization of lung volumes in supine position: the increase of both VC and FEV1 was more pronounced in paraplegic (VC: 84%, $p<0.01$; FEV1: 86%, $p<0.01$) than in tetraplegic patients (VC: 70%, $p=0.22$; FEV1: 39%, $p=0.15$).

Phase angle analysis

The phase angle θ was computed in sitting and supine position for the group of healthy patients, the group of paraplegic patients and the group of tetraplegic patients. The results, reported in Table 5, showed that in healthy subjects θ was equal to 6°±2 in sitting position, and equal to 8°±3 in supine position. In the group of paraplegic patients θ was equal to 16°±4 in sitting position and increased to 23°±6 in supine position. The same analysis for tetraplegic patients showed a phase angle of 28°±6 in sitting position and of 47°±10 in supine position. In sitting position phase angle values were lower than in supine position for all groups ($p<0.05$).

Table 5. Mean values of phase angle analysis for healthy, paraplegic and tetraplegic subjects.

	Sitting	**Supine**
Controls	6±2°	8±3°
Paraplegics	16±4°	23±6°
Tetraplegics	28±6°	47±10°

Konno and Mead diagram

Konno and Mead diagrams were constructed for healthy, paraplegic and tetraplegic subjects both in sitting and in supine position considering one entire respiratory act for each examined subject in QB (Figure 6). In all subjects Konno and Mead loops presented a positive slope and a counterclockwise direction. In healthy subjects Konno and Mead plots resulted in curve similar to a straight line both in sitting and in supine position. Paraplegic subjects, instead, presented an ellipse shaped loop in sitting position, which became wider in supine position. The same behaviour was observed in tetraplegic subjects, with even wider loops.

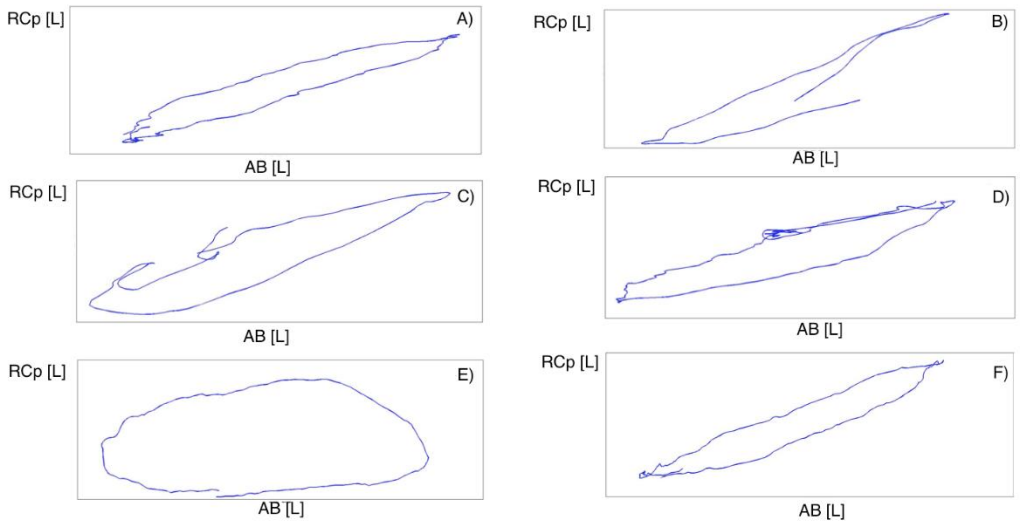

Figure 6. Konno and Mead diagrams. From top to bottom Konno and Mead loops for one healthy subject, one paraplegic subject and one tetraplegic subject (supine position on the left, sitting position on the right).

Discussion

Respiratory functional parameters

In the present study VC and FEV1, indirectly obtained by OEP, were used as synthetic parameters of respiratory function. SCI patients presented overall lower values of VC and FEV1 than healthy subjects. These data agree with data derived from spirometry already described in literature: in tetraplegic and paraplegic subjects with high lesion level there is a restrictive dysfunction due to neuromuscular weakness, characterized by a significant reduction in VC, FEV1, as well as total lung capacity (TLC), expiratory reserve volume (ERV) and inspiratory capacity (IC), together with a significant increase in residual volume (RV) and a reduced or equal functional residual capacity [25-31].

We also observed that VC and FEV1 were significantly influenced by posture. In particular such values were smaller in sitting position in SCI patients compared to the control group and increased in supine position for both groups, but sensibly more for the group of SCI patients (VC +79%, FEV1 +66%). These data are in accordance with previous studies conducted with spirometry [32-35], which showed that FVC, IC and FEV1 increase in supine position. Authors hypothesised that in such position diaphragm increases its inspiratory excursion, since its muscle fibers are longer and operate at a more favourable point of their length/tension curve. According to this hypothesis supine position in SCI subjects would therefore restore a normal ventilatory condition. To this point believing that SCI patients breath better in supine than in sitting position would be reasonable.

The comparison between paraplegics and tetraplegics showed that lung functional parameters values were lower for tetraplegics than for paraplegics, although these differences did not reach significance. These findings are coherent with those reported in literature and, in particular, with data from Baydur's study [32], even if in this study tetraplegic patients showed much lower values than paraplegics. This difference could be explained observing that in our study paraplegic patients had an injury level between T1 and T8, whereas in Baydur's study the lesion level ranged between T1 and L4: since the same authors showed that functional parameters improve with the lowering of the lesion, it might be that these patients had less severe impairment than paraplegic patients of our study. The power in detecting differences between paraplegic and tetraplegic patients is also limited by the small sample size.

Breathing kinematics

In order to understand if supine position facilitates breathing, respiratory kinematics was studied. OEP, infact, allows the analysis of volume variations of CW and of its compartments with relation to posture. This is not possible with common spirometry.

Data of the present study show that the "disease" factor has a determinant effect on volume variations of thorax and CW in every condition, since RC and CW are reduced in SCI patients

compared to healthy subjects, whereas AB is comparable between the two groups. In SCI subjects there is a smaller contribution of RC and a greater contribution of AB to total CW volume in every condition. These differences are even more evident in HP. Chronic SCI patients, indeed, undergo progressively reduced compliance of the rib cage, due to denervation of intercostal muscles, spasticity and increased stiffness of joints and ligaments. Increased compliance of the abdomen is observed in the meanwhile, due to muscle denervation[1]. The analysis of "posture" showed that in supine position the more involved compartment is AB in both groups, but in particular in SCI subjects. This phenomenon could be considered strange, since in the group of patients abdominal wall is denervated and a voluntary activation of AB is not possible. However it is our opinion that, as previously described [1,29], abdominal content in supine position, is moved towards diaphragm, and, acting as an abdominal press, the diaphragm increases its radium of curvature. In this way this muscle can work at a more favourable point of its tension/length curve. Abdominal fulcrum also provides appositional forces at the insertion of diaphragm to the lower ribs, allowing diaphragm fibers to be parallel oriented to the intercostal insertions, instead of being perpendicular. This causes the expansion of the lower portion of the rib cage and the consequent increase of abdominal excursions.

As for "type of breathing" factor, an interaction with posture and disease is witnessed. In HP there is a global increase of both thoracic and abdominal volumes in all groups, but to a lesser extent in the group of SCI patients. In healthy subjects accessory breathing muscles (scalene, sternocleidomastoids, trapezii, pectoralis major) are used to increase intensity and frequency of respiration. Tetraplegic patients lack of intercostal muscles, which are almost denervated. For this reason in QB accessory breathing muscles, which are preserved in our sample group, are already recruited to replace the lost function of intercostals and work almost to the top level of their performance. In HP, therefore, there is fewer muscle reserve to be used in SCI patients with respect to healthy subjects. At the same time abdominal muscles, which in healthy subjects act as voluntary

muscles during HP, are not working in SCI subjects. However, an increased excursion of AB is witnessed since diaphragmatic function is preserved and this muscle is voluntary recruited.

Synchronization of thorax and abdomen during breathing

Previous considerations about respiratory mechanics seem to encourage the opinion that chronic SCI patients regain part of respiratory function in supine position, because diaphragm works more efficiently. However, in order to examine in depth the behaviour of SCI patients we used data derived from the OEP to make phase angle analysis and Konno and Mead diagrams, highlighting some issues that usual spirometry is not able to point out. Phase angle analysis showed that, in all groups, the phase angle θ increased in supine position, meaning that in this posture the phase shift between RCp and AB increased. However, in the group of healthy subjects in any position, the phase angle was lower, meaning that movement of RCp and AB was mostly synchronous. In the group of paraplegic patients, instead, θ was higher than in healthy subjects in both postures and the phase shift between compartments increased in supine position. This behaviour was even more evident in the group of tetraplegic patients, meaning that the phase shift between the two compartments was even higher. This accounts for a less favourable thoracic-abdominal mechanics in supine position. In examined subjects the direction of the Konno and Mead loop was counterclockwise, therefore the AB (diaphragm) movement preceded the RC (intercostal muscles). This is possible thanks to the preservation of the diaphragm in this SCI sample.

The Konno and Mead model is one of the first models of the thoracic-abdominal wall motion described in literature. The analysis was based on the assumption that when muscles contract weakly, the deformation of the rib cage and of the abdominal wall can be considered negligible. According to this hypothesis, the thoracic-abdominal wall, in a given posture, can be considered as a system consisting of two parts, the rib cage and the abdomen-diaphragm system, which can move independently one another. Each one of these two parts is represented by a free coordinate (the

volume), therefore the system has two degrees of freedom. In the presence of a constraint, when the system is closed (i.e., the airways are closed), the system has only one degree of freedom, therefore changes in volume of the rib cage must be equal and opposite to those of the abdomen, namely both compartments must move in phase. Konno and Mead demonstrated that, for a given lung volume, there is one only relationship between the rib cage and the abdomen movement (isovolumic line), assuming that the spine doesn't extend. Isovolumic lines are almost parallel, and therefore the relationship between movement and volume changes for both parts is approximately linear. In clinical terms this means that during QB the coordination of the diaphragm, the intercostal muscles and scalene muscles allows the thoracic-abdominal wall to move with one degree of freedom along its line of relaxation, which results from graphically plotting the chest motion against the abdominal motion during the passive lung inflation. Breathing along this line represents the optimal efficiency of the respiratory system [24].

Konno and Mead analysis showed that, while the curve of the healthy subjects group is very close to a straight line and then to the relaxation line, paraplegic and tetraplegic subjects show an ellipse-shaped loop. This means that thorax and abdomen don't move in phase any more and that the respiratory system works less efficiently. The deviation from the normal relaxation line is particularly evident in tetraplegic subjects. In this condition, the synchronous contraction of the neck muscles, including the sternocleidomastoid, the trapezius, the platysma, the mylohyoid and the sternohyoid muscle, acts in order to push the sternum cranially, making possible the expansion of the upper portion of the rib cage, but, at the same time, causes an inward movement of the side walls of the lower rib cage. In contrast, the contraction of the diaphragm is generally associated with the expansion of the lower rib cage and with the collapse of the upper portion. In summary, the synchronization between the diaphragm and the upper portion of the rib cage is abnormal in tetraplegia, probably due to the loss of activity of the intercostal muscles, to the stiffness of the rib cage and to the increased compliance of the abdominal wall. Since the relaxation line represents the most effective breathing, any deviation from this line is suggestive of increased workload for the

respiratory system. Therefore, Konno and Mead data not only demonstrated that the supine position is the less favourable position for SCI subjects, but may also explain why these patients in stress situations (fever, increased secretions, etc.) rapidly develop breathing muscles fatigue [35].

Conclusions

The OEP proved to be a valid and reliable method to assess breathing in patients affected by spinal cord injury, since data about pulmonary function derived from our study agree with those reported in literature using common spirometry. The great advantage of OEP, however, is the possibility to analyse the kinematics of three different compartments of the thoracic-abdominal wall. In chronic SCI patients thoracic compliance is reduced and abdominal compliance is increased. In supine position SCI patients gain proportionally higher volume variations compared to the sitting position, however the supine position reduces the efficiency of the respiratory system. We then hypothesized that, in contrast to what is suggested by spirometry analysis, the supine position for SCI patients is less favourable for breathing, especially in tetraplegic patients. The implementation, based on the model of Konno and Mead, of diagrams describing the level of synchronization of the RCp with the AB and the "phase angle analysis" actually showed that in SCI subjects the thoracic-abdominal wall movement is far from what is defined the "relaxation line". In clinical terms this means that the movement of thoracic and abdominal components is not synchronized and is less effective, and submits the respiratory system to an increased workload. The use of abdominal binders could probably reproduce, in sitting position, the positive effect of gravity that is present in supine position [37, 38] and the diaphragm could work at a more favorable point of its length-tension curve. Further analyses with OEP would be useful to assess the efficacy of abdominal binders, drugs (for example intrathecal baclofen) or electrostimulation (for example frenic nerve and diaphragmatic pacing) in improving respiratory function in SCI patients.

References

[1]. Winslow C, Rozovsky J. (2003) Effect of spinal cord injury on the respiratory system. Am J Phys Med Rehabil 82:803–814.

[2]. Tollefsen E, Fondenes O. (2012 May 15) Respiratory complications associated with spinal cord injury. Tidsskr Nor Laegeforen 132(9):1111-4.

[3]. De Vivo MJ, Black KJ, Stover SL. (1993) Causes of death during the first 12 years after spinal cord injury. Arch Phys Med Rehabil 74:248–54.

[4]. Garshick E, Kelley A, Cohen SA, Garrison A, Tun CG et al. (2005 Jul) Prospective assessment of mortality in chronic spinal cord injury. Spinal Cord 43 (7):408-16.

[5]. Postma K, Bussman J, Haisma J, Van der Woude et al. (2009) Predicting respiratory infection one year after inpatient rehabilitation with pulmonary function measured at discharge in persons with spinal cord injury. J. Rehabilitation Medicine 41: 729-733.

[6]. Donna-Schwake C, Ragette R, Teschler H. (2006) Patterns and predictors of severe chest infections in pediatric neuromuscular disorders. Neuromuscolar Disord 16:325-328.

[7]. Aliverti A, Dellacà R, Pedotti A. (2001 Nov) Optoelectronic plethysmography: a new tool in respiratory medicine. Recenti Prog Med 92 (11):644-7.

[8]. Aliverti A, Pedotti A. (2003 Jan-Mar) Opto-electronic plethysmography. Monaldi Arch Chest Dis 59(1):12-6.

[9]. Aliverti A, Dellacá R, Pelosi P, Chiumello D, Pedotti Aet al. (2000 May) Optoelectronic plethysmography in intensive care patients. Am J Respir Crit Care Med 161(5):1546-52.

[10]. Lanini B, Bianchi R, Binazzi B, Romagnoli I, Pala F et al. (2007 Aug) Chest wall kinematics during cough in healthy subjects. Acta Physiol (Oxf) 190(4):351-8.

[11]. Binazzi B, Lanini B, Bianchi R, Romagnoli I, Nerini M et al. (2006 Mar) Breathing pattern and kinematics in normal subjects during speech, singing and loud whispering. Acta Physiol (Oxf) 186(3):233-46.

[12]. Duranti R, Sanna A, Romagnoli I, Nerini M, Gigliotti F et al. (2004 May) Walking modality affects respiratory muscle action and contribution to respiratory effort. Pflugers Arch 448(2):222-30.

[13]. Vogiatzis I, Stratakos G, Athanasopoulos D, Georgiadou O, Golemati S et al. (2008 Jul) (Epub ahead of print 2008 Mar 5) Chest wall volume regulation during exercise in COPD patients with GOLD stages II to IV. Eur Respir J 32(1):42-52.

[14]. Vogiatzis I, Aliverti A, Golemati S, Georgiadou O, Lomauro A et al. (2005 Mar) Respiratory kinematics by optoelectronic plethysmography during exercise in men and women. Eur J Appl Physiol 93(5-6): 581-7.

[15]. Vogiatzis I, Georgiadou O, Golemati S, Aliverti A, Kosmas E et al. (2005 Sep) Patterns of dynamic hyperinflation during exercise and recovery in patients with severe chronic obstructive pulmonary disease. Thorax 60(9):723-9.

[16]. Georgiadou O, Vogiatzis I, Stratakos G, Koutsoukou A, Golemati S et al. (2007 Feb) Effects of rehabilitation on chest wall volume regulation during exercise in COPD patients. Eur Respir J. 29(2): 284-91.

[17]. Romagnoli I, Gigliotti F, Galarducci A, Lanini B, Bianchi R et al (2004 Sep) Chest wall kinematics and respiratory muscle action in ankylosing spondylitis patients. Eur Respir J. 24(3):453-60.

[18]. Lanini B, Bianchi R, Romagnoli I, Coli C, Binazzi B et al. (2003 Jul 1) Chest wall kinematics in patients with hemiplegia. Am J Respir Crit Care Med 168(1):109-13.

[19]. Lanini B, Masolini M, Bianchi R, Binazzi B, Romagnoli I et al. (2008 Mar 20) Chest wall kinematics during voluntary cough in neuromuscular patients. Respir Physiol Neurobiol 161(1):62-8.

[20]. Miccinilli S, Morrone M, Bastianini F, Molinari M, Scivoletto G, Silvestri S, Ranieri F, Sterzi S. Optoelectronic plethysmography to evaluate the effect of posture on breathing

kinematics in spinal cord injury: a cross sectional study. Eur J Phys Rehabil Med. 2016;52(1):36-47.

[21]. Aliverti A et al. (2001) Compartmental analysis of breathing in the supine and prone positions by optoelectronic plethismography. Annals of Biomedical Engineering 29: 60-70.

[22]. Hammer J, Newth CJL. (2009) Assessment of thoraco-abdominal asynchrony. Paediatric Respiratory Reviews 10:75-80.

[23]. Agostoni E, Mognoni P. (1966) Deformation of the chest wall during breathing efforts. J Appl. Physiol 21: 1827–1832.

[24]. Konno K. And Mead J. (1967) Measurement of the separate volume changes of rib cage and abdomen during breathing J Appl Physiol 22:407-422.

[25]. Schilero GJ, Spungen AM, Buman WA, Radulovic M, Lesser M. (2009) Pulmonary function and spinal cord Injury Respiratory physiology&Neurobiology 166: 129-141.

[26]. Stepp EL, Brown R, Tun CG, Gagnon DR, Jain NB et al. (2008 August) Determinants of Lung Volumes in Chronic Spinal Cord Injury Arch Phys Med Rehabil 89(8): 1499–1506

[27]. Anke A, Aksnes AK, Stanghelle JK, and Hjeltnes N. (1993) Lung volumes in tetraplegic patients according to cervical spinal cord injury level. Scand J Rehabil Med 25: 73–77.

[28]. Forner JV. (1980) Lung volumes and mechanics of breathing in tetraplegics. Paraplegia 18: 258–266.

[29]. Linn WS, Spungen AM, Gong H, Adkins Jr RH, Bauman WA et al. (2001) Forced vital capacity in two large outpatient populations with chronic spinal cord injury. Spinal Cord 39: 263 ± 268.

[30]. Stolzmann K.L., Gagnon D. R., Brown R., Tun C.G et al. (2008 Apr 1) Longitudinal Change in FEV1 and FVC in Chronic Spinal Cord Injury. American Journal of respiratory and critical care medicine 177(7):781-6

[31]. Pithon KR, Martins LEB, Renno ACM, Abreu DCC, Cliquet A Jr (2008) Pulmonary function testing in quadriplegic subjects. Spinal Cord 46: 275–277.

[32]. Baydur A, Adkins R, Milic Emili J (2001) Lung mechanics in individuals with spinal cord injury: effects of injury level and posture. J Appl Physiol. 90: 405–411.

[33]. Estenne M and De Troyer A. (1987) Mechanism of the postural dependence of vital capacity in tetraplegic subjects. Am RevRespir Dis. 135: 367–371.

[34]. Forner JV, Llombardt RL, and Valledor MCV (1977) The flow volume loop in tetraplegics. Paraplegia 15: 245–251.

[35]. Maeda CJ, Baydur A, Waters RL, Adkins RH (1990) The effect of the halovest and body position on pulmonary function in quadriplegia. J Spinal Disord 3: 47–51.

[36]. Brown R, Di Marco AF, Hoit JD, Garshick E (Aug 2006) Respiratory dysfunction and management in spinal cord injury. Respir Care 51(8):853-68; discussion 869-70.

[37]. Wadsworth BM, Haines TP, Cornwell PL, Paratz JD (2009) Abdominal binder use in people with spinal cord injuries: a systematic review and meta-analysis. Spinal Cord 47: 274–285.

[38]. Wadsworth BM, Haines TP, Cornwell PL, Rodwell LT, Paratz JD (2012 Dec) Abdominal binder improves lung volumes and voice in people with tetraplegic spinal cord injury. Arch Phys Med Rehabil 93(12):2189-97.

Chapter IV - MoCap for motion and posture analysis in Parkinson Disease

Introduction

Motion Capture systems have recently found a growing interest in clinical practice for providing objective measures of pathological such as normal movement patterns. These measures show to be useful for clinicians in order to evaluate pathological patterns and to properly correct them. An explicite example is in the way of assessing postural deformities of the human trunk.

The trunk has rarely been studied as an independent object of research, even if the study of trunk kinematics can play a very important role from a clinical perspective. Among advanced non-invasive movement evaluation tools, the most common are based on optoelectronic devices, considered today's gold standard. The optoelectronic approach is based on two hypotheses: some parts of the human body can be approxi-mated to rigid bodies; at least three geometrical points solidly attached to each rigid body can be identified and the 3D coordinates pinpointing their positions measured.

Under these hypotheses, the trunk can be divided into rigid parts and three optical markers must be solidly attached to each. Thus, the motion of each part can be completely defined in space with at least two optoelectronic cameras. Sometimes the parts are identified by geometrical points, without any dimension, thus only a single marker can be associated with each part. Furthermore, the markers cannot always stay in the optical field of the cameras during movement, thus the number of cameras is incremented. Different approximations can produce biomechanical models with a different number of rigid parts. For these reasons, different optoelectronic systems are used in different ways to monitor trunk kinematics, with different aims and different results.

Recently, the author of this paper and at have conducted a pilot study on a group of parkinsonian patients in order to explicite trunk motion abnormalities and then assess the effect of a rehabilitation protocol on those [1].

Parkinson Disease (PD) is a disabling pathology characterized by bradykinesia, rigidity, resting tremor and postural changes that generate an inadequate amplitude of movement [2] progressively reducing patients' autonomy. Axial impairment and gait disturbances consisting in increased cadence and double support phase duration, decreased step length, walking speed and arm swing, are also associated with increased risk of falls in such patients [3-5]. Therefore, a multidisciplinary intervention, including pharmacological and rehabilitative treatment, is recommended to reduce disabling symptoms. Several studies investigated the effects of physical exercise, suggesting the need for permanent treatment for PD patients [6-13]. Most conventional rehabilitative techniques tested for PD have been focused on motor aspects of posture and gait, but little attention has been deserved on sensory and perceptive aspects.

A recent study aimed to evaluate the potential effects of perceptive rehabilitation in PD and reported promising preliminary results for postural balance control and pain symptoms [14]. To date, however, no randomized controlled trial (RCT) has been carried out to compare the effects of perceptive rehabilitation and conventional training in patients with PD. Thus, the main aim of this pilot RCT was to evaluate whether a perceptive rehabilitation training could be more effective than a conventional physical therapy (PT) program for improving postural balance control in patients with PD. The secondary aim was to compare the effects of perceptive rehabilitation, compared to PT, on the gait pattern.

A single center, single blind, randomized controlled trial was conducted on postural abnormalities in forty-three parkinsonian patients. Inclusion criteria were as follows: confirmed diagnosis of idiopathic PD according to the UK Brain Bank Criteria [15]; Hoehn and Yahr stage ≤ 3 determined in the "on" phase [16]; Mini Mental State Examination score > 24 [17]. Exclusion criteria were as follows: severe dyskinesia or "on-off" fluctuations; important modifications of PD medication during the study (i.e. drug changes); deficits of somatic sensation involving the trunk or lower limbs (assessed by means of a physical and neurological examination); vestibular disorders or paroxysmal vertigo; previous thoracic or abdominal surgery; other neurological or orthopedic conditions

involving the trunk or lower limbs (musculoskeletal diseases, severe osteoarthritis, peripheral neuropathy, joint replacement); cardiovascular comorbidity (recent myocardial infarction, chronic heart failure, uncontrolled hypertension, orthostatic hypotension); latex allergy. Prior to testing, eligible participants were randomly assigned in a one-to-one ratio to two arms: a group that performed perceptive rehabilitation and a group that received conventional physical therapy, according to a balanced (restricted) randomization scheme [18]. The investigator (MM) who determined if a subject was eligible for inclusion in the trial was unaware, when this decision was made, of which group the subject would be allocated to (allocation was by sealed opaque envelopes). Another investigator (MS) checked correct patient allocation according to the randomization list. During the study, participants were instructed to take their Parkinson's disease medications regularly and were tested and trained during the "on" phase, 1 to 2.5 hours after taking their morning dose. Participants did not perform any type of rehabilitation in the three months before the study, nor undergo any form of physical therapy other than that scheduled in the study protocol.

Treatment procedures

Each patient underwent a training program consisting of ten, 45-minute sessions (including rest periods), three days a week (Monday, Wednesday, Friday) for four consecutive weeks.

Perceptive Rehabilitation (Su-Per) group

Patients allocated to the experimental group were treated by means of the Surfaces for Perceptive Rehabilitation (Su-Per) that is a therapeutic system aimed to improve the perception of the trunk and its midline by performing some specific cognitive-perceptive tasks [14]. It is based on the perceptive stimuli produced by the interaction of the patient's back with a rigid wood surface supporting over 100 deformable latex cones of various dimensions (height: 3-8 cm; base diameter: 2-4 cm) and elasticity (20%, 40% and 60%) (Figure 1a).

Figure 1a. Surfaces for perceptive rehabilitation.

During the treatment, patients were asked to relax and lay supine on the Su-Per with their hips and knees flexed. Each training session consisted of increasingly difficult tactile and proprioceptive tasks as follows: perceiving the areas of support; indicating the trunk surface perception as well as describing and counting the number of cones in a specific Su-Per area; checking the distribution of the body load on the Su-Per according to the midline and correcting it in order to distribute it symmetrically and uniformly. In order to train patients to increase their body position awareness, patients were trained to recognize contact areas between cones and trunk during costal and diaphragmatic breathing exercises, antiversion of pelvis and pelvic tilt, and flexion and extension of right and left lower limb. The same trained physical therapist treated all the patients in this group and standardized the intensity of each part of the treatment also according to the hyperemic areas

produced on the trunk of patients by the interaction with the latex cones during each training session (Figure 1b).

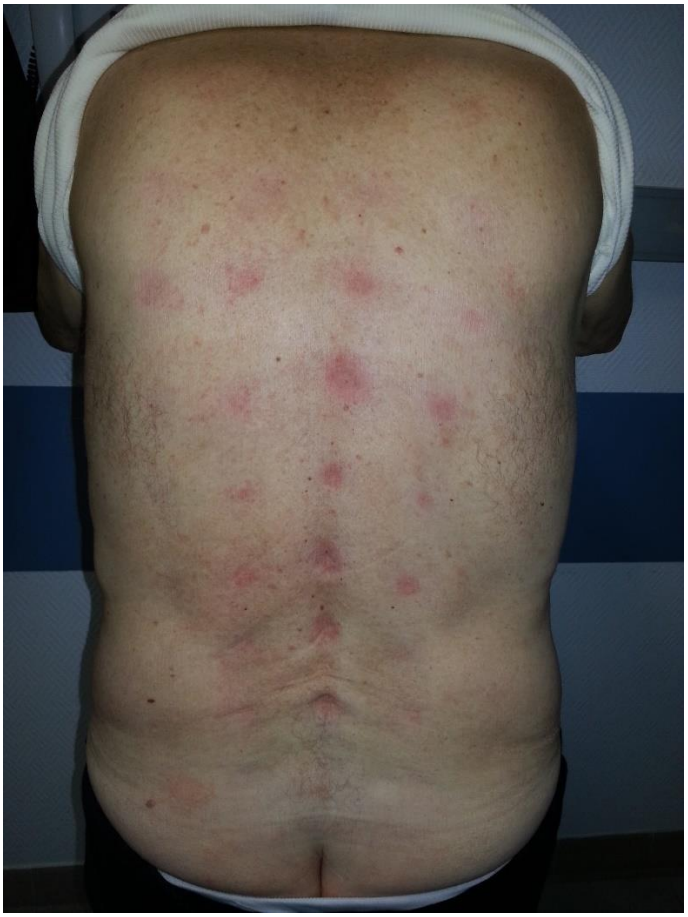

Figure 1b. Hyperemic areas on the patient's back produced by pressure of the perceptive surfaces.

Physical Therapy (PT) group

Patients allocated to the Physical Therapy (PT) group performed a conventional PT program consisting of active joint mobilization of the lower limbs, muscle stretching, coordination and balance exercises according to the European physiotherapy guidelines for Parkinson's disease [19]. Each patient was required to perform exercises in the following sequence: mobilization; stretching and coordination exercises in supine and prone positions; mobilization and coordination exercises in sitting position; stretching and coordination exercises in standing position; coordination and balance

exercises during walking. The same trained therapist treated all the patients in this group and standardized the duration of each part of the treatment.

Evaluation procedures

Patients were evaluated before treatment, immediately after treatment (primary endpoint) and at one month of follow-up. The same rater (MM), who was blinded to the group allocation, evaluated all patients. Asking the assessor to make an educated guess tested the success of blinding. At each check-point, patients were assessed as follows: after the enrolment they underwent a preliminary gait analysis, in order to detect any variation in deambulation pattern between pre and post-physical intervention. This analysis was carried out by using an 8-infrared cameras optoelectronic stereophotogrammetric system (SMART-D system, BTS, Milan, Italy) which recorded the 3D position of 22 retro-reflective spherical markers (15 mm diameter) placed on a series of anatomical landmarks, according to Davis protocol [20-22]. The same stereophotogrammetric system, arranged so as providing full lateral and back views of the subject's trunk, was used to analyze static and dynamic posture of the parkinsonian subjects and its possible modifications after treatment. For this purpose, 9 retro-reflective emispherical markers (10 mm diameter) were placed over the cutaneous projections of the spinous processes of cervical-upper thoracic (C7-T2-T3), dorsal (T5-T6-T8) and lumbar (L1-L3-L5) segments, so as defined by Ranavolo and colleagues [23]. Subjects were required to perform three tasks: i) to maintain a comfortable upright standing position, barefoot with feet parallel, arms alongside the trunk, heels spaced 7 cm apart, open eyes, for 60 seconds (subjects were encouraged to avoid body twisting or asymmetric postures); ii) to maintain the same position for the same time period, but with closed eyes; iii) to execute a full trunk flexion (anterior bending), followed by an extension restoring the trunk to the starting position. For each test, the subject's distance from the recording cameras was set up at 3 meters. Furthermore, all patients underwent a stabilometric assessment by means of a 55 cm-diameter computerized platform (Balance System SD, Biodex Medical Systems Inc., USA), designed to test and train the patients' kinesthetic abilities

by offering twelve increasing-demand levels of stability control on the tilting platform (plus locked position for static measurements). For each subject a static test was performed and then a dynamic one. The static test ("Postural stability") requested the patient to maintain the upright position on the fixed platform for 20 seconds, while the system recorded the de-flexions of the trunk from the center of mass (registered prior to start the test) in any spatial direction. Resulting from this registration, a general index for postural stability was obtained, which was composed by an index evaluating the center of mass displacement along the sagittal plane, and another index evaluating the on-coronal plane oscillations. Moreover, a dynamic test ("Risk of falling") was applied, which consisted of maintaining the center of gravity (represented by a black dot on the screen) at the center of the display, counteracting a three seconds intervals increasingly balance instability, for a total of 20 seconds. The test was repeated for three times at all, and a software calculated the mean score, which was compared to normative age-categorized data.

Primary outcomes

After postural trials acquisition, a dedicated algorithm calculated the position of every marker of the triad (absolute and relative to the others), thus reconstructing the shape of the subject's spine. From this reconstructed model, the dorsal kyphosis and the lumbar lordosis angles were measured and they accounted for the primary outcome measures. Furthermore, we investigated the effects of postural training on stabilometric static postural stability indices (especially those related to sagittal plane).

Secondary outcomes

As secondary outcome measures, we choose to evaluate stabilometric indices obtained from static (coronal plane center of mass deviations) and dynamic (Fall Risk Index) sessions. Moreover, gait pattern spatial-temporal features, immediately dependent on postural behaviors, were analyzed: cadence and its relation with gait phases temporal duration (gait velocity and stride length, measured as mean between left and right side).

Statistical analysis

Since most of the variables failed to show a normal distribution on Shapiro-Wilk test, a non-parametric statistic approach was carried out. Firstly, in order to investigate the effects of proprioceptive rehabilitation program on kyphosis and lordosis angles of parkinsonian patients, a Friedman test for each treatment group throughout the three check-points was conducted. If any significant change emerged, post-hoc analysis by Wilcoxon signed rank test was performed to reveal which differences accounted for clinical meaning. For each of such analyses, a Bonferroni correction for multiple comparisons was applied. Secondly, absolute values and magnitude of change between groups at the three time points were compared by means of Mann-Whitney U test. All values were expressed as median and interquartile range (IQR, 25^{th} and 75^{th} percentiles). IBM SPSS Statistics ver. 20.0 (Chicago, IL, USA) was used for statistical analyses. All tests were two-tailed with a level of significance set at $p<0.05$.

Results

Twenty subjects (11 men and 9 women), median age 73.0 (69.0 to 75.8) years, presenting with idiopathic PD, were recruited from 43 outpatients referring to an Italian Unit of Physical and Rehabilitation Medicine, and assessed for eligibility. The enrolment period was from October 2013 to April 2014. At the end of the recruitment period, ten patients were allocated to each of the treatment groups. No drop-out was observed and no adverse events occurred during the trial in any of the groups. The flow diagram of the study is shown in Figure 2.

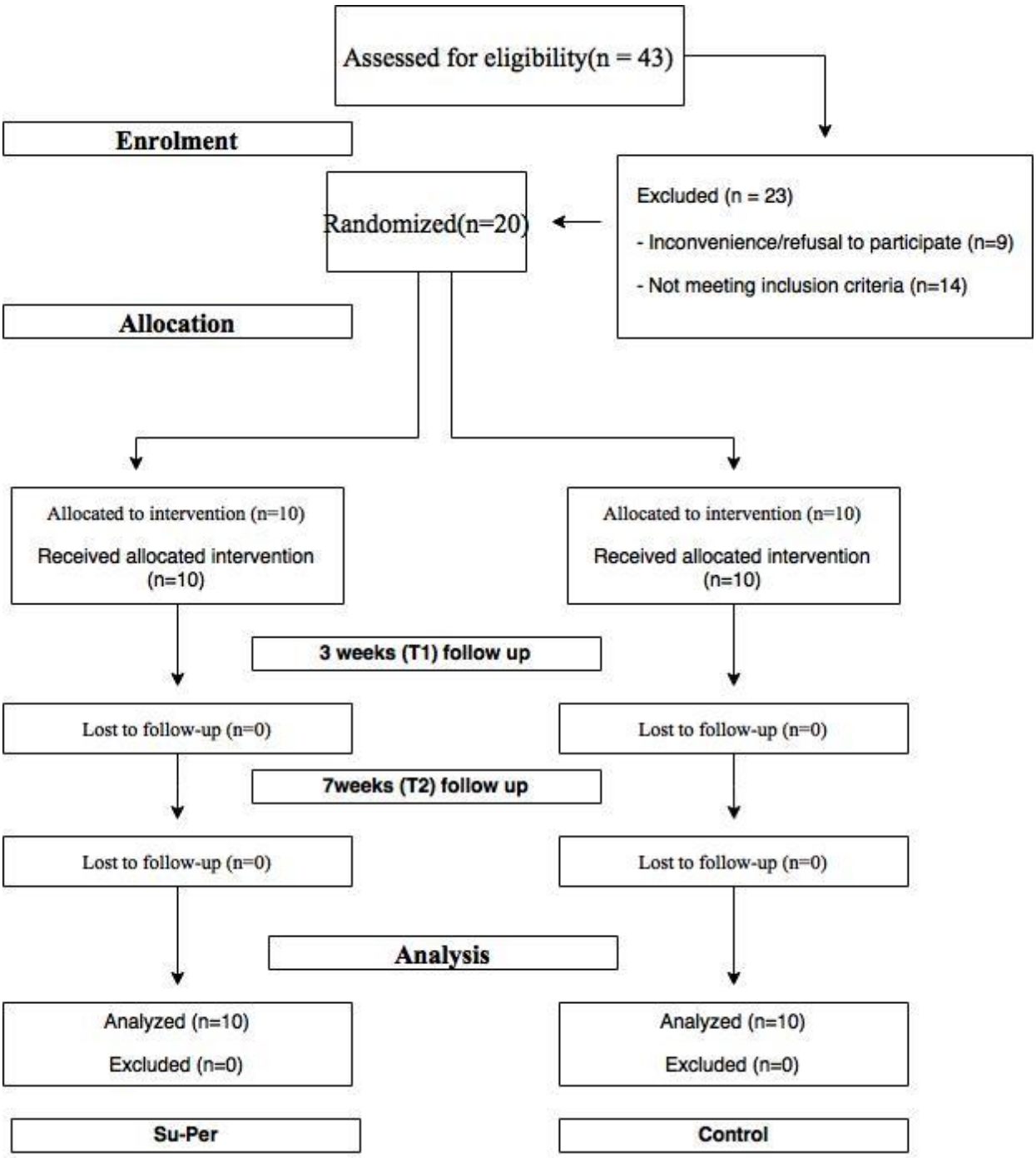

Figure 2. CONSORT flow-chart showing the number of subjects randomized and studied in each group.

Baseline

After randomization, prior to start intervention procedure, all the patients underwent a baseline assessment, including socio-demographic and clinical features. Furthermore, a preliminary gait analysis was carried out in order to assay spatial and temporal characteristics of patients' gait. The baseline comparison between groups did not reveal any difference, thus showing a substantial homogeneity among the enrolled subjects (Table I).

Table I. Baseline demographic, clinical and gait variables of the two enrolled groups.

Parameters*	SuPer group (n=10)	Control group (n=10)	p-value**
Gender (M/F)	1.5	1.5	1.000
Age (yrs)	75.0 (73.0; 76.5)	70.0 (67.5; 72.8)	0.095
BMI	28.1 (26.8; 28.9)	29.2 (27.0; 30.6)	0.226
Hoehn&Yahr grade	3.0 (3.0; 3.0)	3.0 (2.0, 3.0)	0.995
Disease duration (yrs)	6.3 (4.0; 8.4)	6.5 (4.3; 9.0)	0.890
MMSE score	29.0 (27.5; 30.0)	29.5 (28.0; 30.0)	0.689
VAS score (mm)	20.0 (3.0; 55.0)	38.0 (0.0; 56.0)	0.877
BDI score	7.0 (5; 14.5)	9.0 (6.5; 12.8)	0.761
Tinetti Balance+Gait Assessment score	23.0 (20.0: 25.0)	22.0 (19.3; 27.3)	0.970
Stance phase duration (sec)	0.79 (0.74; 0.88)	0.84 (0.75; 0.89)	0.791
Double stance phase duration (sec)	0.20 (0.18; 0.24)	0.18 (0.17; 0.20)	0.496
Cycle duration (sec)	1.14 (1.09; 1.35)	1.30 (1.22; 1.37)	0.185
Cadence (steps/min)	05.90 (89.10; 110.48)	95.25 (89.66; 103.50)	0.384
Cycle lenght (mt)	0.84 (0.65; 0.90)	0.89 (0.76; 1.01)	0.212
Width (mt)	0.15 (0.15; 0.16)	0.19 (0.17; 0.21)	**<0.001**
Normalized velocity (mt)	0.76 (0.67; 0.97)	0.83 (0.71; 0.96)	0.596

*Values are expressed as median (interquartile range), except for gender (ratio). Abbreviations: BMI, Body Mass Index; MMSE, Mini-Mental State Examination; VAS, Visual Analogue Scale; BDI, Beck Depression Inventory.

**Mann-Whitney U test was used for comparisons, except for gender (chi-square test). Statistical significance is in bold type.

Primary outcomes

It was chosen to investigate sagittal plane deviations during a quiet standing trial, due to the assumption that these are the most common postural abnormalities presented by parkinsonian patients. Thus, the primary outcomes were represented by changes of dorsal kyphosis and lumbar lordosis angles after 3 weeks of postural-proprioceptive treatment, such as possible modifications of anterior-posterior postural stability index. The analysis of variance among Su-Per and PT patients

revealed a significant difference in kyphosis angle depending on the kind of treatment they underwent ($\chi^2(2) = 7.200$, $p = 0.027$). Indeed, post-hoc analysis was conducted upon Su-Per group with a Bonferroni correction applied, resulting in a significance level set at $p < 0.009$. Median (IQR) kyphosis angle degrees for the Su-Per group at baseline, at the end of proprioceptive training and after 1 month of follow-up were 57.379 (55.926 to 63.376), 34.312 (27.268 to 55.033) and 56.307 (52.888 to 59.498), respectively. There were no significant differences between baseline and T2 check-point ($Z = -1.886$, $p = 0.059$), and a trend towards increase between T1 and T2 time ($Z = -2.191$, $p = 0.028$); however, a statistically significant reduction was showed in T1 compared to baseline ($Z = -2.701$, $p = 0.007$). As regards physical therapy group, no changes were reported after treatment completion ($\chi^2(2) = 3.800$, $p = 0.150$). Thus, between groups comparison showed a reduced kyphosis angle degree among Su-Per patients at T1 ($U = 22$, $p = 0.035$) (Figure 3). On the contrary, no differences in lumbar lordosis angle were observed both in the Su-Per group ($\chi^2(2) = 3.800$, $p = 0.150$) and in the PT group ($\chi^2(2) = 1.385$, $p = 0.500$). Likewise, sagittal postural stability index did not show any improvement either among Su-Per ($\chi^2(2) = 1.474$, $p = 0.479$) and PT patients ($\chi^2(2) = 2.000$, $p = 0.368$), or between groups for each check time-point (Table II).

Table II. Posturometric and gait variables: within-group and between-group comparison.

	Su-Per group (n=10)			Control group (n=10)		
Parameters[a]	Baseline	3 weeks	Follow-up	Baseline	3 weeks	Follow-up
Kyphosis angle (°)	57,38±7,45	34,31±27,77*	56,31±6,61	58,68±14,69	54,26±21,70§	59,66±15,03
Lordosis angle (°)	39,45±21,66	34,31±20,10	38,00±21,37	42,03±6,75	29,90±3,53	52,21±4,97
APSI	0,40±0,35	0,50±0,63	0,60±0,45	0,60±0,50	0,50±0,60	0,55±0,53
MLSI	0,35±0,43	0,40±0,33	0,40±0,33	0,50±0,33	0,50±0,38	0,55±0,18
FRI	3,60±1,03	3,65±2,30	3,65±2,05	3,5±2,35	3,55±2,65	3,5±2,70
Cadence (steps/min)	105,9±24,49	98,5±16,13	93,15±19,01	95,25±17,11	96,15±6,19	102,53±9,04¥
Stride length (mt)	0,84±0,31	0,79±0,18	0,78±0,30	0,89±0,31	0,90±0,25	0,95±0,18
Normalized Velocity (mt/sec)	0,76±0,38	0,72±0,24	0,72±0,39	0,83±0,34	0,86±0,27	0,92±0,26

[a]Values are median±interquartile range. Abbreviations: APSI, Anterior Posterior Stability Index; MLSI, Medial Lateral Stability Index; FRI, Fall Risk Index. *p<0,01, within-group comparison, T1 vs T0. §p<0,05, between-group comparison at T1. ¥p<0,01, within-group comparison, T2 vs T1.

Secondary outcomes

In order to complete the assessment of patients' postural stability, static and dynamic postural imbalance were investigated. As for static evaluation, the analysis of primary outcomes was completed by adding the results of the medial-lateral stability index modifications. However, no differences were found both in the Su-Per group ($\chi^2(2) = 0.703$, $p = 0.704$) and the PT group ($\chi^2(2) = 0.686$, $p = 0.710$); likewise, no between groups changes were revealed at T0, T1 and T2 checks ($U = 31.5$, $p = 0.154$; $U = 34$, $p = 0.220$; $U = 35$, $p = 0.21$, respectively). Dynamic postural stability was tested by measuring a Fall Risk Index (FRI). However, both within groups and between groups analysis failed to demonstrate any statistically relevant difference. Indeed, Friedman test carried out on FRI as about Su-Per and PT group did not reach significance ($\chi2(2) = 0.200$, $p = 0.905$ and $\chi2(2) = 2.205$, $p = 0.332$, respectively). In the same way, between groups comparison did not show any relevant difference in each of the three check-points ($U = 48$, $p = 0.879$; $U = 42$, $p = 0.545$; $U = 44.5$, $p = 0.677$ for T0, T1 and T2, respectively).

Patients' gait cadence was measured by an optoelectronic system in a dedicated laboratory setting. Not any changes were observed in the Su-Per group ($\chi2(2) = 4.200$, $p = 0.122$), while some differences occurred in the PT group ($\chi2(2) = 7.400$, $p = 0.025$). Thus, post-hoc analysis (with a Bonferroni correction applied) resulted in a significance level set at $p < 0.011$. Median (IQR) cadence among PT patients at baseline, at the end of proprioceptive training and after 1 month of follow-up were 95.250 (88.563 to 105.675), 96.150 (94.763 to 100.950) and 102.525 (96.263 to 105.300), respectively. There were no significant differences between baseline and T1 ($Z = -0.255$, $p = 0.799$), and a trend towards increase between T0 and T2 ($Z = -2.090$, $p = 0.03$), but a significant increase was evident between T1 and T2 ($Z = -2.803$, $p = 0.005$) (Figure 4).

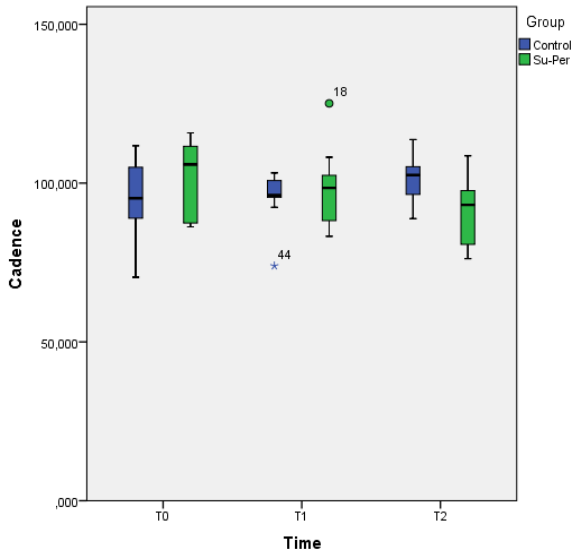

Figure 4. Variation of cadence in Su-Per and PT group.

Finally, gait velocity and mean stride length did not change, either between groups or within groups. As for the former parameter, analysis of variance resulted not significant in the Su-Per group ($\chi^2(2) = 0.359$, $p = 0.836$), whereas for the PT group, despite some apparent differences ($\chi^2(2) = 10.400$, $p = 0.006$), post-hoc analysis with Bonferroni correction for multiple comparisons (which settled the p value at 0.002) lacked to reach any significance. Likewise, mean stride length failed to reveal any improvement over time both in the Su-Per group ($\chi^2(2) = 2.600$, $p = 0.273$) and in the PT

group ($\chi^2(2) = 6.526$, $p = 0.038$), in the latter case by setting the p value for significance at 0.013 after applying Bonferroni correction.

Discussion

The results support the hypothesis that tactile and perceptive stimuli might enhance sensory-motor postural control in PD and showed the efficacy of Su-Per rehabilitative treatment compared to PT, with regard to the primary outcome, in improving postural control in PD patients. Indeed, between groups comparison showed a reduced kyphosis angle degree among Su-Per patients at the end of a short-time treatment.

These results are in accordance with previous studies about the effects of Perceptive Surfaces on posture in chronic non-specific low back pain and in Parkinson Disease [24], and with recent recommendations of Moseley and colleagues [25]. Specifically, Su-Per group obtained a better control of trunk midline on sagittal plane compared to PT group. PD patients usually present impairment in terms of motor control as well as in sensory integration, resulting in static and dynamic postural control deficits. Exercise protocol based on Perceptive Surfaces aims to realign body midline to gravitational axis by means of a perceptive and tactile task (recognition of the different cones), in accordance with other perceptive rehabilitation approaches for the trunk in PD. Also Capecci et al [26] showed that the combination of active posture correction and trunk movements, muscle stretching, and proprioceptive stimulation through Kinesio-taping may usefully impact PD axial symptoms. Repeated training is recommended to avoid vanishing of the effect.

The rehabilitative treatment by Perceptive Surfaces tests the efficacy of an approach that focuses on the reconstruction of patient's perceptive and somesthestic awareness, creating a cognitive consciousness of perceptive afferent flow coming from the trunk. In this way, patients learn to generate internal adaptive strategies.

Trunk midline can be considered as the axis of symmetry around which the body organizes the motor behavior [27]. A promising possibility is therefore to train the patient's ability to recognize the body position with respect to the gravitational axis through perceptive surfaces in contact with the skin [28]. Shenton suggested that proprioceptive inflow may represent an important sensory input to the representation of the body in space [29], as well as processing of the proprioception information is context-depending [30].

The results reinforce the idea that working on the representation of the midline and motor imagery of the trunk, providing a bridge between perception and movement, can give rise to new functional strategies for PD patients. Since rehabilitation is usually considered as a learning process, ascertaining how and to what extent motor learning could be impaired in PD patients is very important.

However, attentional strategies potentially have a high cost in terms of mental effort and fatigue as a result of using cognitive resources to generate the internal cue. External cues may thus require less effort and attention, and their use during more complex activities could facilitate walking [31]. Previous studies showed that PD patients undergoing global postural rehabilitation programs resulted in an increase in gait speed, step/stride cadence, suggesting an effect of such treatment on gait pattern. Furthermore, follow–up evaluations confirmed that all subjects maintained these improvements in the two following months as compared to baseline [32].

The analysis of cadence among patients enrolled in the Su-Per group showed no significant differences between baseline and T1 or between T0 and T2 (although a tendency for enhancement), whereas a significant increase of cadence was evident between T1 and T2 in the PT group. In order to understand if this increase was due to an increase of festination or, on the contrary, to an improvement in gait dexterity, the following spatial and temporal parameters were considered: gait velocity and stride length. However, both within and between-groups comparisons showed no significant differences for such parameters. Previous studies described differences in gait parameters between festinating and non-festinating PD patients, confirming that, although

festination is apparently patterned with increase in speed, global gait velocity is actually reduced and festination is slower than either normal or non-festinating parkinsonian gait. Festinating patients present a reduction in step and stride length and the need to execute more steps to cover similar distances than non-festinating patients. Cadence values were higher in PD patients than in controls even if this difference was not statistically significant [33]. Another finding was the lack of improvement in gait performance of the Su-Per group after treatment. A possible explanation to this result is that a pure proprioceptive treatment in absence of other active cues does not promote learning of motor strategies in PD patients. For this reason, a possible strategy to be followed would be to combine proprioceptive rehabilitation with active motor training in order to extend the benefits of Su-Per treatment also to gait pattern.

Although it is a pilot study, the trial presents some limitations: firstly, the smallness of the sample size, which hampers the generalizability of the study's results. Another likely limitation is represented by the lack of improvement of postural stability indices (static and dynamic) on stabilometric platform, in both groups. This observation may be consequent to a selection bias; indeed, at the baseline assessment, each subject was tested for postural stability and gait performance by means of the Tinetti Balance and Gait Assessment Tool. This task performance exam tests balance and gait abilities under functional conditions, by giving a sub-score ranging from 0 to 16 for balance assessment, and another sub-score for gait whose maximum value is 12. The Tinetti overall score results from the sum of these two sub-scores, being the best performance scored 28. The majority of the patients, in both groups, presented a good baseline stability condition, showing a median score of 23 for Su-Per group, and 22 for PT group. Thus, a ceiling effect of the assessment tool in this selected sample could explain the lack of a significant effect of rehabilitative treatment in such a population. Finally, a longer follow-up could have been useful possibly to clarify the optimal duration of a perceptive rehabilitation program.

Conclusion

The reported findings support the idea that a proprioceptive training, based on the association of many intensive perceptive stimuli during cognitive tasks focused on improving proprioception and sensory integration, may help patients with PD into restoring a correct midline perception and, in turn, to improve postural control. Postural disorders due to PD such as Pisa Syndrome, a tonic lateral flexion of the trunk associated with slight rotation along the sagittal plane, could therefore benefit from this kind of treatment. Further studies are needed to determine if the association of perceptive treatment and active motor treatment would be useful in improving gait dexterity of PD patients.

References

[1] Morrone M, Miccinilli S, Bravi M, Paolucci T, Melgari JM, Salomone G, Picelli A, Spadini E, Ranavolo A, Saraceni VM, Di Lazzaro V, Sterzi S. Perceptive rehabilitation and trunk posture alignment in patients with Parkinson disease: a single blind randomized controlled trial. Eur J Phys Rehabil Med. 2016;52(6):799-809.

[2] Morris ME, Iansek R, Matyas TA, Summers JL. The pathogenesis of gait hypokinesia in Parkinson's disease. Brain 1994;117:1169–81.

[3] Knutsson F. An analysis of parkinsonian gait. Brain 1972;95:475–486.

[4] Murray MP, Sepic SB, Gardner GM, Downs WJ. Walking patterns of men with Parkinsonism. Am J Phys Med 1978;57: 278–294.

[5] Koller WC, Glatt S, Vetere-Overfield B, Hassanein R. Fallsand Parkinson's disease. Clin Neuropharmacol 1989;12:98–105.

[6] Gobbi LT, Oliveira-Ferreira MD, Caetano MJ, Lirani-Silva E, Barbieri FA, Stella F, Gobbi S. Exercise programs improve mobility and balance in people with Parkinson's disease. Parkinsonism Relat Disord. 2009;15:S49–S52.

[7] Reuter I, Engelhardt KS, Baas H. Therapeutic value of exercise training in Parkinson's disease. Med Sci Sports Exerc. 31:1544–1549.

[8] Miyai I, Fujimoto Y, Ueda Y, Yamamoto H, Nozaki S, Saito T, Kang J. Treadmill training with body weight support: its effect on Parkinson's disease. Arch Phys Med Rehabil. 2000;81:849–852.

[9] Scandalis TA, Bosak A, Berliner JC, Helman LL, Wells MR. Resistance training and gait function in patients with Parkinson's disease. Am J Phys Med Rehabil. 2001;80:38–43.

[10] Dibble LE, Hale TF, Marcus RL, Gerber JP, LaStayo PC. High intensity eccentric resistance training decreases bradykinesia and improves quality of life in persons with Parkinson's disease: a preliminary study. Parkinsonism Relat Disord. 2009;15:752–7.

[11] Bergen JL, Toole T, Elliott RG III, Wallace B, Robinson K, Maitland CG. Aerobic exercise intervention improves aerobic capacity and movement initiation in Parkinson's disease patients. NeuroRehabilitation 2002;17:161–8.

[12] Hackney ME, Earhart GM. Health-related quality of lifeand alternative forms of exercise in Parkinson disease. Parkinsonism Relat Disord. 2009;15:644–8.

[13] Nocera J, Horvat M, Ray CT. Effects of home-basedexercise on postural control and sensory organization in individuals with Parkinson disease. Parkinsonism Relat Disord. 2009;15:742–5.

[14] Paolucci T., Morone G., Fusco A., Giuliani M., Rosati E., Zangrando F. et al. Effects of perceptive rehabilitation on balance control in patients with Parkinson's disease. Neurorehabilitation 2014;34:113-20.

[15] Hughes AJ, Daniel SE, Kilford L, Lees AJ. Accuracy of clinical diagnosis of idiopathic Parkinson's disease. A clinico-pathological study of 100 cases. JNNP 1992;55:181-4.

[16] Goetz CG, Poewe W, Rascol O, Sampaio C, Stebbins GT, Counsell C, Giladi N, Holloway RG, Moore CG, Wenning GK, Yahr MD, Seidl L. Movement Disorder Society Task Force Report on the Hoehn and Yahr Staging Scale: Status and Recommendations. The Movement Disorder Society Task Force on Rating Scales for Parkinson's disease. Movement Disorders 2004;19:1020–8.

[17] Folstein MF, Folstein SE, McHugh PR "Mini Mental State" a practical method for grading the cognitive state of patients for the clinicians. J Psychiat Res. 1975;12:189–98.

[18] Suresh K. An overview of randomization techniques: An unbiased assessment of outcome in clinical research. J Hum Reprod Sci. 2011;4:8–11.

[19] Keus S, Munneke M, Graziano M, Paltamaa J, Pelosin E, Domingos J, Bruhlmann S, Ramaswamy B, Prins J, Struiksma C, Rochester L, Nieuwboer A, Bloem B European physiotherapy guideline for Parkinson's disease [ParkinsonNet and the Royal Dutch Society for Physical Therapy (KNGF)-2014].

[20] Aliverti A., Pedotti A. Opto-electronic Plethysmography. Monaldi Arch Chest Dis. 2003;59:12-16.

[21] Aliverti A, Dellacà R, Pedotti A. Optoelectronic plethysmography: a new tool in respiratory medicine. Recenti Prog Med. 2001;92:644-7.

[22] Aliverti A, Dellacà R, Pelosi P, Chiumello D, Gattinoni L, Pedotti A. Compartmental analysis of breathing in the supine and prone positions by optoelectronic plethismography. Annals of Biomedical Engineering 2001;29:60-70.

[23] Ranavolo A, Don R, Draicchio F, Bartolo M, Serrao M, Padua L, Cipolla G, Pierelli F, Iavicoli S, Sandrini G. Modelling the spine as a deformable body: Feasibility of reconstruction using an optoelectronic system. Appl Ergon. 2013;44:192-9.

[24] Paolucci T, Fusco A, Iosa M, Grasso MR, Spadini E, Paolucci S, et al. The efficacy of a perceptive rehabilitation on postural control in patients with chronic nonspecific low back pain. Int J Rehabil Res. 2012;35:360-6.

[25] Moseley GL, Gallagher L, Gallace A Neglect-like tactile dysfunction in chronic back pain. Neurology. 2012;79:327-32.

[26] Capecci M, Serpicelli C, Fiorentini L, Censi G, Ferretti M, Orni C, et al. Postural rehabilitation and Kinesio taping for axial postural disorders in Parkinson's disease. Arch Phys Med Rehabil. 2014;95:1067-75.

[27] Fabri M, Polonara G, Salvolini U, Manzoni T. Bilateral cortical representation of the trunk midline in human first somatic sensory area. Hum Brain Mapp. 2005;25:287-96.

[28] Lee BC, Martin BJ, Ho A, Sienko KH. Postural reorganization induced by torso cutaneous covibration. J Neurosci. 2013;33:7870-6.

[29] Shenton JT, Schwoebel J, Coslett HB. Mental motor imagery and the body schema: evidence for proprioceptive dominance. Neurosci Lett. 2004;370:19-24.

[30] Ivanenko YP, Dominici N, Daprati E, Nico D, Cappellini G, Lacquaniti Locomotor body scheme F. Hum Mov Sci. 2011;30:341-51.

[31] Ceravolo MG Rehabilitation goals and strategies in Parkinson's disease. Eur J Phys Rehabil Med. 2009;45:205-8.

[32] Vitale C, Agosti V, Avella D, Santangelo G, Amboni M, Rucco R, Barone P, Corato F, Sorrentino G. Effect of Global Postural Rehabilitation program on spatiotemporal gait parameters of parkinsonian patients: a three-dimensional motion analysis study. Neurol Sci. 2012;33:1337-43.

[33] Merello M, Fantacone N, Balej J. Kinematic study of whole body center of mass position during gait in Parkinson's disease patients with and without festination. J Mov Disord. 2010;25:747-54.

Chapter V- MoCap systems for gait analysis: application to foot drop syndrome

Introduction

Motion analysis has developed greatly during the last 30 years, focusing mainly on gait. There are several reasons for this; the quite standard activity of walking, for example, but also the importance of gait impairment in neurological and orthopedic diseases both in adults and children. The development of movement essentially in the sagittal plane has allowed the development of standard protocols [1]. Gait analysis is a comprehensive assessment increasing its diffusion in clinical settings. One of its milestone applications is in the filed of prosthesis and orthosis prescription, evaluation and realization. Ankle-foot-orthoses (AFOs) are frequently prescribed for hemiparetic patients to compensate for the foot drop syndrome, in order to compensate for malfunctioning of the neuromuscolar system and improve subject walking ability. Research works on new prototypes of AFOs can be found in the literature [1, 2]. Also, the effects of commercial AFOs on gait capabilities were widely studied. Park et al [3] investigated changes in the gait due to anterior and posterior AFOs. No statistically significant differences were reported. On the contrary, Chen et al [4] showed that a posterior AFO was able to improve rear-foot dorsi-flexion during the whole gait cycle with respect to an anterior AFO and decrease rear-foot inversion with respect to the absence of AFO. Lehmann et al [5] studied the effect of different trimlines of plastic AFOs on ankle motion; in the study of Hiroaki et al [6] the effect of plastic AFOs on gait stability was investigated.

Spatio-temporal parameters [7,8], kinematic and kinetic indicators [9,10,11], walking speed [12,13,14], balance [15,16], and energy cost functions [7,17,18,10,25] were proposed in the literature to assess patient walking capabilities. Several studies [7-18] showed the beneficial effects of wearing AFOs, while some other studies [19,20,21] reported very limited advantages. In the

studies of Don et al [23] and Merlo et al [24] quantitative indexes were used to assess Charcot-Marie-Tooth patients with foot drop and plantar flexion failure. As explained by Bregman et al [22], the controversial results found in the literature could be justified by the orthosis mechanical properties, which differently matched patients' individual impairment.

Motion capture can be a useful tool in guiding proper prescription of orthoses for foot drop syndrome in hemiparetic patients. An example is represented by a recent study conducted bythe author in collaboration with Zollo et al [26] which carried out a comparative evaluation of two commercial AFOs with different mechanical properties, i.e. solid versus dynamic AFO, by means of quantitative indicators of subject gait capabilities.

Two commercial orthoses (i.e. the Codivilla Spring and the Toe-Off) were considered for the study. The Codivilla Spring is a solid AFO with a rigid structure that increases both plantar-flexion and dorsi-flexion resistance [27]. The Toe-Off is a dynamic AFO with a flexible structure capable of storing elastic energy during stance and releasing it during swing. The analysis resorts to quantitative indicators describing patient performance during gait in terms of spatio-temporal, kinematic and muscular features. The main subgoals are: (a) to assess the capability of the AFOs to improve walking in the case of a specific disorder, i.e. the foot drop, thus focusing on dorsi-plantar flexion correction; (b) to compare the corrective action of two different off-the-shelf orthoses, i.e. a solid and a dynamic AFO; (c) to evaluate the capability of the orthoses to rebalance the behaviour of the two limbs (paretic and contralateral); (d) to verify the effect of the AFO on the behaviour of the contralateral limb.

For these purposes, ten patients underwent a biomechanical gait analysis through a stereo-photogrammetric system (BTS Smart D) in three different conditions: shoes without AFO, shoes with a solid AFO and shoes with a dynamic AFO. From the recorded gait patterns a set of 22 quantitative indexes were extracted. Finally, a statistical analysis based on Friedman non-parametric tests with Wilcoxon post-hoc test and Bonferroni correction was carried out to compare patients' gait performance in the three aforementioned conditions.

Materials and methods

Subjects

Table 1 shows anamnestic data of the ten chronic hemiparetic patients (7 men, 3 women) with foot drop syndrome who met inclusion criteria and volunteered to participate in the study. Inclusion criteria were the following: 1) diagnosis of a single, unilateral stroke at least six months prior to enrolment, verified by brain imaging; 2) sufficient walking capability to walk without assistance, with or without support; 3) sufficient cognitive and language abilities (Mini-Mental Status Score ≥ 22 or interview for aphasic subjects). None of the subjects was hemiplegic or affected by chronic deformities of the lower limb. Subjects neither had other types of ankle foot anomalies, such as the equinus varus foot, nor was affected by other pathologies involving locomotion.

Table 1 – Demographic and etiologic characteristics of the hemiparetic subjects

Subject	Gender	Age (years)	Diagnosis	Affected limb	Height (cm)	Weight (Kg)	Time from
1	F	74	ISC	L	152	53	18
2	M	66	HAE	R	174	78	17
3	M	76	ISC	R	163	88	205
4	F	69	ISC	R	165	66	24
5	M	74	ISC	R	167	80	183
6	M	44	HAE	R	170	75	12
7	M	71	ISC	L	173	75	69
8	M	55	HAE	L	174	90	21
9	F	52	ISC	R	174	70	84
10	M	62	ISC	L	168	80	11

F: female, M: male, ISC: ischemic, HAE: hemorrhagic, R: right, L: left

Materials

Two commercial models of AFOs were analysed and compared (Figure 1). They are a solid and a dynamic AFO typically prescribed in the clinical practice. The solid orthosis (by M.T.O. Spa) is made of polypropylene, has a posterior leaf and is called "Codivilla-spring". The dynamic orthosis, called "Toe-Off" (by Allard International), is made of carbon fibre, fiberglass and Kevlar and has an anterior leaf.

(a) (b)

Figure 1 – (a) Solid AFO; (b) Dynamic AFO

A biomechanical gait analysis was carried out through a stereo-photogrammetric system (BTS Smart D) (Figure 2) made of 8 infrared cameras capturing the movement of 20 passive and retro-reflecting markers, 2 digital cameras for the simultaneous acquisition of the video (BTS VIXTA) and 8 miniaturized probes with active EMG electrodes (BTS FREEEMG 300) positioned on the lateral gastrocnemius, tibialis anterior, biceps femoris and rectus femoris muscles. The markers were placed on the patient's body according to the Davis protocol [27] (Figure 3a).

(a) (b) (c)

Figure 2 -a) EMG probes, b) infrared camera, c) passive and retro-reflecting markers

(a) 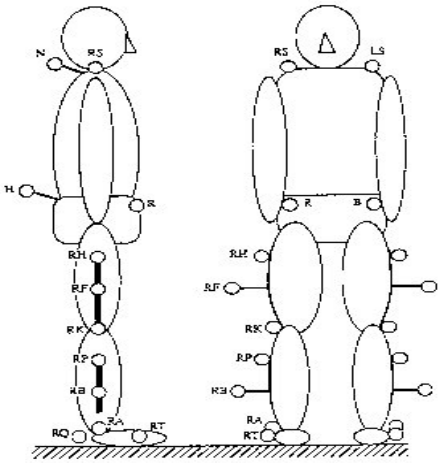 (b)  (c)  (d) 

Figure 3 – (a) Markers positioning in Davis protocol; -Ambulation of a patient during the gait analysis: b) without AFO, c) with solid AFO, d) with dynamic AFO.

Experimental Protocol and Evaluation

The clinical protocol included a preliminary wash-out phase followed by three randomly ordered walking sessions, performed in the same day: (i) 5 walking trials without orthosis, (ii) 5 walking trials with the Codivilla-spring, (iii) 5 walking trials with the Toe-Off. Each subject was instructed to walk with a self-paced speed along a 3-m walkway (Figure 3). During the trials the subjects were allowed to use ambulation aids.

Patients were assessed by means of clinical scales and quantitative indicators extracted from the gait motion analysis. The following clinical scales were used: Lower Extremity Fugl-Meyer, Mini Mental State Examination, Modified Ashworth Scale, Ranges of Motion, and Timed Up and Go Test.

Data Analysis

Spatio-temporal, kinematic and electromyographic indicators were used for the biomechanical analysis. Friedman non-parametric tests with Wilcoxon post-hoc test was used to carry out three comparative analyses of patient performance: (i) without orthosis versus Codivilla-spring;(ii) without orthosis versus Toe-Off, (iii) Codivilla-spring versus Toe-Off. A Bonferroni correction was applied ($p < 0.167$). Furthermore, the behaviour of the two limbs (paretic and contralateral) was compared through a Wilcoxon test. Finally, the effect of the orthosis on the contralateral limb was evaluated.

Spatio-temporal indicators

A stride is the time between two consecutive heel–floor contacts of the same limb, and is segmented in a stance phase and a swing phase. Cadence, step length, stride length, stride time, percentage of swing phase and percentage of double stance phase were evaluated.

Kinematic indicators

Twelve kinematic indicators were computed to quantify patient motion capabilities at ankle, knee and hip levels. For the ankle the following parameters were evaluated: angle between the floor and the foot at initial contact; range of motion (i.e. ROM) of the dorsi-plantar-flexion (during swing and stance phases); dorsi-flexion peak during the swing phase. Because of the specific pathology addressed by this study, i.e. the foot drop, only ankle dorsi-plantar flexion was monitored. It is also worth considering that patients enrolled for this study had not other types of ankle foot anomalies, such as the equinus varus foot, as shown by the clinical evaluation. For the knee ROM of the flexion-extension angle was computed. For the hip the following indicators were calculated: ROM of the flexion-extension angle (during swing and stance phases); flexion peak during the swing phase; ad/abduction ROM during the swing phase; pelvic frontal ROM (during swing and stance phases).

EMG indicators

The following four electromyographic parameters were computed:

a) Co-activation index (CI), expressed as [28]

$$CI = \frac{EMG_L}{EMG_H} * \left(\frac{EMG_L + EMG_H}{2}\right)$$

where EMGL is the activity of the less active muscle and EMGH the activity of the more active muscle. CI is used to evaluate the simultaneous activation of agonist/antagonist muscles in four different intervals of the stance phase (i.e. loading response, mid-stance, terminal stance and pre-swing) and in three different intervals of the swing phase (i.e. initial swing, mid-swing and terminal swing).

b) Tibialis anterior activation index (TAAI), calculated as [29]

$$\frac{\text{sum of TA activity between toe off and toe strike}}{\text{sum of TA activity during one complete gait cycle}}$$

It represents the capacity of the TA to be active during the swing phase.

c) Push-off index (POI), used to determine the activity of the calf during the push-off phase and computed as [29]

$$\frac{\text{sum of calf activity from 11\% of gait cycle before heel rise to 9\% of gait cycle after heel rise}}{\text{sum of calf activity during one complete gait cycle}}$$

d) Premature calf activation index (PCAI), defined as [29]

$$\frac{\text{sum of calf activity toe strike} + 20\% \text{ of the gait cycle}}{\text{sum of calf activity during one complete gait cycle}}$$

It allows identifying abnormal premature calf activity in early stance.

Results

Clinical evaluation

The results of the clinical evaluation are reported in terms of mean value and SD: Fugl-Meyer: 66.85(±6.62); Mini Mental State Examination: 26(±2.29); Modified Ashworth Scale: 1.10(±0.31); Timed Up and Go Test: No AFO: 27.86(±9.35) s; solid AFO: 28.57(±11.5) s; dynamic AFO: 26.73(±8.84) s.

Quantitative evaluation

The computed spatio-temporal indices are shown in Table 2. The Friedman test showed no statistically significant differences among the three analysed walking conditions. A statistical significant difference was observed only in the comparison between the paretic and contralateral limbs for the percentage of swing phase (p=0.0018 without orthosis; p=0.0022 for the solid AFO; p=0.0235 for the dynamic AFO) as well as for the percentage of double support phase (p=0.0154 without orthosis; p=0.0185 for the solid AFO; p=0.0023 for the dynamic AFO).

Table 2 - Spatio-temporal data in hemiparetic patients

Parameter		Shoes	Solid AFO	Dynamic AFO
Cadence [step/min]		56.68 ± 9.08	58.38 ± 15.77	57.51 ± 13.51
Stride time [s]	A	2.03 ± 0.48	1.95 ± 0.61	2.05 ± 0.66
	U	2.08 ± 0.41	1.96 ± 0.57	2.16 ± 0.68
Step length [m]	A	0.28 ± 0.08	0.30 ± 0.10	0.28 ± 0.08
	U	0.28 ± 0.11	0.26 ± 0.01	0.23 ± 0.10
Stride length [%]	A	0.57 ± 0.16	0.60 ± 0.21	0.55 ± 0.21
	U	0.59 ± 0.20	0.58 ± 0.19	0.58 ± 0.20
percentage of the swing phase [%]	A	31.37 ± 7.90[1c]	32.57 ± 7.90 [c]	31.67 ± 10.10 [c]
	U	21.12 ± 5.00	19.30 ± 6.70	22.02 ± 8.10
percentage of the double support phase [%]	A	18.88 ± 7.30[c]	17.58 ± 5.50 [c]	17.07 ± 5.50 [c]
	U	26.76 ± 7.50	26.87 ± 10.8	29.26 ± 11.60

Data are mean ± SD

A: affected limb. U: unaffected limb

[1]a) Mean of this condition differed significantly from mean of Shoes condition; b) mean of solid AFO differed significantly from mean of dynamic AFO; c) mean of contralateral differed significantly from mean of paretic limb

Table 3 reports mean and SD of kinematic indicators for ankle, knee and hip. The solid as well as the dynamic AFO led to a statistically significant reduction of the ROM of the dorsi-plantar-flexion of the affected ankle during stance with respect to the ambulation without AFO (solid AFO: $p=0.008$, dynamic AFO: $p=0.011$). The angle between the floor and the foot at initial contact changed towards positive values for both orthoses. The variation was significant only for the solid AFO ($p=0.008$). The other examined kinematic parameters did not show statistically significant changes in the use of AFOs compared to the walking without AFO.

The mean value of EMG activity over all the subjects is drawn in Figure 4 for the two muscular couples of Tibialis Anterior – Lateral Gastrocnemius and Rectus Femoris – Biceps Femoris. Quantitative indicators extracted from EMG signals are reported in Tables 4-5. Significant results were retrieved only for the co-activation index.

Table 3 - Kinematic data in hemiparetic patients

Parameter [°]		Shoes	Solid AFO	Dynamic AFO
Ankle:				
angle at initial contact (sagittal plane)	A	-1.63 ± 6.3[c]	3.98 ± 3.8[a]	3.64 ± 3.9
	U	5.33 ± 3.6	6.33 ± 5.0	7.08 ± 3.9
dorsi-plantar flexion RoM during the stance phase	A	16.41 ± 6.4	11.11 ± 3.1[a, c]	10.02 ± 1.9[a, c]
	U	19.21 ± 5.6	18.76 ± 5.5	18.16 ± 6.5
dorsi-plantar flexion RoM during the swing phase	A	6.56 ± 5.6	4.60 ± 2.6[c]	3.92 ± 3.9[c]
	U	7.50 ± 3.4	9.67 ± 5.0	9.43 ± 6.4
dorsi flexion peak during the swing phase	A	1.09 ± 9.2[c]	5.71 ± 5.9[c]	2.57 ± 9.2
	U	9.12 ± 3.7	11.57 ± 4.4	9.79 ± 2.7
Knee:				
flexion RoM during the stance phase	A	11.88 ± 5.8	13.58 ± 6.5	10.81 ± 3.9
	U	10.31 ± 4.3.	9.69 ± 4.3	8.12 ± 2.3
flexion peak during the swing phase	A	31.72 ± 12.0[c]	28.44 ± 8.4[c, b]	20.76 ± 13.0[c,a]
	U	55.16 ± 8.4	54.58 ± 8.5	52.54 ± 12.9
Hip:				
flexion/extension RoM during the stance phase	A	23.07[c] ± 9.1	23.69 ± 10.1[c]	19.52 ± 8.8[c]
	U	33.44 ± 7.3	31.66 ± 7.7	31.16 ± 7.8
flexion/extension RoM during the swing phase	A	15.26 ± 8.6	18.01 ± 4.0	15.60 ± 7.4
	U	19.10 ± 7.9	21.14 ± 10.7	18.58 ± 8.6
flexion peak during the swing phase	A	32.49[c] ± 13.9	33.57 ± 11.4	30.20 ± 17.7[c, a]
	U	40.66 ± 15.1	39.44 ± 13.5	37.61 ± 17.3
ad/abduction RoM during the swing phase	A	5.57 ± 3.9	4.88 ± 1.7	4.41 ± 1.6
	U	4.60 ± 1.5	4.59 ± 2.3	4.97 ± 3.1
pelvic tilt RoM during the stance phase	A	7.59 ± 4.2	7.38 ± 3.2	6.78 ± 3.0
	U	8.42 ± 4.2	7.90 ± 3.8	7.93 ± 4.1[c]
pelvic tilt RoM during the swing phase	A	6.82 ± 4.4[c]	6.72 ± 4.0[c]	6.21 ± 4.6[c]
	U	2.74 ± 1.9	2.93 ± 2.7	3.02 ± 1.7

Data are mean ± SD. A: affected limb. U: unaffected limb.

On the other hand, data on the affected and unaffected limbs pointed out that both AFOs have the effect of reducing the asymmetry between the two limbs in terms of ankle angle at initial contact and hip flexion peak (the difference between affected and unaffected limbs is not significant).

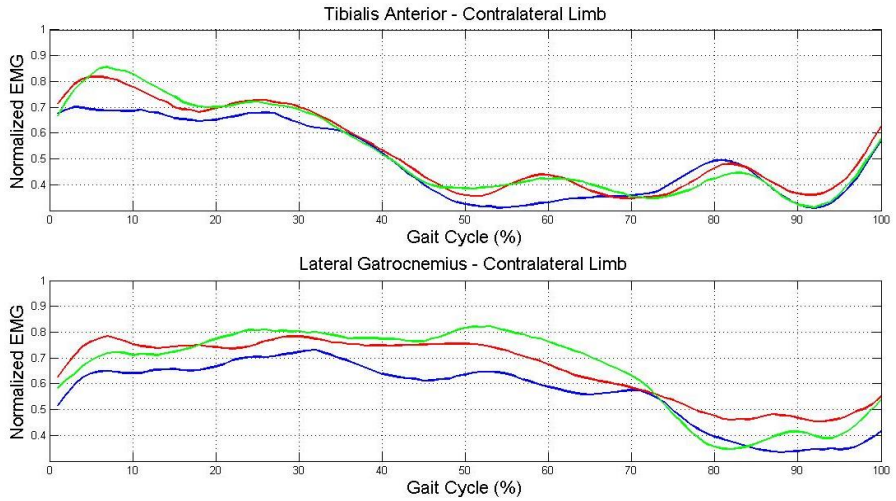

(a)

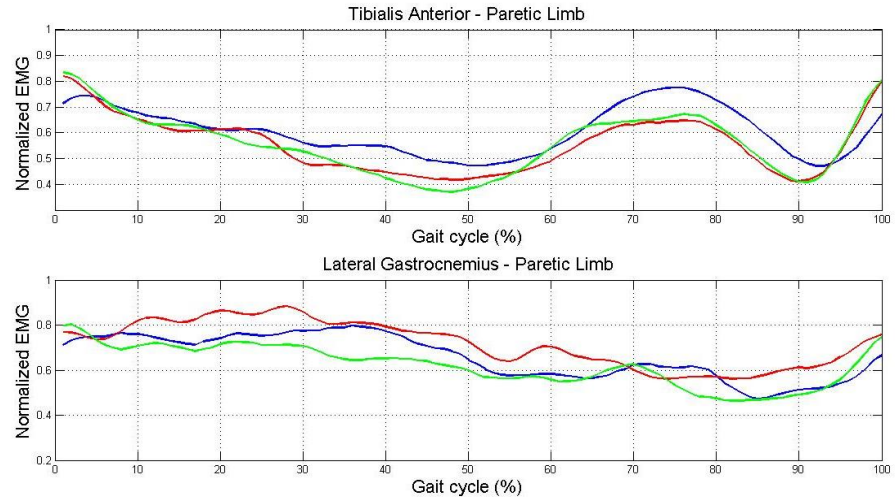

(b)

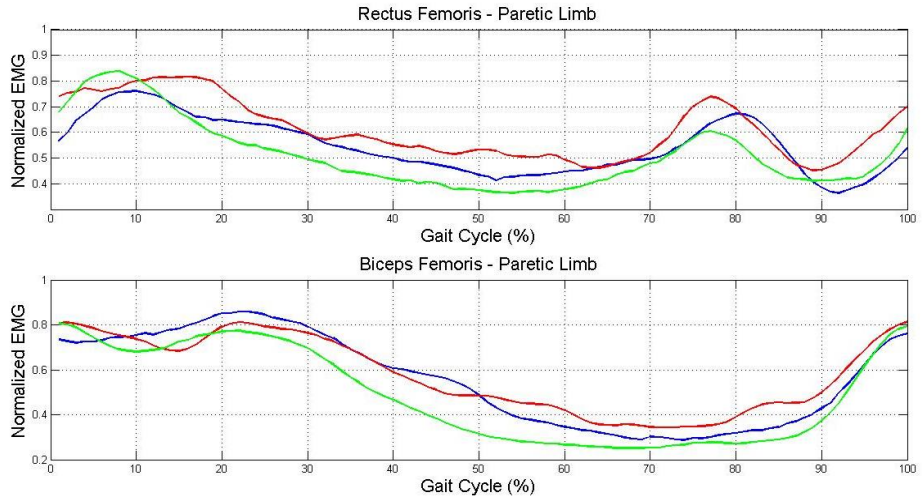

(c)

Figure 4- EMG mean envelope for the couple of muscles (a) Tibialis Anterior-Gastrocnemius of the paretic limb, (b) Tibialis Anterior-Gastrocnemius of the contralateral limb, (c) Rectus Femoris – Biceps Femoris of the paretic limb (blue: without AFO; red: solid AFO; green: dynamic AFO).

Consider first the couple of muscles Tibialis Anterior – Lateral Gastrocnemius in Table 4. For the paretic limb, in each stance sub-phase except for the pre-swing, CI values related to the solid AFO were higher than ones for the dynamic AFO. This difference however was not statistically significant. On the contralateral limb, during mid-stance and terminal stance CI values obtained with Toe-Off and without orthosis were higher than values obtained for the paretic limb ($p=0.050$ and $p=0.036$ without orthosis; $p=0.036$ and $p=0.017$ with the dynamic AFO).

As regards the swing phase, in both limbs during the initial swing there were not significant differences with and without orthosis. For the paretic side, in the terminal swing both AFOs caused an increase of CI, although significance was not reached. For the contralateral limb, during initial swing and terminal swing CI values were lower than CI values obtained for the paretic limb with both solid ($p=0.017$ and $p=0.012$) and dynamic AFO ($p=0.012$ and $p=0.036$). In the mid-swing, the difference between CI values in the contralateral and paretic limbs was significant only for the solid AFO ($p=0.025$) and without orthosis ($p=0.025$).

Table 4 – Coactivation Index in hemiparetic patients

Parameter		Shoes	Solid AFO	Dynamic AFO
Tibialis Anterior-Gastrocnemius Co-activation index		*during mid-stance*		
	A	0.401 ± 0.194[c]	0.533 ± 0.249	0.460 ± 0.223[c]
	U	0.632 ± 0.177	0.595 ± 0.202	0.644 ± 0.171
		during terminal stance		
	A	0.303 ± 0.136[c]	0.382 ± 0.206	0.304 ± 0.137[c,]
	U	0.520 ± 0.151	0.410 ± 0.130	0.445 ± 0.114
		during initial swing		
	A	0.455 ± 0.273	0.478 ± 0.253[c]	0.443 ± 0.164[c]
	U	0.250 ± 0.125	0.214 ± 0.070	0.224 ± 0.108
		during mid-swing		
	A	0.413 ± 0.203[c]	0.396 ± 0.181[c]	0.340 ± 0.162
	U	0.247 ± 0.127	0.263 ± 0.157	0.226 ± 0.096
		during terminal swing		
	A	0.409 ± 0.214	0.583 ± 0.101 [c]	0.554 ± 0.180[c]
	U	0.297 ± 0.113	0.336 ± 0.166	0.337 ± 0.153
Rectus Femoris – Biceps Femoris Co-activation index		*during loading response*		
	A	0.639 ± 0.239	0.703 ± 0.222	0.685 ± 0.186
	U	0.622 ± 0.160	0.563 ± 0.215	0.527 ± 0.202
		during mid-stance		
	A	0.533 ± 0.227	0.688 ± 0.117[c]	0.533 ± 0.209
	U	0.562 ± 0.176	0.488 ± 0.118	0.410 ± 0.151 [a,]
		during terminal stance		
	A	0.348 ± 0.124 [c]	0.416 ± 0.198	0.269 ± 0.115
	U	0.553 ± 0.211	0.442 ± 0.204[a]	0.409 ± 0.165[a]
		during pre-swing		
	A	0.229 ± 0.154	0.263 ± 0.226	0.150 ± 0.087[, c]
	U	0.404 ± 0.233	0.325 ± 0.169	0.306 ± 0.155
		during initial swing		
	A	0.207 ± 0.174	0.283 ± 0.283	0.209 ± 0.208
	U	0.252 ± 0.121	0.190 ± 0.136	0.187 ± 0.116
		during mid swing		
	A	0.290 ± 0.170[c]	0.338 ± 0.203[c]	0.249 ± 0.130
	U	0.220 ± 0.125	0.227 ± 0.137	0.207 ± 0.092
		during terminal swing		
	A	0.436 ± 0.101	0.537 ± 0.176	0.418 ± 0.110
	U	0.469 ± 0.191	0.398 ± 0.187	0.422 ± 0.151

Data are mean ± SD. A: affected limb. U: unaffected limb.

Table 5 - Electromyographic data in hemiparetic patients

Parameter		Shoes	Solid AFO	Dynamic AFO
Tibial anterior activation index	A	0.41 ± 0.13	0.47 ± 0.11	0.43 ± 0.16
	U	0.21 ± 0.07	0.28 ± 0.10	0.27 ± 0.09
Premature calf activation index	A	0.24 ± 0.10	0.23 ± 0.06	0.23 ± 0.02
	U	0.20 ± 0.05	0.22 ± 0.06	0.21 ± 0.02
Push-off index	A	0.24 ± 0.05	0.21 ± 0.07	0.21 ± 0.03
	U	0.24 ± 0.06	0.24 ± 0.04	0.24 ± 0.03

Data are mean ± SD. A: affected limb. U: unaffected limb.

Consider now the couple of muscles Rectus femoris – Biceps femoris. For the paretic side, all along the stance phase the Codivilla spring made the CI increase with respect to the Toe-Off and the absence of orthosis. However, this behaviour did not produce significant variations. During the terminal stance and the subsequent pre-swing, the Toe-Off induced a notable CI reduction with respect to the absence of AFO; because of the Bonferroni correction, the variation was not significant but close to the threshold ($p=0.025$). For the contralateral limb, there were no statistically significant changes in the performed multiple analysis.

Along the swing phase, the Codivilla spring generally provided higher CI values than the Toe-Off, although the difference was not significant. In the mid-swing, the difference between CI values in the contralateral and paretic limbs was significant only for the solid AFO ($p=0.017$) and without orthosis ($p=0.025$).

Discussion

Three walking sessions (without AFO, with an anterior dynamic AFO and with a posterior solid AFO), randomly ordered, were carried out for each patient. A biomechanical gait analysis based on the Davis protocol was carried out through a stereo-photogrammetric system (BTS Smart D). Spatio-temporal, kinematic and electromyographic changes in patients ambulation patterns were measured through quantitative indices.

The results showed that both AFOs can reduce the ROM of the dorsi-plantar-flexion angle of the ankle, thus proving that the use of the AFO is effective in correcting the foot drop syndrome, independently on the specific type of orthosis. No relevant difference was retrieved in the spatio-temporal parameters probably because of the short time the patient used the orthoses. Furthermore, both devices showed a balancing effect between the two limbs, with different co-activation patterns of the involved muscles (Table 4).

In detail, for the couple of muscles Tibialis Anterior-Gastrocnemius, it was observed a clear increase of the CI on the paretic side during mid-stance with both AFOs (with respect to the absence of AFO). It was probably caused by the proprioceptive stimulus related to the presence of the external device. Lower CI could be observed for the Toe-Off (although not statistically significant), probably because of its elastic structure.

CI values obtained without orthosis and with Toe-Off on the contralateral limb during mid-stance were similar and higher than values obtained for the paretic limb. This may be due to the longer time duration of the stance phase and to the major effort for the ankle stabilization. Additionally, the combined effect of the elastic features and the anterior leaf of the Toe-Off caused a reduction of the tibialis anterior activity of the paretic limb (Figure 4a) and, consequently, a lower CI value in mid-stance and terminal stance phases with respect to the contralateral limb. In the terminal stance, both orthoses reduced the CI on the contralateral limb with respect to the absence of AFO because of the "push" effect of the orthoses during pre-swing. The expected consequence is the positive effect on the contralateral side of reducing co-contraction. This is confirmed by the increased activity of the gastrocnemius for both AFOs compared to the absence of orthosis (see Figure 4b), while tibialis anterior activity is similar.

During the initial swing, the use of orthoses (independently on the specific type) did not entail significant CI differences in the two limbs with respect to the ambulation without orthosis. Both orthoses enabled a more effective clearance of the paretic limb (confirmed by the lower activity of the tibialis anterior in presence of AFOs (Figure 4a)). The effect was more evident in the Toe-Off

that, because of the elastic material, allowed storing energy in the stance phase and releasing it in the swing phase. This behaviour was sharpened in the subsequent mid-swing. Furthermore, in the mid-swing CI values were significantly higher on the paretic side than on the contralateral side for the solid AFO and the absence of AFO (Table 4). Correspondingly, Figure 4a points out that the absence of orthosis caused higher tibialis anterior activity. With the Toe-Off the gastrocnemius was less active than with the Codivilla spring, thus getting the behaviour of the paretic limb closer to the contralateral limb.

On the other hand, for the couple of muscles Rectus femoris – Biceps femoris, CI values for the Codivilla spring were higher than the other two cases all along the stance phase. The solid AFO caused the reduction of the ankle ROM with respect to the ambulation without orthosis and, due to the mechanical stiffness of the material, caused the major involvement of the knee in the trunk weight-bearing. Correspondingly, the rectus femoris was more activated also because of the posterior leaf. This behaviour is particularly evident in the mid-stance (Figure 4c). During the terminal stance and the pre-swing, the Toe-Off induced a large (close to significance) CI reduction with respect to the absence of AFO; this was due to its mechanical elasticity, and consequent energy release.

All along the swing phase, the Codivilla spring provided higher CI values than the Toe-Off. The elastic properties of the Toe-Off coupled to the anterior leaf contributed to generate an extensor torque on the knee that reduced the rectus femoris activity and correspondingly the CI (Figure 4c).

Despite the limited number of subjects, the obtained results were encouraging because they showed that: wearing an AFO did not lead to drawbacks on patient ambulation and provided a corrective action on the typical deficit of dorsi-flexion of patients with foot drop, as expected. Moreover, AFOs played an important role in recovering the balance between the two limbs. Finally, in terms of muscular activation, the anterior dynamic AFO was more beneficial than the posterior solid AFO because of the lower co-contraction of the couple of muscles involved in gait.

Future efforts will be addressed to: (a) increase the number of patients, in order to enforce the statistical significance of the reported results, (b) add force data and kinetic indices, which are expected to point out more relevant differences between the two devices; (c) extend the study to other ankle foot pathologies in hemiparetic subjects (e.g. equinus varus foot), thus modifying the Davis protocol currently used by the optoelectronic system; (d) define clinical guidelines for the prescription of the two devices.

References

[1] Yamamoto S, Hagiwara A, Mizobe T, Yokoyama O, Yasui T. Development of an ankle–foot orthosis with an oil damper. Prosthet Orthot Int 2005; 29: 209-219.

[2] Ferris DP, Gordon KE, Sawicki GS, Peethambaran A. An improved powered ankle–foot orthosis using proportional myoelectric control.Gait& Posture 2006; 23: 425-428.

[3] Park JH, Chun MH, Ahn JS, Yu JY, Kang SH. Comparison of gait analysis between anterior and posterior ankle foot orthosis in hemiplegic patients. Am J Phys Med Rehabil 2009; 88: 630–634.

[4] Chen C-C, Hong W-H, Wang C-M, Chen C-K, Wu KP-H, Kang C-F, Tang SF. Kinematic features of rear-foot motion using anterior and posterior ankle-foot orthoses in stroke patients with hemiplegic gait. Arch Phys Med Rehabil 2010; 91: 1862-8.

[5] Lehmann JF, Esselman PC, Ko MJ, Smith JC, deLateur BJ, Dralle AJ. Plastic Ankle-Foot Orthoses: evaluation of function. Arch Phys Med Rehabil 1983; 64: 402-7.

[6] Hiroaki A, Akira M, Kazuyoshi S, Naoki S, Shin-Ichi I. Improving gait stability in stroke hemiplegic patients with a plastic Ankle-Foot-Orthosis. Tohoku J. Exp. Med., 2009; 218: 193-199.

[7] Franceschini M, Massucci M, Ferrari L, Agosti M, ParoliC.Energy cost and gait assessment for hemiplegic walking: effects of an ankle-foot orthesis.Eur Med Phys 2002; 38: 57-64.

[8] Esquenazi A, Ofluoglu D, Hirai B, Kim S. The effects of an Ankle-Foot Orthosis on temporal spatial parameters and asymmetry of gait in hemiparetic patients.PM&R, 2009; 1.11: 1014-1018.

[9] Desloovere K, Molenaers G, Van Gestel L, Huenaerts C, Van Campenhout A, Callewaert B, Van de Walle P, Seyler J. How can push-off be preserved during use of an ankle foot orthosis in children with hemiplegia? A prospective controlled study. Gait Posture 2006; 24: 142-151.

[10] Brehm MA, Harlaar J, Schwartz M. Effect of ankle-foot orthoses on walking efficiency and gait in children with cerebral palsy. J Rehabil Med 2008; 40: 529-534.

[11] Van Gestel L, Molenaers G, Huenaerts C, Seyler J, Desloovere K. Effect of dynamic orthoses on gait: a retrospective control study in children with hemiplegia. Dev Med Child Neurol 2008; 50: 63-67.

[12] Lehmann JF, Condon SM, Price R, DeLateur BJ. Gait abnormalities in hemiplegia: their correction by ankle-foot orthoses. Arch Phys Med Rehabil1987;68: 763-71.

[13] De Wit DC, Buurke JH, Nijlant JM, IJzerman MJ, Hermens HJ. The effect of an ankle-foot orthosis on walking ability in chronic stroke patients: a randomized controlled trial. ClinRehabil 2004; 18: 550-557.

[14] Beckerman H, Becher J, Lankhorst GJ, Verbeek AL. Walking ability of stroke patients: efficacy of tibial nerve blocking and a polypropylene ankle-foot orthosis. Arch Phys Med Rehabil 1996; 77: 1144-1151.

[15] Cakar E, Durmus O, Tekin L, Dincer U, Kiralp MZ. The ankle-foot orthosis improves balance and reduces fall risk of chronic spastic hemiparetic patients. Eur J PhysRehabil Med 2010; 46.3: 363-368.

[16] Wang RY, Yen L, Lee CC, Lin PY, Wang MF, Yang YR. Effects of an ankle-foot orthosis on balance performance in patients with hemiparesis of different durations. ClinRehabil 2005; 19: 37-44.

[17] Danielsson A, Sunnerhagen KS. Energy expenditure in stroke subjects walking with a carbon composite ankle foot orthosis. J Rehabil Med 2004; 36: 165-168.

[18] Buckon CE, Thomas SS, Jakobson- Huston S, Moor M, Sussman M, Aiona M. Comparison of three ankle-foot orthosis configurations for children with spastic diplegia. Dev Med Child Neurol 2004; 46: 590-598.

[19] Ridgewell E, Dobson F, Bach T, Baker R. A systematic review to determine best practice reporting guidelines for AFO interventions in studies involving children with cerebral palsy. Prosthet Orthot Int 2010; 34: 129-145.

[20] Morris C. A review of the efficacy of lower-limb orthoses used for cerebral palsy. Dev Med Child Neurol 2002; 44: 205-211.

[21] Figueiredo EM, Ferreira GB, Maia Moreira RC, Kirkwood RN, Fetters L. Efficacy of ankle-foot orthoses on gait of children with cerebral palsy: systematic review of literature. Pediatr Phys Ther. 2008; 20: 207-223.

[22] Bregman DJJ. The optimal ankle foot orthosis: the influence of mechanical properties of Ankle Foot Orthoses on the walking ability of patients with central neurological disorders. 2011.

[23] Don R, Serrao M, Vinci P, Ranavolo A, Cacchio A, Ioppolo F, Paoloni M, Procaccianti R, Frascarelli F, De Santis F, Pierelli F, Frascarelli M, Santilli V. Foot drop and plantar flexion failure determine different gait strategies in Charcot-Marie-Tooth patients. Clinical Biomechanics 2007; 22.8: 905-916.

[24] Merlo A, Farina D, Merletti R. A fast reliable technique for muscle activity detection from EMG signals. IEEE Trans Biomed Eng 2003; 50: 316-323.

[25] Cavagna GA, Thys H, Zamboni A. The sources of external work in level walking and running. J. Physiol. 1976; 262: 639-657.

[26] Zollo L, Zaccheddu N, Ciancio AL, Morrone M, Bravi M, Santacaterina F, Laineri Milazzo M, Guglielmelli E, Sterzi S. Comparative analysis and quantitative evaluation of ankle-foot orthoses for foot drop in chronic hemiparetic patients. Eur J Phys Rehabil Med. 2015;51(2):185-96.

[27] Yamamoto S, Ebina M, Miyazaki S, Kawai H, Kubota T. Development of a new ankle-foot orthosis with dorsiflexion assist. Part 1: Desirable characteristics of ankle-foot orthoses for hemiplegic patients. J ProsthetOrthot.1997; 9.4: 174-179.

[28] Davis R, Ounpuu S, Gage J. A gait analysis data collection and reduction technique. Human Mov Science 1991; 10: 575-587.

[29] Don R, Ranavolo A, Cacchio A, Serrao M, Costabile F, Iachelli M, Camerota F, Frascarelli M, Santilli V. Relationship between recovery of calf-muscle biomechanical properties and gait pattern following surgery for Achilles tendon rupture. Clinical Biomechanics 2007; 22: 211-220.

[30] Burridge JH, Wood DE, Taylor PN, McLella DL. Indices to describe different muscle activation patterns, identified during treadmill walking, in people with spastic drop-foot. Medical Engineering & Physics 2001; 23: 427-434.

Chapter VI - MoCap systems for posture and gait analysis: application to amputee patients.

Introduction

In the last chapter, the author reports some preliminary data of an ongoing pilot study involving a single upper limb amputee patient compared to a group of healthy age-matched controls. The rationale is to investigate how an external object can alterate human trunk motion, depending whether the object is recognized as one's own body parts (embodiment) or not. Prosthetic limbs are an example of external objects capable becoming embodied, which can be observed in everyday environment. Postural control commonly is regulated by a series of internal and external circuits which maintain balance of the body center of mass. As regards the upper limbs, there are difficulties in the way of defining a standard for motion analysis, the result mainly of the different tasks and functions of this body segment [2]. Trunk activity can be considered more similar to the upper than the lower extremities in terms of complexity. Trunk movements play an important role in many human activities, contributing to the movement of the whole body [3-5]; in fact the trunk offers stability to the limbs, allowing them to operate properly [6]. For these reasons, the trunk has been studied in relation to limb movements during simple activities (e.g. gait or reaching) and modifications to trunk kinematics have been observed when comparing healthy and pathological subjects [7-9]. Nevertheless, the trunk has rarely been studied as an independent object of research, even if the study of trunk kinematics can play a very important role from a clinical perspective. Even more rarely, the trunk has been studied in relation to the function of the stump in case of upper limb amputation. In this preliminary study we have analyzed, by means of a motion analysis and a stabilometric system, the trunk sagittal and coronal deviations induced by wearing different prostheses on an upper limb chronic amputee patient, in order to describe the influence of an

embodied prosthesi on postural control and compare it with a not-embodied. To reinforce this aim, we decided to conduct a postural balance dynamic analysis by means of a stabilometric platform.

Materials and methods

Subjects

Nineteen healthy subjects (10 males, 9 females; age 53,47±11,52; BMI 25,88±4,14) were enrolled as a control group in order to make comparison with a post-traumatic upper limb amputee female patient (age 40; BMI 27,39). The level of amputation was across the radius bone of the left arm, and the onset of amputation was twenty-nine years ago. The patient was familiar with a cosmetic prosthesis, which serves her to attempt activities of daily living.

Experimental protocol

The experimental protocol was set up as follows: an instrumental gait analysis followed by a postural analysis in static and dynamic conditions; gait and postural analysis were carried out in the same laboratory setting by using the same stereophotogrammetric motion analysis system (SMART-DX system, BTS, Milan, Italy). In order to complete the trunk analysis, we conducted a stabilometric assessment on a computerized tilting platform (Balance System SD, Biodex Medical Systems Inc., NY, USA). All the experimental measurements were completed on the same day for each subject, in order to avoid any possible bias due to learning effect.

Experimental setup

Gait analysis was carried out on a six meters walkaway by using an 8-infrared cameras optoelectronic system which recorded the three-dimensional position of 22 retro-reflective spherical markers (15 mm diameter) placed on a series of anatomical landmarks, according to Davis protocol [19-21]. The same stereophotogrammetric system, arranged so as to provide full lateral and back views of the subject's trunk, was used to analyze static and dynamic posture of the subjects. This was obtained by placing 9 retro-reflective emispherical markers (10 mm diameter) over the

cutaneous projections of the spinous processes of cervical-upper thoracic (C7-T2-T3), dorsal (T5-T6-T8) and lumbar (L1-L3-L5) segments, as defined by Ranavolo [10-12]. Subjects were required to perform three tasks: to maintain a comfortable upright standing position, barefoot with feet parallel, arms alongside the trunk, heels spaced 7 cm apart, open eyes, for 30 seconds (subjects were encouraged to avoid body twisting or asymmetric postures); to perform a full trunk flexion (anterior bending), followed by an extension restoring the trunk to the starting position. Each test was repeated three times in order to obtain a mean value. For each test, the subject's distance from the recording cameras was set up at 3 meters. Furthermore, all patients underwent a stabilometric assessment by means of a 55 cm-diameter computerized platform (Balance System SD, Biodex Medical Systems Inc., NY, USA), designed to test and train the patients' kinesthetic abilities by offering twelve increasing-demand levels of stability control on the tilting platform (plus locked position for static measurements). For each subject a static test was performed and then a dynamic one. The static test ("Postural stability") requested the patient to maintain the upright position on the fixed platform for 20 seconds, while the system recorded the de-flexions of the trunk from the center of mass (registered prior to start the test) in any spatial direction. Resulting from this registration, a general index for postural stability was obtained, which was composed by an index evaluating the center of mass displacement along the sagittal plane, and another index evaluating the on-coronal plane oscillations. Moreover, a dynamic test ("Risk of falling") was applied, which consisted of maintaining the center of gravity (represented by a black dot on the screen) at the center of the display, counteracting a 3-seconds intervals increasingly balance instability, for a total of 20 seconds. The test was repeated for three times at all, and a software calculated the mean score, which was compared to normative age-categorized data.

Amputee patient

The analysis of the postural and gait performance of the amputee patient was conducted under three distinct conditions: i) wearing her own cosmetic prosthesis; ii) wearing a commercial myoelectric prosthesis (I-limb, Touch Bionics Inc., UK); iii) wearing a research myoelectric prosthesis (IH2

Azzurra, Prensilia s.r.l., Italy); iv) without any prosthesis at all.

Fig. I-Limb Touch Bionics

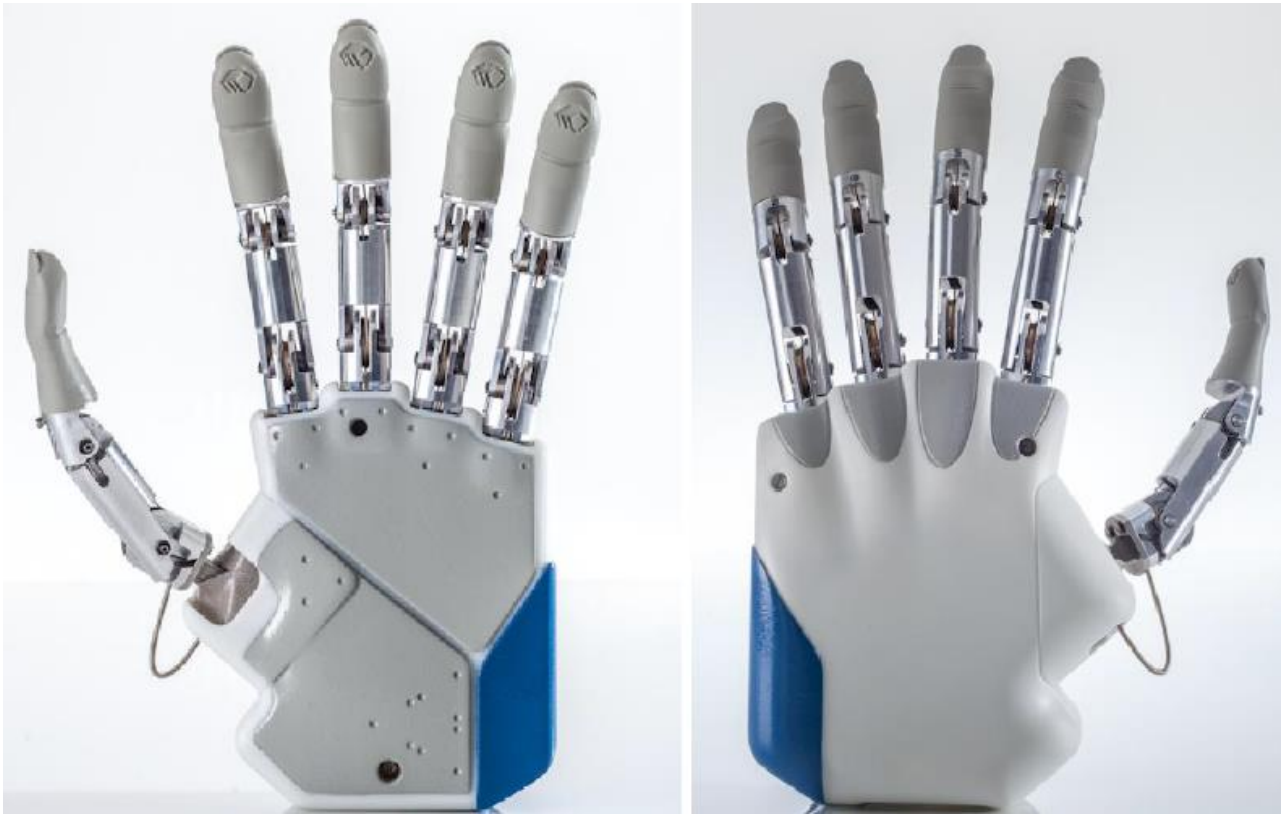

Fig. 1 Palm and dorsum view of IH2 Azzurra (left hand version).

The main difference between I-Limb and Prensilia is in the weight: I-Limb has a weight of 623 g, while IH2 Azzurra comes to be slightly more heavy (640 g).

Results

Gait parameters

According to embodiment principles [13], as shown in table I, the amputee patient showed a better gait performance using her own cosmetic prosthesis. Indeed, holding a myoelectric prosthesis as well as walking without any prosthesis implies a substantial worsening of gait parameters. Thus, by wearing cosmetic prosthesis, it can be observed a better cadence (113,80 steps/min) than in the other two conditions (107,00 steps/min as for no prosthesis walking, and 105,00 steps/min wearing a myoelectric prosthesis). This finding reflects a slight reduction of mean normalized velocity (velocity/height) from 1,10 m/s (without prosthesis) and 1,09 m/s (myoelectric prosthesis) to 1,06 m/s walking with cosmetic prosthesis.

Comparison between left and right side, keeping in mind the left side of amputation, pointed out no differences among the three conditions as regards the right healthy side both for spatial (right step 0,49 m) and all temporal parameters except for swing phase duration (0,39 s with myoelectric prosthesis vs 0,44 s wearing cosmetic prosthesis or not). Left side comparison indicates a clear reduction of stride duration by walking with cosmetic prosthesis (0,99 s vs 1,12 s not wearing prosthesis vs 1,13 s wearing myoelectric prosthesis). Table I reports quantitative data about gait parameters for amputee patient and control group.

Tab. I. Gait spatio-temporal parameters.

	Patient			Control group
	None	Cosmetic	Myoelectric	Mean (SD)
tRSTRIDE(s)	1,12	1,17	1,15	1,15 (0,14)
tRSTANCE (s)	0,69	0,73	0,76	0,75 (0,10)
tRSWING (s)	0,44	0,44	0,39	0,41 (0,05)
tLSTRIDE (s)	1,12	0,99	1,13	1,19 (0,16)
tLSTANCE (s)	0,70	0,69	0,74	0,77 (0,12)
tLSWING (s)	0,42	0,43	0,39	0,44 (0,05)
dSTEPW (m)	0,16	0,15	0,15	0,17 (0,03)
dRSTRIDE (m)	1,01	1,02	1,02	1,06 (0,17)
dRSTEP (m)	0,49	0,49	0,49	0,50 (0,09)
dLSTRIDE (m)	1,01	0,91	1,04	1,09 (0,15)
dLSTEP (m)	0,45	0,45	0,46	0,49 (0,08)
velMEANnorm (m/s)	1,10	1,06	1,09	0,96 (0,21)
velRSTRIDE (m/s)	0,90	0,88	0,89	0,89 (0,19)
velRSWING (m/s)	2,08	2,02	2,22	2,13 (0,45)
velLSTRIDE (m/s)	0,90	0,87	0,91	0,90 (0,18)
velLSWING (m/s)	2,08	2,11	2,25	2,14 (0,38)
CAD (steps/min)	107,00	113,80	105,00	94,29 (14,86)

tRSTRIDE=Right stride time; tRSTANCE=Right stance time; tRSWING=Right swing time; tLSTRIDE=Left stride time; tLSTANCE=Left stance time; tLSWING=Left swing time; tLSTRIDE=Left stride time; tLSTANCE=Left stance time; tLSWING=Left swing time; dSTEPW=step width; dRSTRIDE=Right stride length; dRSTEP=Right step length; dLSTRIDE=Left stride length; dLSTEP=Left step length; velMEANnorm=normalized mean velocity; velRSTRIDE=Right stride velocity; velRSWING=Right swing velocity; velLSTRIDE=Left stride velocity; velLSWING=Left swing velocity; CAD=gait cadence.

Static posture

Two main sagittal curves of the trunk were measured in standing position: the thoracic kyphosis and the lumbar lordosis. Both the curves were obtained by defining the 5^{th} order polynomial function interpolating the coordinates of the 9 markers placed on the skin projection of three triplets of markers (cervical, dorsal, lumbar), as previously described. Thus, the kyphosis angle was defined as the angle between the line perpendicular to the interpolating function passing through C7 and the line perpendicular to the interpolating function passing through the point in which the trunk curve

changes passing from the cervical to the thoracic segment. Likewise, the lumbar lordosis was defined as the corresponding angle between the perpendicular lines to the interpolating function passing through the point of inversion from thoracic to lumbar segment, and through L5 respectively.

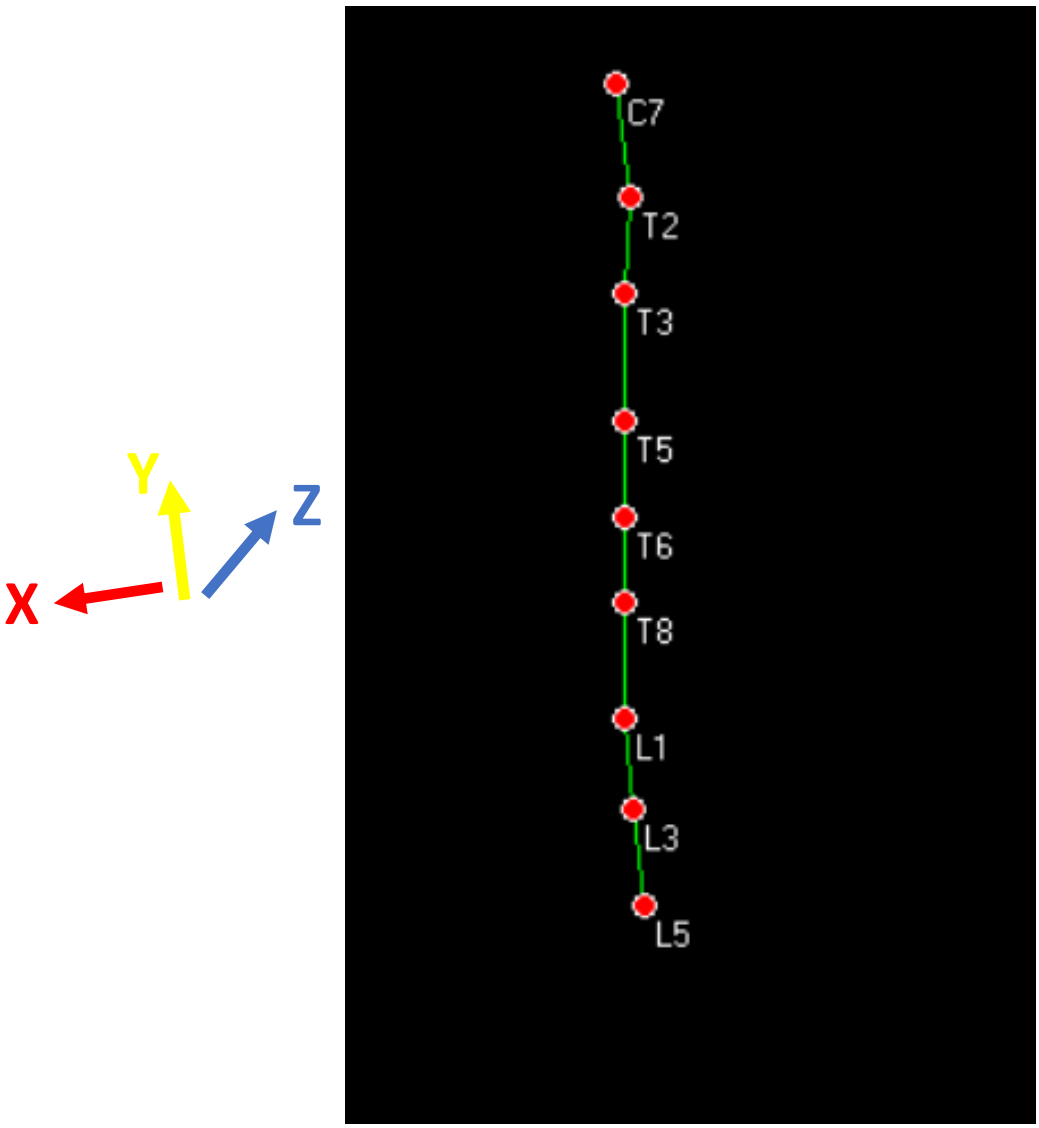

Fig. 1. Kinematic representation of the spine by optoelectronic system (9-markers protocol). Angle on the sagittal plane (flexion-extension) is defined as the angle between the Y-axis and the projection of the couple L5-L3 on the YZ-plane. Likewise, angle on the coronal plane (abduction-adduction) is defined as the angle between the Z-axis and the projection of the couple L5-L3 on the XZ-plane.

Notably, control subjects presented kyphosis angle (43,34± 1,34 degrees) smaller than the amputee patient (53,13± 2,81 degrees), while lordosis angle resulted more pronounced (78,02± 0,60 degrees vs 69,66± 1,59 degrees, respectively). Moreover, if comparing trunk angles of the amputee patient wearing three different prosthetic devices and without wearing any prosthesis, we observed a substantial homogeneity in lumbar lordosis angle values (69.05± 1.00 degrees wearing no prosthesis; 68.84± 1.24 degrees wearing her own cosmetic device, 70.52± 2.53 degrees wearing the I-limb prosthesis, and 70.23± 1.23 degrees wearing the IH2 Azzurra). As regards kyphosis angle, a slight reduction was revealed by wearing IH2 Azzurra (49.38± 3.00 degrees) if compared to the other three conditions (55.37± 1.91 degrees without prosthesis; 53.30± 2.81 degrees with cosmetic prosthesis; 54.50± 3.50 degrees with I-limb). Fig. 2 highlights differences in angular values of thoracic and lumbar curve of the amputee patient in static upright posture.

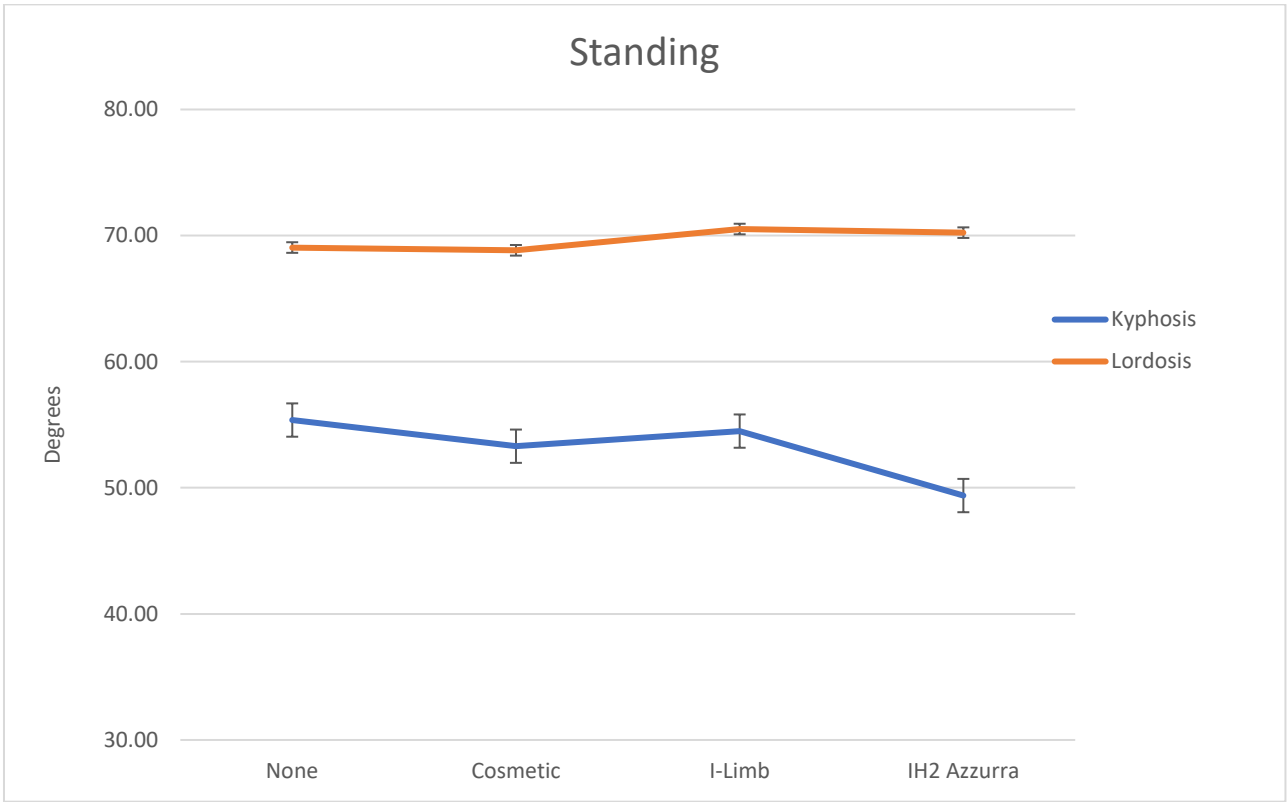

Fig.2. Thoracic kyphosis and lumbar lordosis angles of the amputee patient in static upright posture, under four different conditions (see text for details).

Bending

Dynamic posture was investigated by optoelectronic analysis of trunk motion on sagittal plane; at this purpose, controls and patient were required to slowly bend forward their trunk as much as possible, and then return to the standing upright position by extending their trunk.

Overall trunk excursion in anterior bending showed to be similar in controls (51.11± 4.66 degrees) and the amputee patient (50.61± 1.24 degrees). If considering the amputee patient in her wearing conditions, we observed a clear reduction in overall sagittal excursion of the spine by wearing heavy myoelectric prosthesis (46.68± 0.63 degrees wearing IH2 Azzurra, and 47.68± 1.49 degrees wearing I-Limb) with respect to cosmetic (54.25± 0.57 degrees) and no prosthesis (57.49± 1.60 degrees). Fig. 3 remarks these differences.

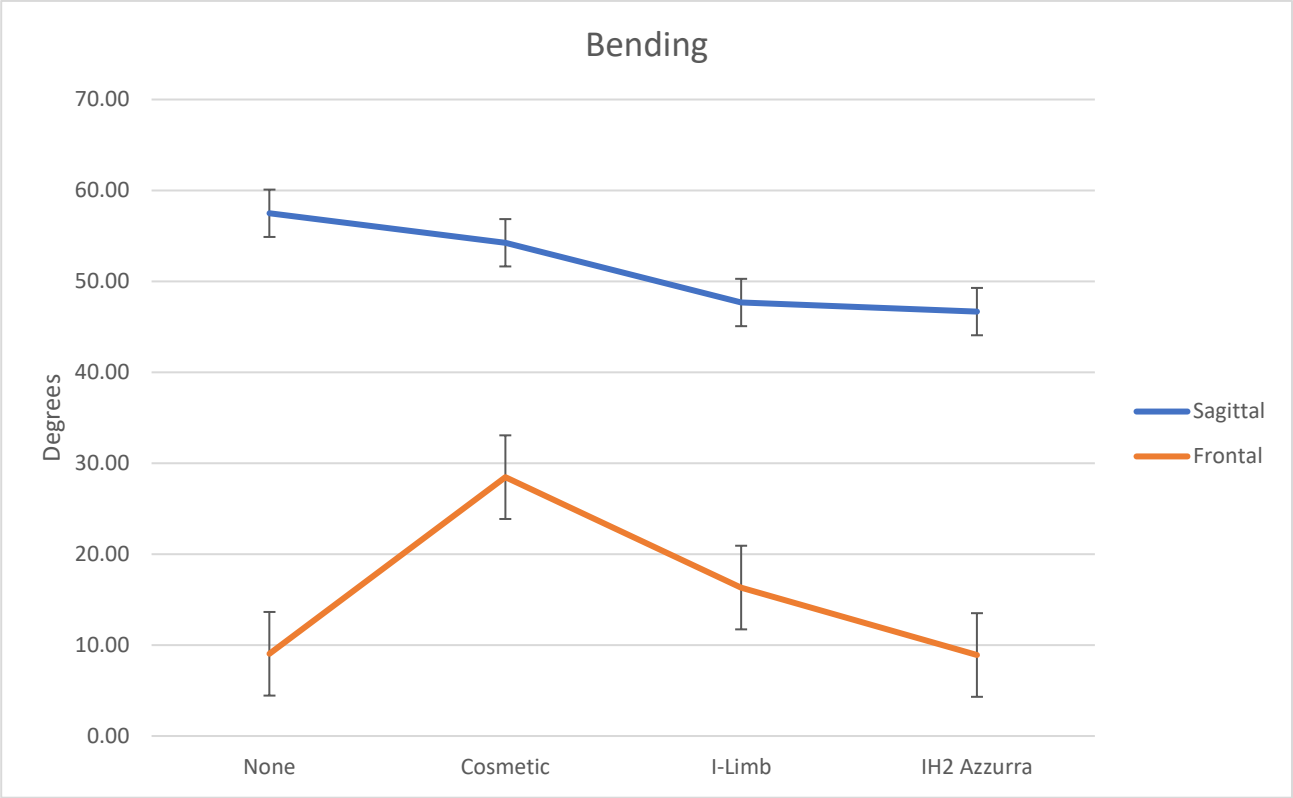

Fig. 3. Sagittal and frontal excursions in anterior bending test for the amputee patient, under four different conditions (see text for details).

Furthermore, in order to study influence of wearing upper limb prosthesis and the different weights of the devices (or the absence of any of these) on postural symmetry on the coronal plane, we evaluated also the frontal excursions of the trunk during the anterior bending test. As depicted in figure 3, cosmetic prosthesis determines a major frontal range of motion of trunk during the anterior bending (28.47± 0.51 degrees), while no prosthesis condition and IH2 Azzurra provide less trunk deviation (9.05± 1.31 degrees vs 8.91± 1.32 degrees, respectively). I-Limb causes a mean moderate trunk coronal deviation, but with a wide standard deviation (16.33± 4.69 degrees), resulting similar to the corresponding excursions among control subjects (14.36± 4.79 degrees). Interestingly, observing the direction of trunk lateral deviation of the amputee patient during the bending test, a frontal deviation towards the contralateral (right) side to the stump was evident for all the conditions except for the Prensilia, which causes a deviation towards the ipsilateral (left) side to the stump.

Stabilometric assessment

To evaluate the effects of wearing a prosthesis on postural balance, we conducted a stabilometric test on a tilting computerized platform (Balance SD System, Biodex Medical Systems Inc., NY, USA). The Biodex Balance System SD allows to assess a patient's neuromuscular control in a closed-chain, multi-plane test by quantifying the ability of the patient to maintain dynamic bilateral postural stability on either a static or unstable surface. The degree of surface instability is controlled by the system's microprocessor-based actuator. In a dynamic test, once the session begins, the patient's ability to control the platform angle is quantified as a variance from the locked (level) position, as well as degrees of deflection over time. A large variance may be indicative of poor neuromuscular response. Further insight into specific neuromuscular activation patterns is realized with the quantification of anterior/posterior and medial/lateral platform tilt.

Static testing measures the angular excursion of the patient's Center of Gravity (COG). Body height is a factor for static measures. A person's COG is approximately 55% of their height. Based on a

selected height, an appropriate static measure scaling is applied. Good static testing scores can lead to a progression into dynamic testing and training. The Postural Stability test emphasizes a patient's ability to maintain a center of balance. The patient's score, or "Stability Index", on this test assesses deviations from center, thus a lower score is more desirable than a higher score. The Stability Index is the average position from the center. The Stability index does not indicate how much the patient swayed, but only his body position. Indeed, the standard deviation is indicative of sway.

Limits of Stability (LOS) test challenges patients to move and control their center of gravity within the base of support. During each test trial, patients must shift their weight to move the cursor from the center along a target path and back as quickly and with as little deviation as possible. The same process is repeated for each of the targets. Target paths activate in a random order. This test is a good indicator of dynamic control within a normalized sway envelope. Poor control, inconsistent, or increased times suggests further assessment for lower extremity strength, proprioception, vestibular, or visual deficiencies. Sway information—or what the clinician and patient will see as "Angle (°)" on the display screen—is collected by positioning the patient on the static platform and sampling and recording patient movement. The system employs a series of strain gauges to determine variation in the patient's resultant center of pressure (COP). The center of pressure is the patient's center of gravity (COG) projection on the platform resulting from postural position (sway angle) and patient height. Data is sampled at the rate of 20Hz. Each recorded sample consists of a (X, Y) coordinate. The sway angle "Angle (°)" is derived from the position of the patient's COG from zero and the height of the patient's COG (taken as .55 times the patient height.).

The Balance System SD Fall Risk test allows identification of potential fall candidates. Test results are compared to age-dependent normative data. Scores higher than normative values suggest further assessment for lower extremity strength, proprioception, and vestibular or visual deficiencies.

The results of the "Postural stability" test, which registers the body sway around the center of mass in static conditions with open eyes, point out a better stability of the amputee patient (overall stability index OSI = 0.4 without prosthesis) than controls (OSI = 1.05). The worse score in overall

stability index among control subjects can be ascribed to both the antero-posterior and the medio-lateral deviations (APSI = 0.74 and MLSI = 0.84, respectively). For the amputee patient, even if changing the worn prosthesis, OSI does not differ from the condition without prosthesis (OSI = 0.5 wearing either cosmetic or myoelectric prosthesis). The body sway is expressed by the standard deviation of OSI (OSISD); while the control subjects present OSISD equal to 0.41 (0.38 for the antero-posterior component, 0.33 for the medio-lateral), the amputee patient shows a comparable global sway (OSISD = 0.49 without prosthesis). Notably, OSISD reduces if wearing cosmetic prosthesis (OSISD = 0.4) if compared to the myoelectric (OSISD = 0.46) and the medio-lateral component seems to give the greater contribution (MLSISD = 0.2), equally to that recorded without wearing any prosthesis. On the contrary, the myoelectric prosthesis seems to reduce the antero-posterior oscillation (APSISD = 0.29) if compared to the other two conditions (APSISD = 0.5 if no wearing prosthesis, and APSISD = 0.4 if wearing cosmetic prosthesis). Table II reports data on stabilometric parameters

Tab. II Stabilometric assessment

	Patient			Controls
	None	Cosmetic	Myoelectric	Mean
OSI	0,4	0,5	0,5	1,05
OSISD	0,49	0,4	0,46	0,41
APSI	0,3	0,4	0,3	0,74
APSISD	0,5	0,4	0,29	0,38
MLSI	0,2	0,2	0,4	0,84
MLSISD	0,19	0,2	0,42	0,33
OSL	49	49	48	53,13
ASL	63	64	65	69,88
PSL	27	52	40	48,63
RSL	76	60	38	62,38
LSL	77	47	83	65,88
LST	51	46	46	126,38
FRI	1,6	1,3	1,7	2,13

OSI=overall stability index; OSISD=OSI standard deviation; APSISD=APSI standard deviation; MLSISD=MLSI standard deviation; MLSI=medio-lateral stability index; ASL/PSL=anterior/posterior stability limit; RSL/LSL=right/left stability limit; FRI=fall risk index; LST=limit stability time; OSL=overall stability limit.

Discussion

A prosthetic upper-limb incorporated into an amputee's body may affect motor control over the whole body in addition to body representation. A recent qualitative study suggested that a prosthetic arm can maintain amputees' body posture [14]. Prosthetic arms (both functional and aesthetic) can compensate for asymmetric and/or disturbed body balance due to limb amputation, which may cause uneven load and consequently back and neck pain. The authors pointed out that everyday activities, such as walking and swimming, also benefit from stabilization engendered by use of an upper-limb prosthesis. Given this, it is natural to think that a lower-limb prosthesis would play a similar role because the legs bear one's body weight and generate one's gait. Indeed, studies have investigated the effects of a lower-limb prosthesis resulting in a perturbed postural control [15] and an asymmetric gait [16]. Moreover, because walking with a unilateral lower-limb prosthesis is likely to rely more on the intact side and thus show an asymmetric gait pattern, long-term use of the

lower-limb prosthesis may cause musculoskeletal distortion [7]. In contrast, it remains unclear whether and how an upper-limb prosthesis modulates amputees' postural control and how the frequency of use and embodiment of an upper-limb prosthesis affects postural modulation; the suggestion by Wijk and Carlsson [14] has yet to be empirically examined.

Human body posture is maintained by online comparison of the desired body parts' locations with their actual locations on the basis of multisensory afferent information supplied by those body parts, that is, a feedback system [18-20]. Additionally, since the feedback system is not sufficient to maintain posture, anticipatory motor control computed by internal forward models is also used, that is, a feedforward system [21,22]. Both systems need to sense the current location of body parts and their movement sequence, although humans do not have organs by which to directly perceive these data. Instead, implicit body representation can play a key role as a template of a balanced body and a reference for postural control [23,24]. Thus, it is assumed that a coherent body representation may be sufficient to maintain their body posture, even in amputees presumably with altered afferent information due to the amputation. If so, a prosthetic arm may restore an amputee's body representation by being incorporated as a part of his or her body [25,26], and consequently stabilize his or her body posture. Thus, we expected that amputees whose prosthetic arm belongs to their body representation would show well-stabilized postural control, whereas those whose prosthesis is not incorporated into their body would show relatively disturbed postural control because the prosthesis can behave as a perturbation. The preliminary data reported in this section seem to confirm this orientation. Indeed, the amputee patient of the study showed a reduced kyphosis angle, during the standing test, when wearing the more heavy prosthesis, thus resulting in a trunk reaction towards an overextension in order to compensate for anterior sliding of body gravitational center. Likewise, as regards frontal oscillations during a bending trial, the more heavy prostheses seem to better stabilize body medial-lateral sway, even if the Prensilia tends to pull down the trunk towards ipsilateral side.

References

[1] Davis RB, Õunpuu S, Tyburski D, Gage JR. A gait analysis data col-lection and reduction technique. Hum Mov Sci 1991;10:575-87.

[2] Rau G, Disselhorst-Klug C, Schmidt R. Movement biomechanics goes upwards: from the leg to the arm. J Biomech 2000;33:1207-16.

[3] Maaswinkel E, Griffioen M, Perez RSGM, van Dieën JH. Methods for assessment of trunk stabilization, A systematic review. J Electro-myogr Kinesiol 2016;26:18-35.

[4] Smania N, Picelli A, Romano M, Negrini S. Neurophysiological basis of rehabilitation of adolescent idiopathic scoliosis. Disabil Rehabil 2008;30:763-71.

[5] Villafañe JH, Zanetti L, Isgrò M, Cleland JA, Bertozzi L, Gobbo M, et al. Methods for the assessment of neuromotor capacity in non-specific low back pain: Validity and applicability in everyday clinical practice. J Back Musculoskelet Rehabil 2015;28:201-14.

[6] Sihvonen T, Lindgren KA, Airaksinen O, Manninen H. Movement disturbances of the lumbar spine and abnormal back muscle elec-tromyographic findings in recurrent low back pain. Spine (Phila Pa 1976) 1997;22:289-95.

[7] Needham R, Stebbins J, Chockalingam N. Three-dimensional kin-ematics of the lumbar spine during gait using marker-based systems: A systematic review. J Med Eng Technol 2016;40:172-85.

[8] Barton GJ, Hawken MB, Foster RJ, Holmes G, Butler PB. The effects of virtual reality game training on trunk to pelvis coupling in a child with cerebral palsy. J Neuroeng Rehabil 2013;10.

[9] Ferrarin M, Rizzone M, Lopiano L, Recalcati M, Pedotti A. Effects of subthalamic nucleus stimulation and L-dopa in trunk kinematics of patients with Parkinson's disease. Gait Posture 2004;19:164-71.

[10] Don R, Capodaglio P, Cimolin V, Benedetti MG, D'Osualdo F, Frigo C, et al. Instrumental measures of spinal function: Is it worth? A state-of-the art from a clinical perspective. Eur J Phys Rehabil Med 2012;48:255-73.

[11] Ranavolo A, Don R, Draicchio F, Bartolo M, Serrao M. Modelling the spine as a deformable body: Feasibility of reconstruction using an optoelectronic system. Appl Ergon 2013;44:192-9.

[12] Leardini A, Biagi F, Belvedere C, Benedetti MG. Quantitative comparison of current models for trunk motion in human movement anal-ysis. Clin Biomech 2009;24:542-50.

[13] Imaizumi S, Asai T, Koyama S. Embodied prosthetic arm stabilizes body posture, while unembodied one perturbs it. Consciousness and Cognition 2016;45:75-88.

[14] Wijk U, Carlsson I. Forearm amputees' views of prosthesis use and sensory feedback. Journal of Hand Therapy. 2015;28(3):1880-2.

[15] Fernie GR, Holliday PJ. Postural sway in amputees and normal subjects. Journal of Bone and Joint Surgery. 1978;60(7):895-8.

[16] Winter DA, Sienko SE. Biomechanics of below-knee amputee gait. Journal of Biomechanics. 1988;21(5):361-7.

[17] Gailey, R., Allen, K., Castles, J., Kucharik, J., Roeder, M. Review of secondary physical conditions associated with lower-limb amputation and long-term prosthesis use. Journal of Rehabilitation Research and Development. 2008;45(1):15–29.

[18] Mergner T, Rosemeier T. Interaction of vestibular, somatosensory and visual signals for postural control and motion perception under terrestrial and microgravity conditions: A conceptual model. Brain Research Reviews. 1998;28(1-2):118-35.

[19] Peterka RJ. Sensorimotor integration in human postural control. Journal of Neurophysiology. 2002;88(3):1097-1118.

[20] Peterka RJ, Loughlin PJ. Dynamic regulation of sensorimotor integration in human postural control. Journal of Neurophysiology. 2004;91(1):410-423.

[21] Collins JJ, de Luca CJ. Open-loop and closed-loop control of posture: A random-walk analysis of center-of-pressure trajectories. Experimental Brain Research. 1993;95(2), 308–318.

[22] Van der Kooij H, Jacobs R, Koopman B, Grootenboer H. A multisensory integration model of human stance control. Biological Cybernetics. 1999;80(5):299–308.

[23] Di Fabio RP, Emasithi A. Aging and the mechanisms underlying head and postural control during voluntary motion. Physical Therapy. 1997;77(5):458–475.

[24] Gurfinkel VS, Ivanenko YP, Levik YS, Babakova IA. Kinesthetic reference for human orthograde posture. Neuroscience. 1995;68(1):229–243.

[25] De Vignemont F. Habeas corpus: The sense of ownership of one's own body. Mind & Language. 2007;22(4):427–449.

[26] Mayer A, Kudar K, Bretz K, Tihanyi J. Body schema and body awareness of amputees. Prosthetics and Orthotics International. 2008;32(3):363–382.

Conclusion

In this paper we have presented some interesting clinical uses of optoelectronic motion analysis systems. Such systems have shown a great reliability as for detecting even small movements, like those of thoraco-abdominal wall. This is a major advantage of this kind of motion capture, as demonstrated by the diffusion oh this kind of analysis for studying respiratory diseases. In particular, the possibility to measure several compartments independently has been shown to be very useful for clinical puroposes.To point out this advantage, we showed how posture (sitting or supine) can influence breathing kinematics among spinal cord injured patients, and the synchronization between upper thoracic and abdominal compartments. Other examples of how useful marker-based stereophotogrammetric systems in clinical practice are represented by the analysis of trunk alignment in Parkinson disease and the assessement of ankle foot orthoses in gait analysis, as well as for postural stability in amputee patients.Future directions of research would be to make motion analysis systems even more invasive; in this way of research, wearable sensors as well as sensorized fabrics promise to enhance body movements analysis, thus avoiding the limits of a laboratory setting

List of publications

Published journal papers

1. Pezzuto A, Morrone M, Mici E. Unusual jaw metastasis from squamous cell lung cancer in heavy smokers: Two case reports and review of the literature. Medicine (Baltimore). 2017;96(21):e6987.

2. Massaroni M, Carraro E, Vianello A, Miccinilli S, Morrone M, Levai K, Schena E, Saccomandi P, Sterzi S, Dickinson JW, Silvestri S. Optoelectronic Plethysmography in Clinical Practice and Research: A Review. Respiration 2017;93(5):339-354.

3. Miccinilli S, Morrone M, Bastianini F, Molinari M, Scivoletto G, Silvestri S, Ranieri F, Sterzi S. Optoelectronic plethysmography to evaluate the effect of posture on breathing kinematics in spinal cord injury: a cross sectional study. Eur J Phys Rehabil Med. 2016;52(1):36-47.

4. Sterzi S, Giordani L, Morrone M, Lena E, Magrone G, Scarpini C, Milighetti S, Pellicciari L, Bravi M, Panni I, Ljoka C, Bressi F, Foti C. The efficacy and safety of a combination of glucosamine hydrochloroide, chondroitin sulfate and bio-curcumin with exercise in the treatment of knee osteoarthritis: a randomized, double-blind, placebo-controlled study. Eur J Phys Rehabil Med. 2016;52(3):321-30.

5. Morrone M, Miccinilli S, Bravi M, Paolucci T, Melgari JM, Salomone G, Picelli A, Spadini E, Ranavolo A, Saraceni VM, Di Lazzaro V, Sterzi S. Perceptive rehabilitation and trunk posture alignment in patients with Parkinson disease: a single blind randomized controlled trial. Eur J Phys Rehabil Med. 2016;52(6):799-809.

6. Zollo L, Zaccheddu N, Ciancio AL, Morrone M, Bravi M, Santacaterina F, Laineri Milazzo M, Guglielmelli E, Sterzi S. Comparative analysis and quantitative evaluation of ankle-foot orthoses for foot drop in chronic hemiparetic patients. Eur J Phys Rehabil Med. 2015;51(2):185-96.

Published international conference proceedings

1. Massaroni C, Schena E, Saccomandi P, Morrone M, Sterzi S, Silvestri S. Evaluation of optoelectronic plethysmography accuracy and precision in recording displacements during quiet breathing simulation. Conf Proc IEEE Eng Med Biol Soc. 2015 Aug;2015:1291-4.